

Synthesis of functional 1,2-dithiolanes from 1,3-bis-*tert*-butyl thioethers

Georg M. Scheutz^a, Jonathan L. Rowell^a, Fu-Sheng Wang^b, Khalil A. Abboud^a, Chi-How Peng^b, and Brent S. Sumerlin^{*,a}

^aGeorge & Josephine Butler Polymer Research Laboratory, Center for Macromolecular Science & Engineering, Department of Chemistry, University of Florida, Gainesville, FL 32611, USA

^bDepartment of Chemistry and Frontier Research Center on Fundamental and Applied Sciences of Matters, National Tsing Hua University, 101, Sec 2, Kuang-Fu Rd., Hsinchu 30013, Taiwan

Table of Contents	Page
S1. General Information	2
S2. Instrumentation	2
S3. Supplementary Figures	4
S4. Synthesis of 1,2-Dithiolane Derivatives	21
S5. Synthesis of 1,3-<i>tert</i>-Butyl Thioether Substrates	31
S6. Starting Material Synthesis	40
S7. NMR Spectra and Additional Characterization	48
S8. X-Ray Crystallography	84
S9. Computational Details	88
S10. References	94

S1. General Information

Reagents and solvents were purchased from commercial sources and used without further purification. Anhydrous THF, Et₂O, and DCM were obtained by passing the solvent through two sequential activated alumina columns in a MBRAUN solvent purification system. All solvent mixtures are given in volume ratios. Thin-layer chromatography (TLC) was performed on SiO₂-60 F254 aluminum plates with visualization by UV light or staining with KMnO₄. Flash column chromatography was performed using silica gel (40–60 μm particle size, 60 Å pore size) from VWR. The melting points (T_m) of the solid compounds were determined via differential scanning calorimetry.

S2. Instrumentation

Nuclear Magnetic Resonance (NMR) Spectroscopy. 500 (125) MHz ¹H (¹³C) NMR spectra were recorded on an INOVA 500 MHz spectrometer. Chemical shifts (δ) are given in parts per million (ppm) relative to TMS and referenced to residual protonated solvent purchased from Cambridge Isotope Laboratories, Inc. (CDCl₃: δ¹H 7.26 ppm, δ¹³C 77.16 ppm). Abbreviations used are s (singlet), d (doublet), t (triplet), q (quartet), p (pentet), sept (septet), b (broad), and m (multiplet).

High Resolution Mass Spectrometry (HRMS). HRMS was conducted on an Agilent 6220 TOF spectrometer with electro spray ionization (ESI).

Gas Chromatography-Electron Ionization Mass Spectrometry (GC-EIMS). GC-EIMS spectra were recorded on a Thermo Scientific DSQ II after sample introduction via GC (Thermo Scientific Trace GC Ultra).

Raman Spectroscopy. Raman characterization was carried out using a LabRAM ARAMIS (Horiba Jobin Yvon) with a 633 nm HeNe laser as excitation source. Spectra

were recorded with a confocal hole size of 200 μm , 1800 g/mm grating and averaged over 32 scans in LabSPEC 5 (Horiba Jobin Yvon). All Raman spectra were baseline subtracted and normalized using OriginPro 8.5.

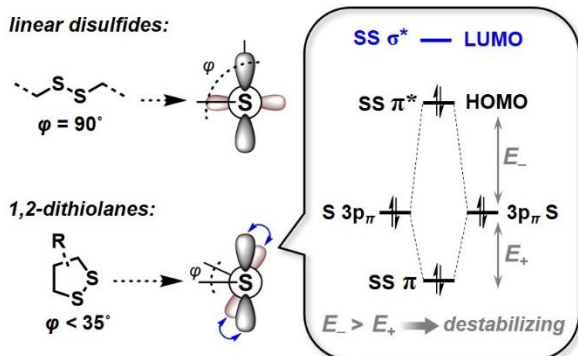
UV-Vis Spectroscopy. UV-vis characterization was conducted on a Molecular Devices Spectra Max M2 spectrophotometer with Greiner Bio-one 96-well clear-bottom polypropylene reader plates.

Fourier-Transform Infrared (FTIR) Spectroscopy. FTIR spectra were collected on neat samples using a PerkinElmer Spectrum One FTIR spectrometer equipped with a PIKE MIRacle single-reflection ATR accessory containing a diamond crystal sample plate. Spectra were processed using PerkinElmer Spectrum 10 software.

Differential Scanning Calorimetry (DSC). DSC analysis was performed on a TA Q1000 DSC (TA Instruments, New Castle, DE) equipped with an autosampler and refrigerated cooling system 90, using aluminum hermetic sealed pans. The peak maximum of the endothermic melting peak was used as T_m .

S3. Supplementary Figures

A. Bergson (1958)



B. Whitesides et al. (1987)

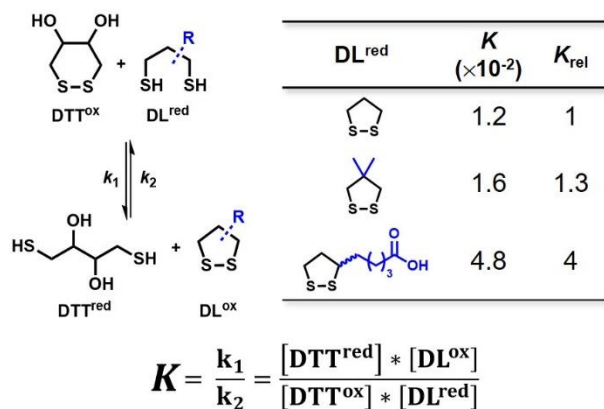


Figure S1. The effect of CSSC dihedral angle (φ) and ring substitution on 1,2-dithiolane reactivity. (A) The simplified molecular orbital diagram for the disulfide bond as introduced by Bergson¹ (and refined by Boyd)² explains the increased closed shell repulsion at low φ , due to the energy penalty from the out-of-phase (i.e., antibonding; E_-) interaction, which outcompetes the stabilizing in-phase (i.e., bonding; E_+) interaction. The increased HOMO energy level at low φ decreases the energy of the first electronic transition, resulting in a distinct red shift of the disulfide chromophore absorbance. (B) Ring substitution can stabilize the ring-closed (oxidized) five-membered disulfide scaffold.³ For example, the equilibrium constant (K) for the reaction between oxidized dithiothreitol (DTT^{ox}) and the reduced 1,3-dithiol (DL^{red}) is 1.3-times higher for 4,4-dimethyl-1,2-dithiolane than for unsubstituted 1,2-dithiolane.

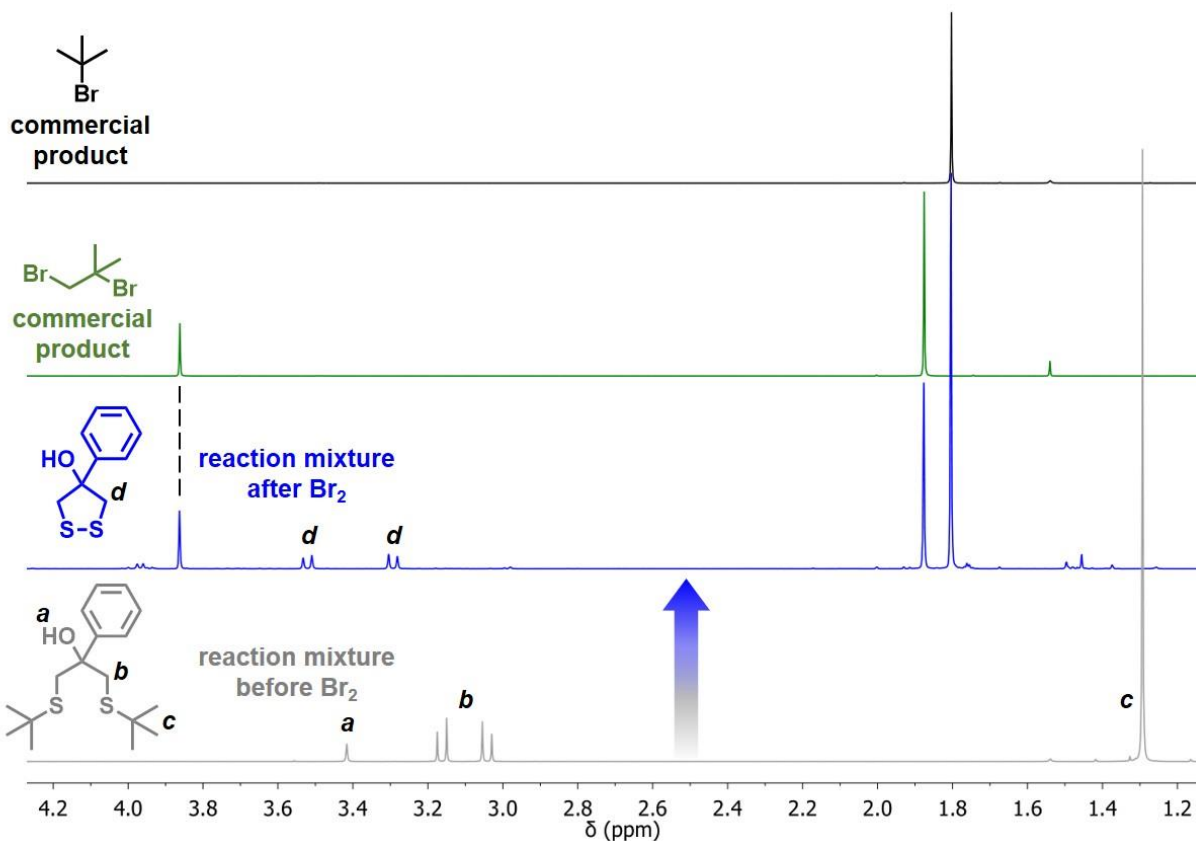


Figure S2. Stacked ^1H NMR spectra of the crude reaction mixture before addition of bromine (grey) and after the addition of bromine (blue), showing full conversion of the 2-phenyl-1,3-bis-*tert*-butyl thioether starting material. Notable are the ^1H NMR spectral signals indicative of the formation of 1,2-dibromo-2-methylpropane (3.86 and 1.88 ppm) and *tert*-butyl bromide (1.80 ppm). Spectra of commercial 1,2-dibromo-2-methylpropane (green) *tert*-butyl bromide (black) are shown on top. The products were further detected by GC-MS (Figures S3–S5).

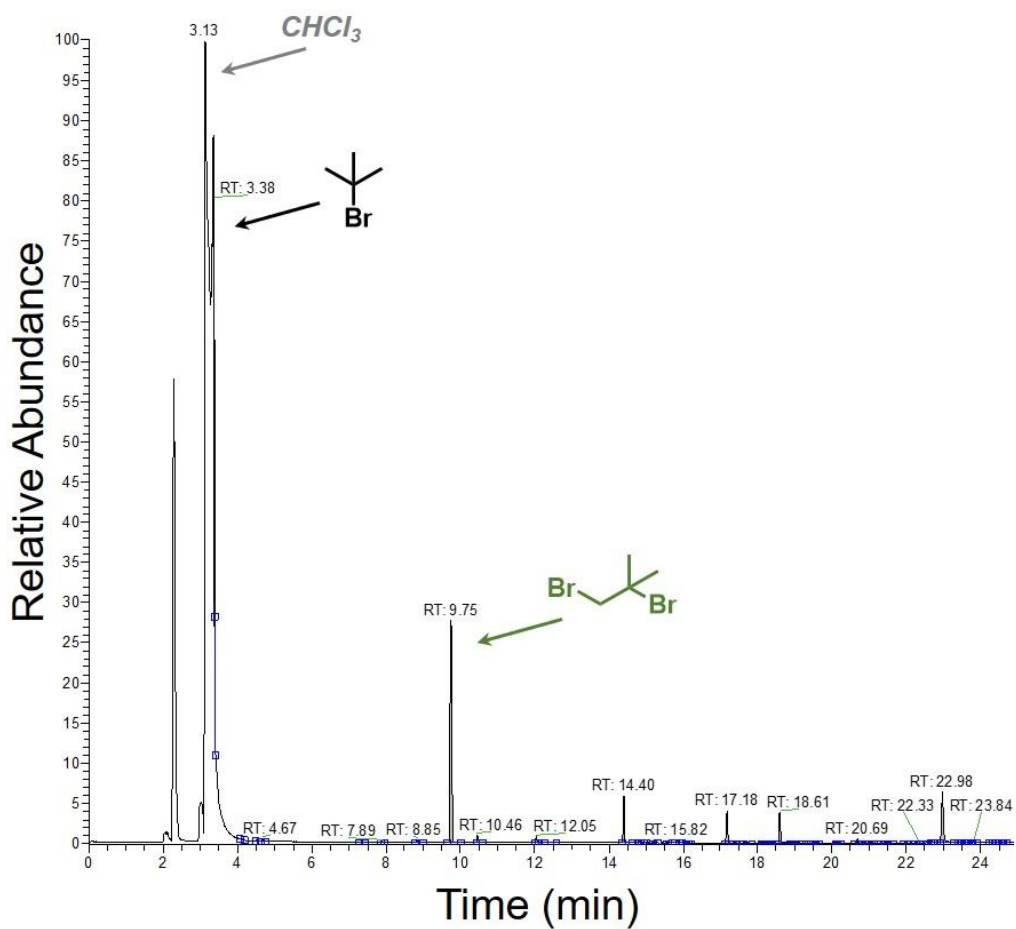


Figure S3. Chromatogram of the GC-MS analysis of the crude reaction at full conversion of the starting material. The substances eluting at 3.38 and 9.75 min were identified as 1,2-dibromo-2-methylpropane and *tert*-butyl bromide (Figures S4 and S5).

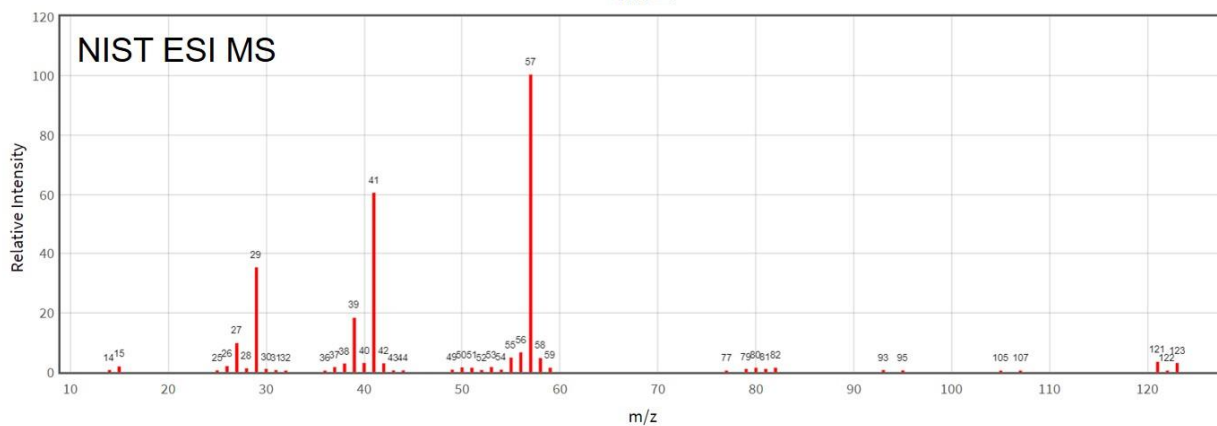
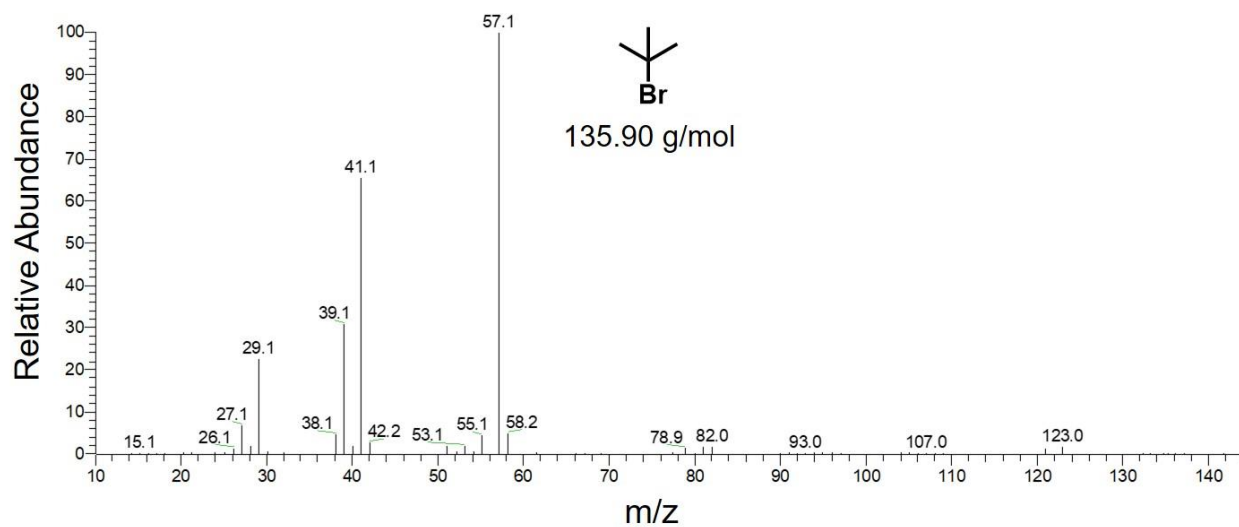


Figure S4. Mass spectrum (top) of the compound eluting at 3.38 min in the chromatogram of Figure S3 revealing a fragmentation pattern that matches the spectrum (bottom) of *tert*-butyl bromide obtained from NIST.⁴

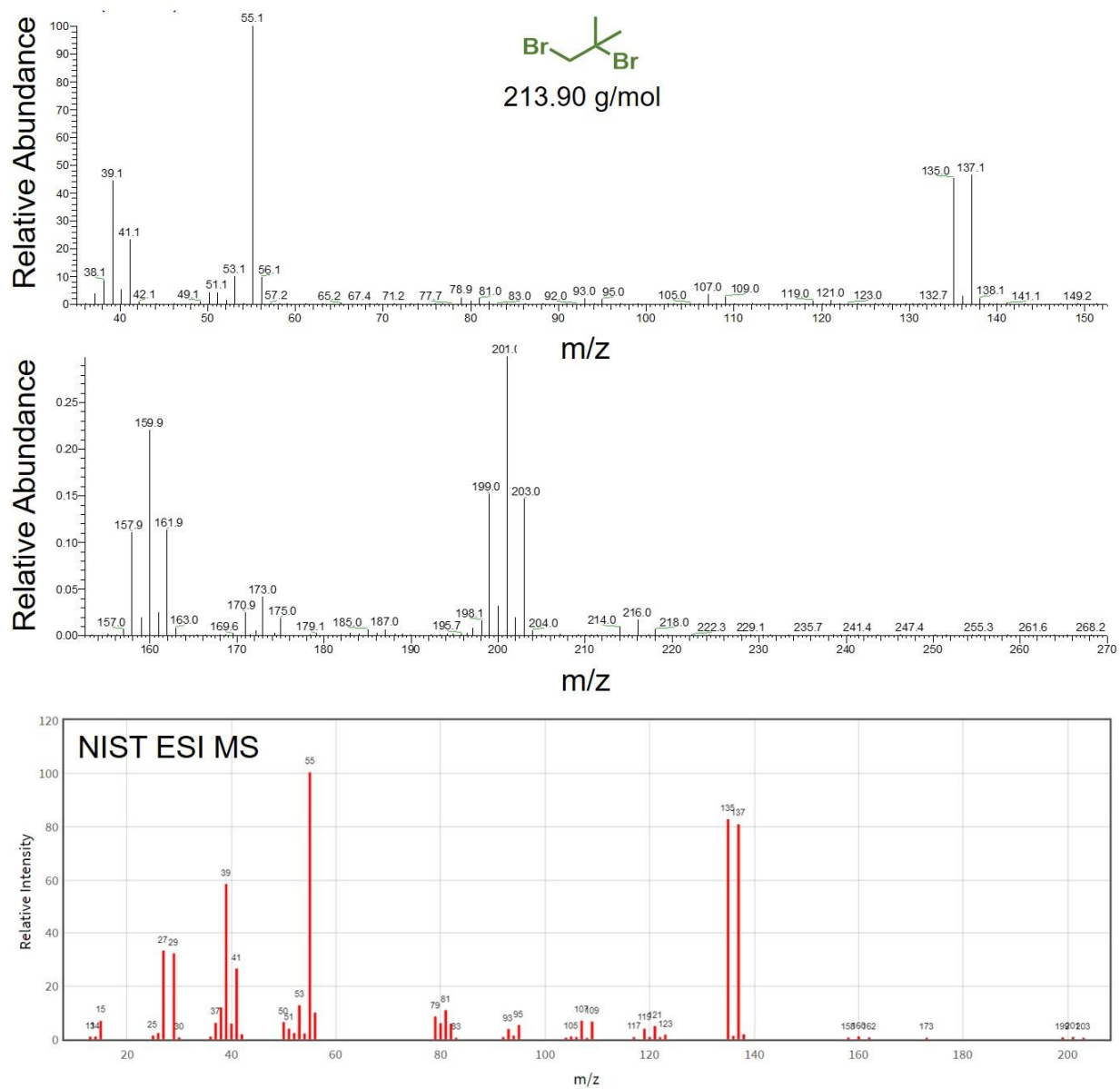


Figure S5. Mass spectrum (top and middle) of the compound eluting at 9.75 min in the chromatogram of Figure S3 revealing a fragmentation pattern that matches the spectrum (bottom) of 1,2-dibromo-2-methylpropane obtained from NIST.⁵

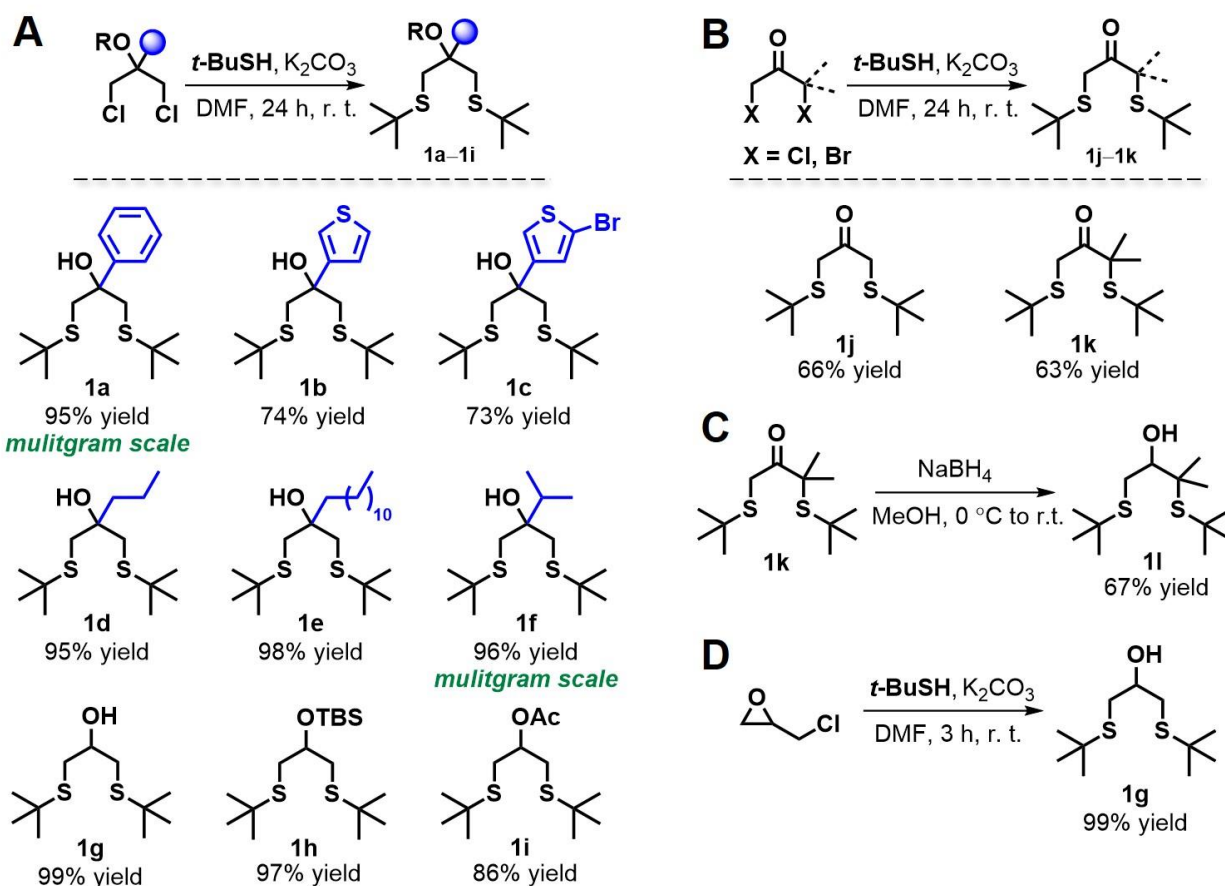


Figure S6. 1,3-Bis-*tert*-butyl thioether synthesis from 1,3-dichloropropan-2-ol derivatives (A) and α,α' -halogenated ketones (B). NaBH_4 reduction of **1k** provided hydroxy thioether **1l** (C). The successful synthesis of **1g** from 2-(chloromethyl)oxirane suggests that substituted oxiranes can potentially serve as substrates (D).

Discussion of the 1,3-bis-*tert*-butyl thioether synthesis: Reaction of *tert*-butylthiol (*t*-BuSH) with 1,3-dichloropropan-2-ol derivatives furnished the desired *tert*-butyl thioethers. Most substrates were obtained in good purity without the need for chromatographic purification, and the reaction conditions could be easily applied to multigram scales. Common protecting groups (**1h** and **1i**) were tolerated under the reaction conditions, showing that the hydroxy functionality is not essential to the transformation (Figure S6A). α,α' -Halogenated ketones under the same conditions provided 1,3-bis-*tert*-butyl thioethers in moderate yields. Notably, generation of **1k** from 2,4-dibromo-2-methylbutan-3-one involved the conversion of a tertiary bromide into a thioether, which is unlikely to occur via nucleophilic substitution under basic conditions. Since 2,4-dibromo-2-methylbutan-3-one rapidly decomposed upon exposure to K_2CO_3 and DMF in the absence of *t*-BuSH, we believe that this transformation followed a more complex reaction

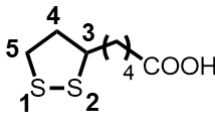
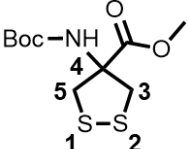
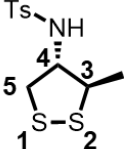
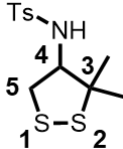
sequence, potentially a Favorskii-type rearrangement intercepted by ring-opening of the cyclopropanone intermediate with *t*-BuSH (Figure S6B).

Table S1. Disulfide (S–S) bond lengths and dihedral angles for various 1,2-dithiolanes obtained from crystal structures available at the Cambridge Crystallographic Data Center (CCDC). The dihedral angles are given as absolute values.

	C12DL	DiMeDL	Gerradine ^a		Guinesine-B <i>p</i> -bromophenylc arbamate ^b	Asparagusic Acid ^c
			ring A	ring B		
	bond length (Å)					
S–S	2.064	2.065	2.078	2.062	2.035	2.077
	dihedral angle (°)					
C5SSC3	35.2	23.4	0.6	23.4	36.4	25.4
SSC3C4	51.3	43.2	28.3	44.4	47.7	46.3
SC3C4C5	49.0	51.3	51.4	52.0	39.4	53.7
C3C4C5S	18.8	32.2	50.7	31.7	8.6	31.4
C4C5SS	14.1	1.0	27.1	0.3	20.7	0.5

^a Values from ref. 6; CCDC deposition number 1166300. ^b Values from ref. 7; CCDC deposition number 1280887. ^c Values from ref. 8; CCDC deposition number 723720.

Table S2. Disulfide (S–S) bond lengths and dihedral angles for various 1,2-dithiolanes obtained from crystal structures available at the Cambridge Crystallographic Data Center (CCDC). The dihedral angles are given as absolute values.

	Lipoic Acid^a	Boc-COOMe- 1,2-DL^b	Me-NHTs- 1,2-DL^c	DiMe-NHTs- 1,2-DL^d
				
	bond length (Å)			
S–S	2.053	2.056	2.059	2.045
	dihedral angle (°)			
C5SSC3	34.5	31.4	0.5	27.2
SSC3C4	43.0	47.4	27.5	44.0
SC3C4C5	36.3	47.8	49.5	49.0
C3C4C5S	7.7	20.6	49.8	27.8
C4C5SS	20.0	10.46	26.2	3.8

^aValues from ref. 9; CCDC deposition number 1270584. ^bValues from ref. 10; CCDC deposition number 181737. ^cValues from ref. 11; CCDC deposition number 288574. ^dValues from ref. 12; CCDC deposition number 648189.

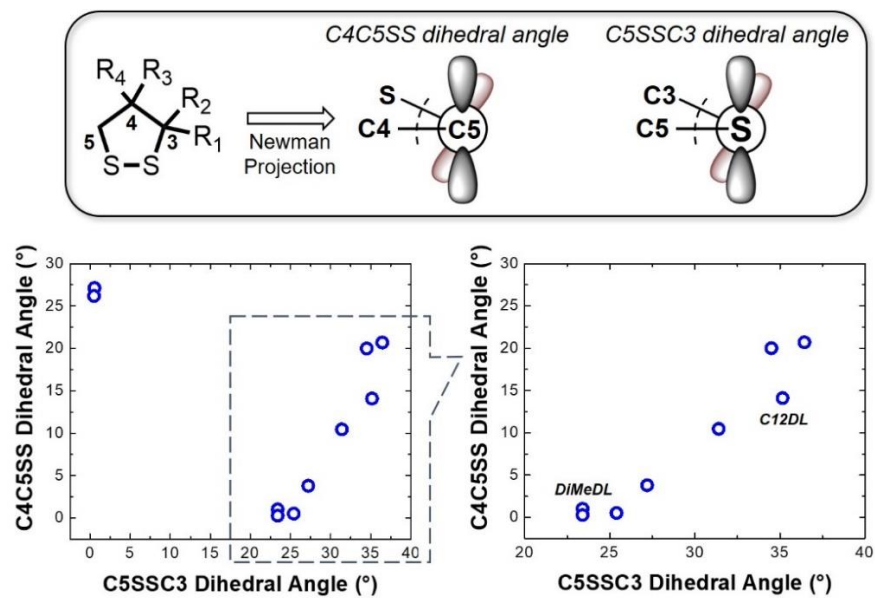


Figure S7. Plot of C4C5SS dihedral angle versus C5SSC3 dihedral angle (left) of the compounds listed in Tables S1 and S2. Expansion for C5SSC3 dihedral angle above 20° (right) revealed an almost linear relationship with substantially eclipsed C4C5SS conformation for 1,2-dithiolanes with C5SSC3 dihedral angles around 25°.

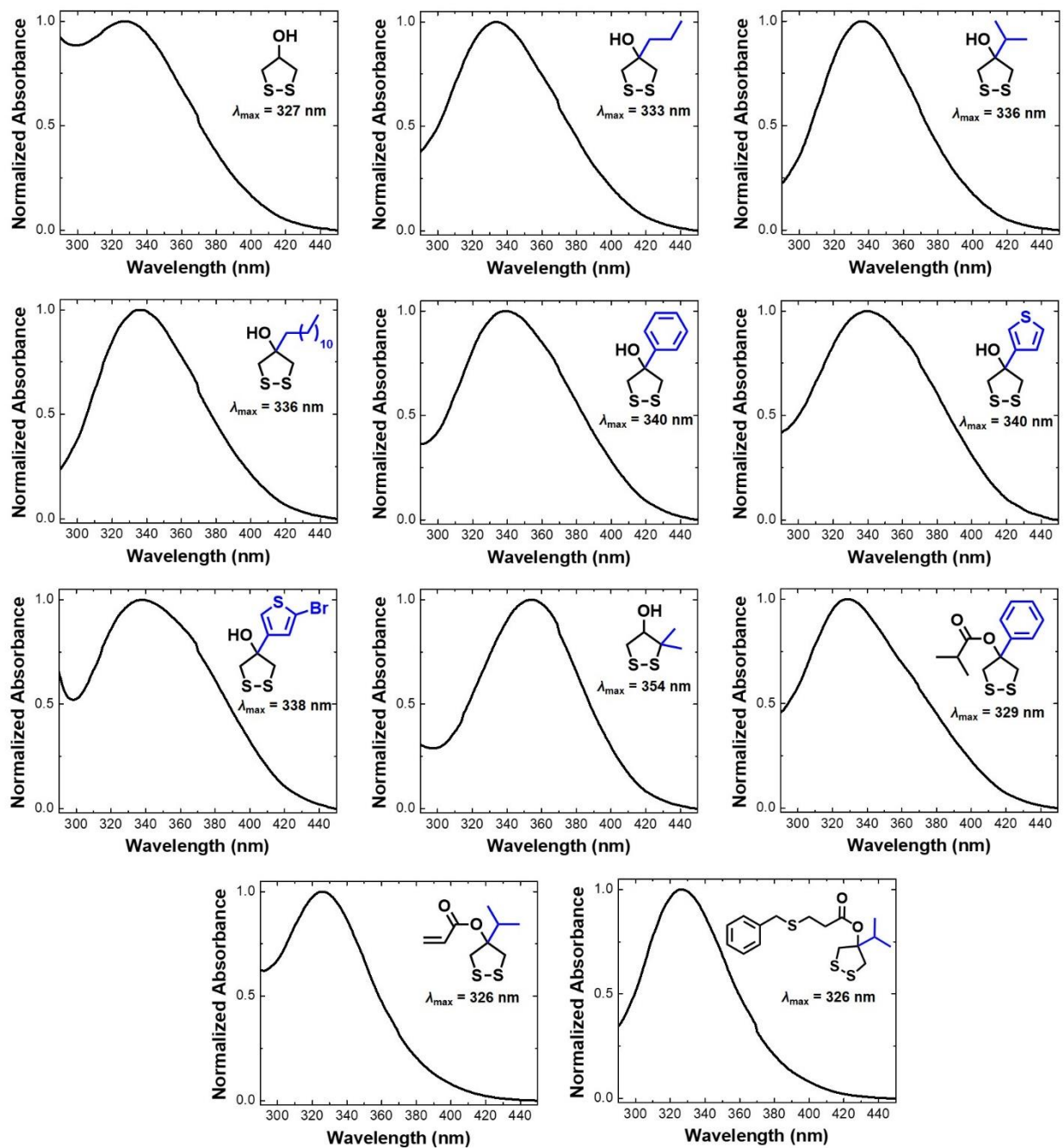


Figure S8. Normalized UV-vis spectra for the 1,2-dithiolane substrates at 10 mM in DMSO. Notably, esterification of the hydroxyl functionality resulted in a shift of the maximum absorbance to lower wavelengths. For example, λ_{\max} of **PhDL** shifted from 340 to 329 nm upon transformation to the isopropanoate ester **2**. We believe this is due to substantial geometric changes caused by the sterically demanding isopropanoate ester group geminal to the phenyl substituent. However, electronic effects upon conversion of the hydroxy functionality into an ester cannot be ruled out.

Table S3. Maximum absorbance wavelength (λ_{\max}) obtained from UV-vis spectroscopy of 1,2-dithiolane substrates. Estimation of CSSC dihedral angles (φ) based on λ_{\max} using the protocol reported by Kilgore and Raines.¹³

Compound	λ_{\max} (nm)	φ (estimated) ^a (°)	φ (experimental) ^b (°)
HDL	327	40.0	
<i>n</i> PrDL	334	37.5	
<i>i</i> PrDL	336	36.8	
C12DL	336	36.8	35.2
PhDL	340	35.4	
TphDL	340	35.4	
TphBrDL	338	36.1	
DiMeDL	354	30.8	23.4

^aCalculated via the relationship $\varphi = \pm \arcsin [(460 \text{ nm} - \lambda_{\max}) / 207 \text{ nm}]$ from ref.13; ^bObtained from X-ray crystal structures.

Discussion of the CSSC dihedral angle (φ) estimation: Although we found good agreement between X-ray crystal structure and calculated φ for **C12DL** with 35.2° and 36.8°, respectively, the estimated φ for **DiMeDL** of 30.8° differed substantially from 23.4° as obtained by X-ray crystallography. We believe this discrepancy can be attributed to additional substituent effects, such as hyperconjugative interactions,¹³ from the di-methyl substitution on the carbon in α -position to the S–S bond. Similar effects have been observed in vibrational spectroscopy of disulfides.^{14–15}

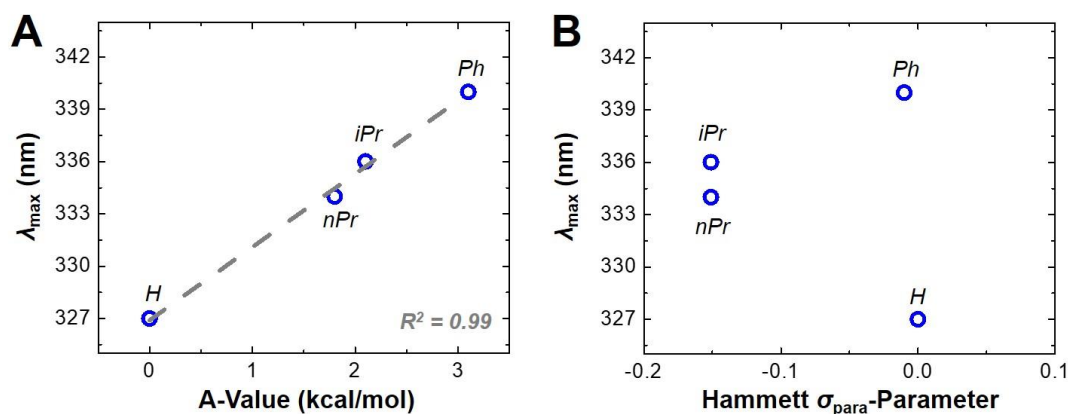


Figure S9. Investigations of the relationship between λ_{\max} and steric and electronic substituent effects. (A) λ_{\max} increases linearly with substituent A-values, obtained from ref. 16. (B) No correlation between λ_{\max} and Hammett σ_{para} -parameter¹⁷ was found. A-value and σ_{para} -parameter of an ethyl group was used for nPr in both plots, since no such values are available for nPr.

Discussion steric and electronic substituent effects: Using A-values as a measure of steric bulk,¹⁶ we found a linear relationship between λ_{\max} (and thus φ) and substituent A-value. These results suggest that λ_{\max} increases with increasing substituent size, reflecting decreasing φ with larger substituents. However, A-values were available only for a fraction of the substituents used in this report and more detailed future studies will be necessary to elucidate this phenomenon fully.

The plot of λ_{\max} against Hammett σ_{para} -parameter¹⁷ as indicator of electronic influence of the substituent did not show any correlation, indicating a predominantly steric nature of the effect.

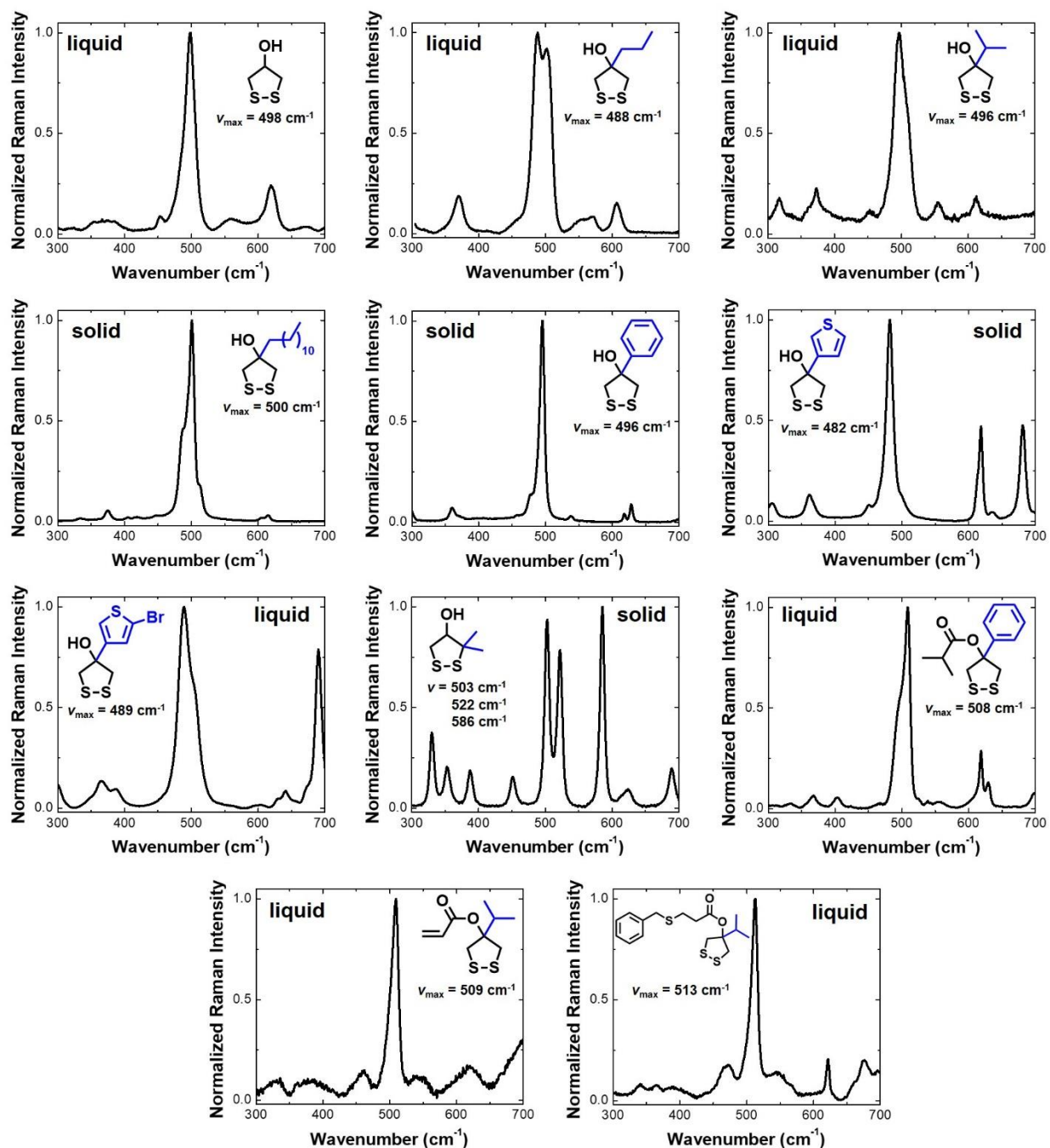


Figure S10. Normalized Raman spectra for the 1,2-dithiolane substrates. The physical state of the compounds potentially affects the Raman scattering signature. For example, the otherwise very similar compounds **TphDL** (solid) and **BrTphDL** (liquid) demonstrated shifted maximum signal wavenumbers (v_{\max}) and additional signals in the solid sample. The spectrum of **DiMeDL** is distinctly different, potentially due to the geminal di-substitution in α -position to the S–S bond.

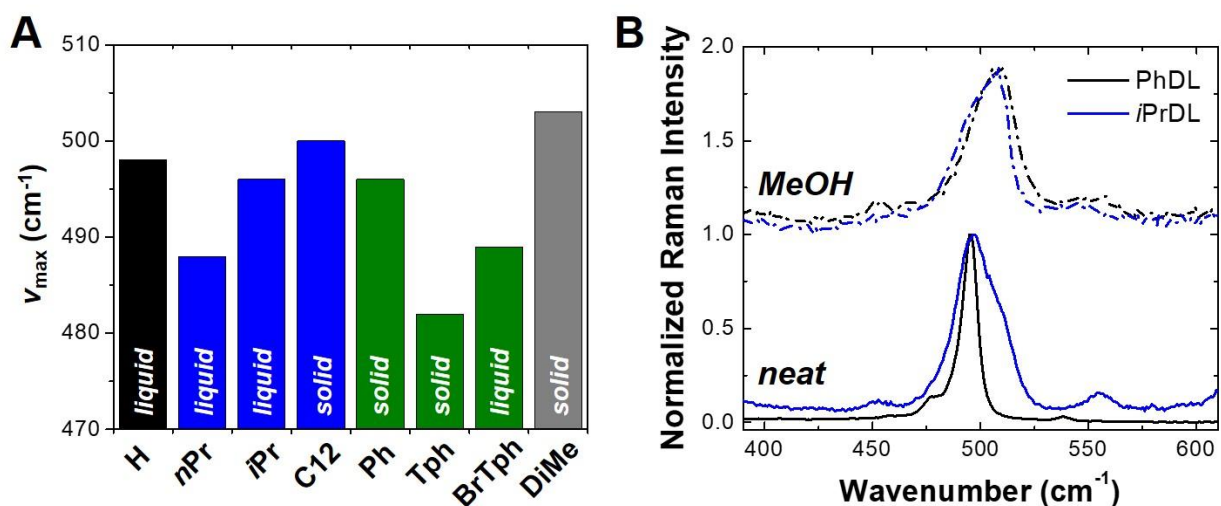


Figure S11. (A) Maximum Raman signal wavenumbers (ν_{\max}) for various 1,2-dithiolane substituents. (B) Overlaid Raman scattering spectra of **PhDL** (solid) and **iPrDL** (liquid) neat and solvated in methanol (MeOH). The shift of ν_{\max} and the change of the signal shape suggests solvation effects on the Raman scattering.

Discussion of the Raman spectroscopy results: The S–S stretching frequency (ν_{SS}) in Raman spectroscopy was suggested to depend linearly on the CSSC dihedral angle,^{15,18} which has been the subject of scientific debate.^{19–20} We found no particular trend of ν_{SS} for different substrates but instead rather scattered values in the range of 482 to 503 cm^{-1} , matching reported values¹⁵ for 1,2-dithiolanes. Furthermore, our results suggest that the physical state of the compound (i.e., solid or liquid) and chemical environment (i.e., neat or solvated) can dramatically affect the determination of ν_{SS} .

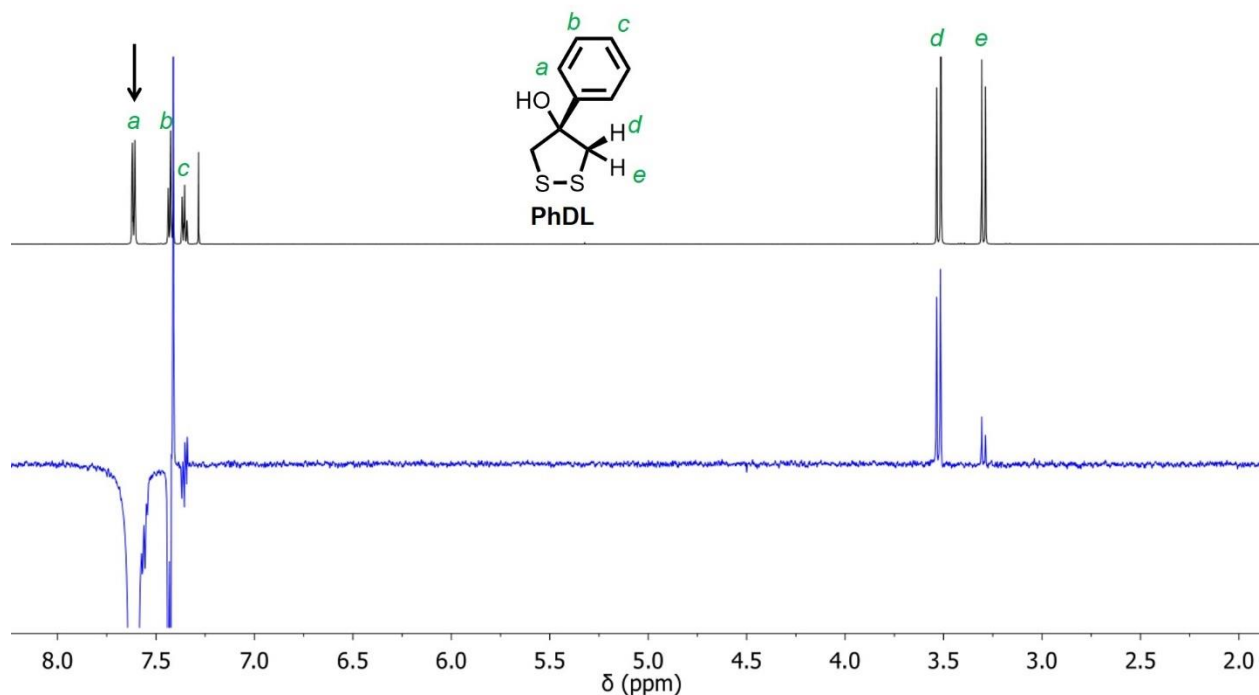


Figure S12. Methylene H-assignment of **PhDL** using NOE experiments. The more downfield proton is spatially closer to the phenyl ring. The NOE excitation is indicated with the black arrow.

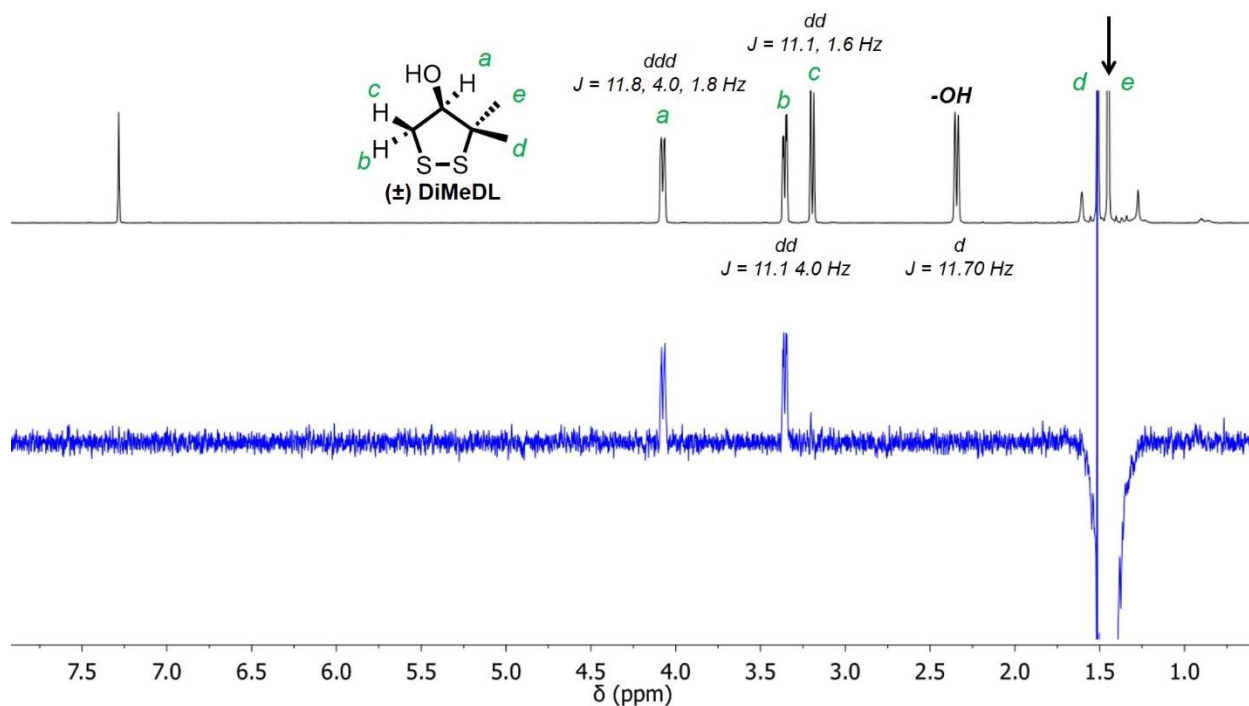


Figure S13. H-Assignment of **DiMeDL** using NOE experiments and J values. The NOE excitation is indicated with the black arrow.

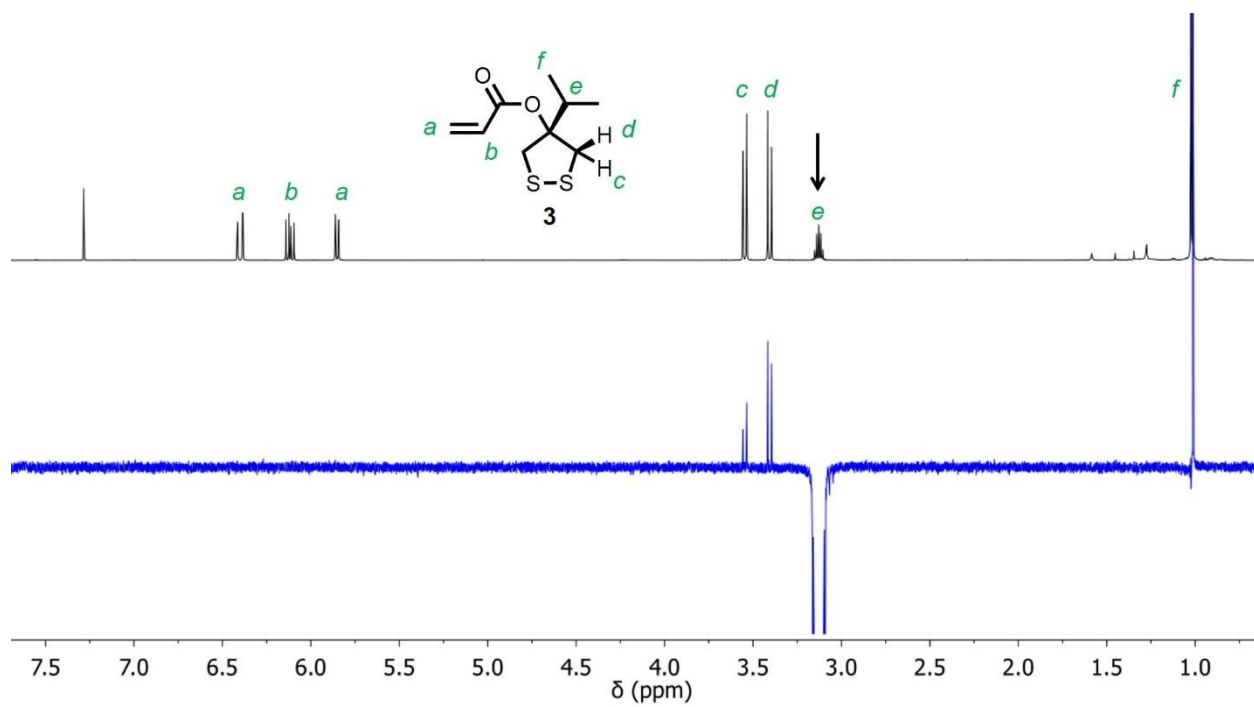


Figure S14. Methylene H-assignment of **3** using NOE experiments. The more downfield proton is spatially closer to the acrylate group. The NOE excitation is indicated with the black arrow.

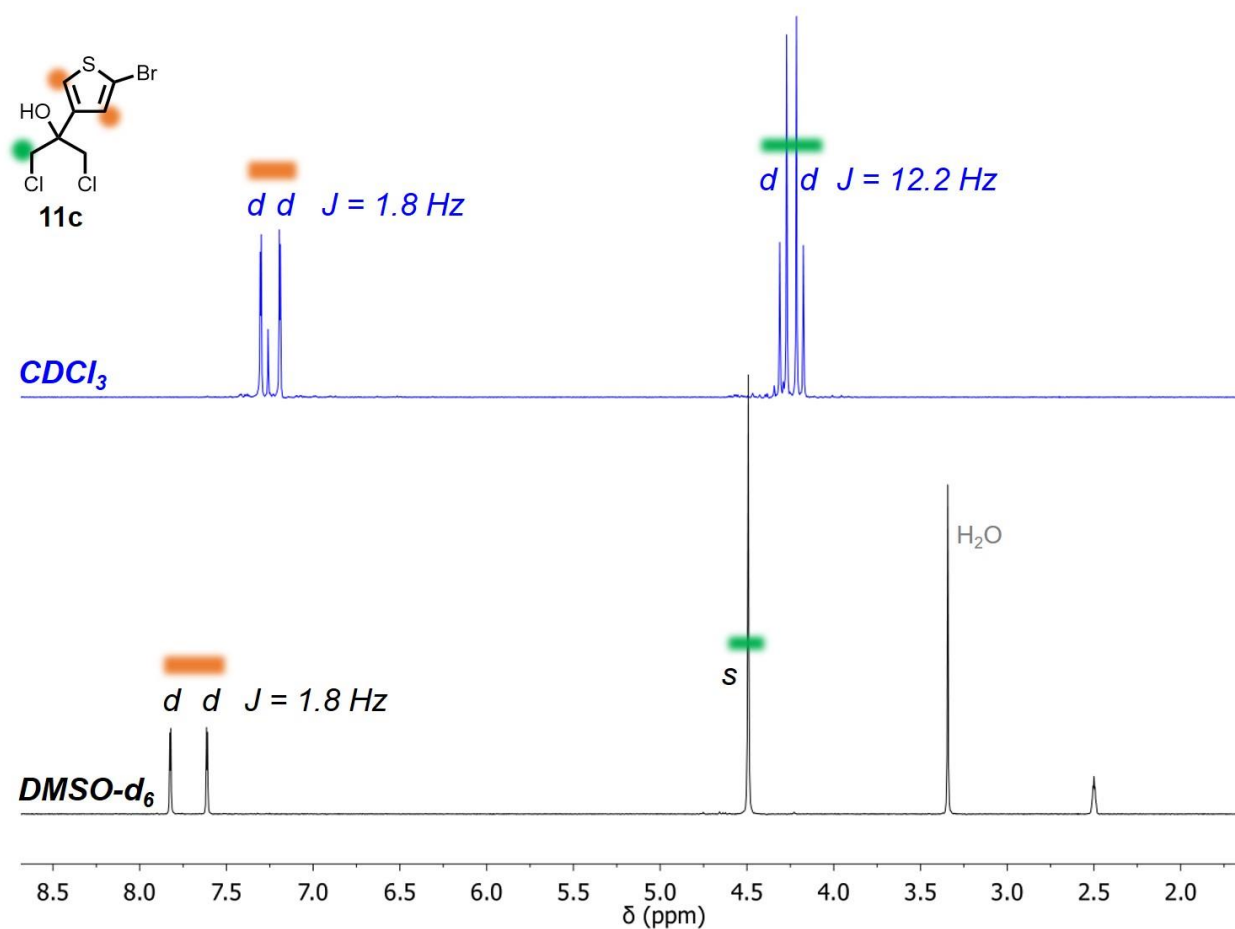
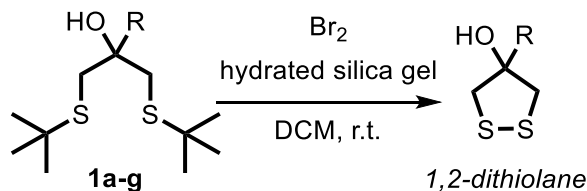


Figure S15. Investigation of the methylene proton (green) splitting into doublets observed for all symmetric 1,3-bis-*tert*-butyl thioethers and 1,3-dihalide substrates reported herein. Comparison of the ¹H NMR splitting pattern of **11c** in CDCl₃ and DMSO-*d*₆. The splitting of the methylene protons (green) into a doublet ($J = 12.2$ Hz) is likely due to intramolecular hydrogen bonding favoring one conformer, as it has been reported for β -hydroxy thioderivatives.²¹ This hypothesis is corroborated by the collapse of the two doublets into one singlet in DMSO-*d*₆, disrupting the hydrogen bonds.

S4. Synthesis of 1,2-Dithiolane Derivatives

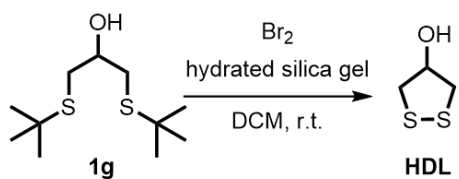
General procedure for the synthesis of the 1,2-dithiolane derivatives



Hydrated silica gel was prepared by mixing silica gel with deionized water in a 2:1 (wt/wt, silica/ H_2O) ratio until a free-flowing powder was obtained.

In a representative procedure, the 1,3-bis-*tert*-butyl thioether derivative (1 equiv.) and hydrated silica gel ($[\text{g}]_{\text{silica gel}}/[\text{mmol}]_{\text{thiol}} = 2$) were added to DCM. The total volume of DCM was adjusted to a final 1,3-bis-*tert*-butyl thioether concentration of 0.05 M. Under vigorous stirring, Br_2 (1.2–1.5 equiv., 0.3 M in DCM) was added slowly dropwise until a slightly brownish solution color persisted, which usually coincided with total disappearance of the starting material as determined by TLC analysis. The mixture was filtered through a fritted funnel and methyl acrylate (10 equiv.) was added to scavenge any adventitious thiol impurities. After stirring for 2 h, half of the DCM was evaporated and replaced with hexanes over three evaporation-dilution cycles. Importantly, the crude mixture should never be too concentrated, since this was found to easily induce polymerization. The crude mixture was then loaded in hexanes onto a silica column and the desired 1,2-dithiolane derivative was obtained after flash column chromatography.

4-Hydroxy-1,2-dithiolane (HDL)



1g	0.250 g	1.06 mmol
hydr. silica	2.1 g	
Br_2	0.237 g	1.48 mmol
DCM	22 mL	

HDL was obtained as a pale-yellow liquid after flash column chromatography on silica gel

(Et₂O/hexanes 1/2) in 52% yield (0.663 g, 0.513 mmol). **HDL** readily polymerizes upon concentration and should only be handled under dilute conditions.

$R_f \sim 0.10$ in EtOAc/hexanes (1/7)

¹H NMR (500 MHz, CDCl₃) δ 4.95 (dtt, $J = 11.1, 3.7, 1.7$ Hz, 1H), 3.20 (dd, $J = 11.6, 1.7$ Hz, 2H), 3.13 (dd, $J = 11.6, 3.8$ Hz, 2H), 2.48 (d, $J = 11.1$ Hz, OH)

¹³C NMR (125 MHz, CDCl₃) δ 75.6, 47.1

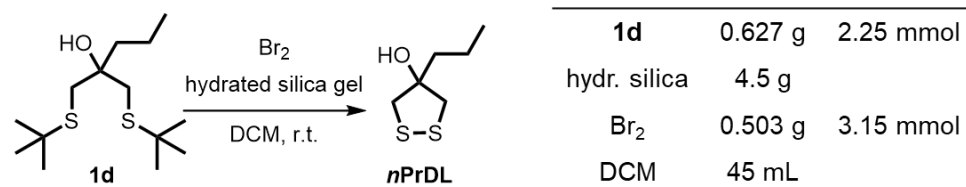
UV-vis (λ_{max} , nm; 10 mM in DMSO) 327

Raman (S–S ν_{max} , cm⁻¹; neat) 489

FTIR (ν_{max} , cm⁻¹) 3363, 3310, 2922, 2852, 1406, 1201, 1166, 1017

This compound has been reported before with ¹H and ¹³C NMR shifts in DMSO-d₆.²²

4-*n*-Propyl-4-hydroxy-1,2-dithiolane (*nPrDL*)



nPrDL was obtained as a yellow liquid after flash column chromatography on silica gel (Et₂O/hexanes 1/10) in 64% yield (0.237 g, 1.44 mmol). ***nPrDL*** readily polymerizes upon concentration and should only be handled under dilute conditions.

$R_f \sim 0.24$ in EtOAc/hexanes (1/15)

¹H NMR (500 MHz, CDCl₃) δ 3.06 (d, $J = 11.2$ Hz, 2H), 3.02 (d, $J = 11.2$ Hz, 2H), 2.95 (b, OH), 1.81 (m, 2H), 1.56 (m, 2H), 0.98 (t, $J = 7.3$ Hz, 3H)

¹³C NMR (125 MHz, CDCl₃) δ 85.3, 49.9, 40.1, 19.0, 14.7

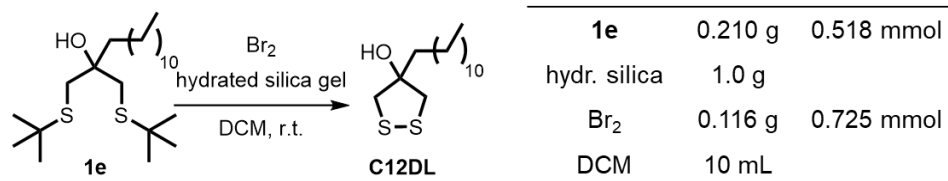
GC-EIMS: calculated 164.0, found 164.0 (HRMS in our hands did not yield sufficient ionization.)

UV-vis (λ_{max} , nm; 10 mM DMSO) 333

Raman (S–S ν_{\max} , cm^{-1} ; neat) 488

FTIR (ν_{\max} , cm^{-1}) 3442, 2958, 2928, 2871, 1465, 1378, 1342, 1207, 1029, 994, 865

4-Dodecyl-4-hydroxy-1,2-dithiolane (C12DL)



C12DL was obtained as a yellow solid after flash column chromatography on silica gel (Et_2O /hexanes 1/10) in 67% yield (0.099 g, 0.341 mmol).

$R_f \sim 0.36$ in EtOAc /hexanes (1/9)

$T_m = 43.7\text{ }^\circ\text{C}$

$^1\text{H NMR}$ (500 MHz, CDCl_3) δ 3.05 (d, $J = 11.2$ Hz, 2H), 3.02 (d, $J = 11.2$ Hz, 2H), 2.95 (s, OH), 1.82 (m, 2H), 1.52 (m, 2H), 1.29 (b, 18H), 0.88 (t, $J = 6.9$ Hz, 3H)

$^{13}\text{C NMR}$ (125 MHz, CDCl_3) δ 85.4, 49.9, 37.9, 32.1, 30.3, 29.80, 29.78, 29.71, 29.65, 29.5, 25.7, 22.8, 14.28

Crystal structure: Figure S84

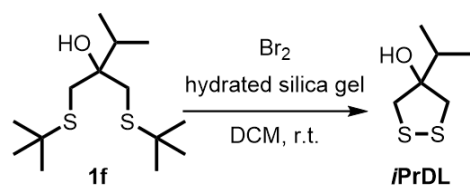
GC-EIMS: calculated 290.3, found 290.2 (HRMS in our hands did not yield sufficient ionization.)

UV-vis (λ_{\max} , nm; 10 mM in DMSO) 336

Raman (S–S ν_{\max} , cm^{-1} ; neat) 500

FTIR (ν_{\max} , cm^{-1}) 3437, 2915, 2848, 1473, 1345, 1202, 1067, 1009, 730

4-Isopropyl-4-hydroxy-1,2-dithiolane (**iPrDL**)



1f	0.423 g	1.52 mmol
hydr. silica	3.0 g	
Br_2	0.292 g	1.83 mmol
DCM	30 mL	

iPrDL was obtained as a yellow liquid after flash column chromatography on silica gel (Et_2O /hexanes 1/10) in 78% yield (0.193 g, 1.12 mmol).

$R_f \sim 0.27$ in EtOAc/hexanes (1/15)

$^1\text{H NMR}$ (500 MHz, CDCl_3) δ 3.08 (d, $J = 11.2$ Hz, 2H), 3.03 (d, $J = 11.1$ Hz, 2H), 2.85 (d, $J = 0.88$ Hz, OH), 2.02 (sept, $J = 6.8, 0.84$ Hz, 1H), 1.11 (d, $J = 6.8$ Hz, 6H)

$^{13}\text{C NMR}$ (125 MHz, CDCl_3) δ 88.1, 48.8, 35.6, 19.0

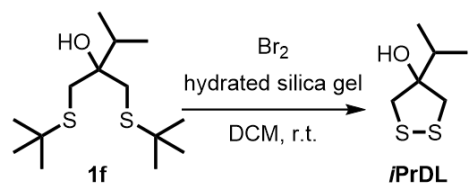
GC-EIMS: calculated 164.0, found 164.0 (HRMS in our hands did not yield sufficient ionization. However, the further functionalized products **3** and **4** were found suitable for HRMS.)

UV-vis (λ_{max} , nm; 10 mM in DMSO) 336

Raman (S–S ν_{max} , cm^{-1} ; neat) 496

FTIR (ν_{max} , cm^{-1}) 3477, 2965, 2935, 2878, 1468, 1366, 1217, 1104, 999, 874, 730

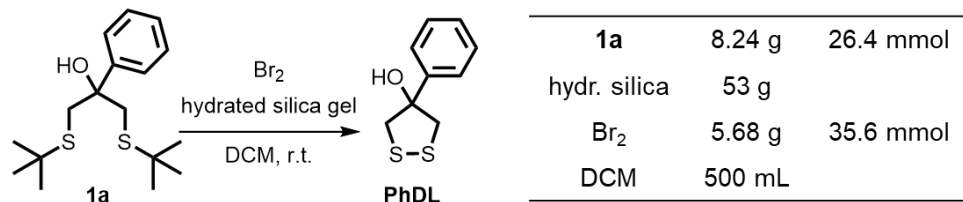
Gram-scale synthesis of 4-isopropyl-4-hydroxy-1,2-dithiolane (**iPrDL**)



1f	6.42 g	23.1 mmol
hydr. silica	46 g	
Br_2	4.79 g	30.0 mmol
DCM	460 mL	

iPrDL was obtained as a yellow liquid after flash column chromatography on silica gel (Et_2O /hexanes 1/10) in 79% yield (2.98 g, 18.2 mmol).

4-Hydroxy-4-phenyl-1,2-dithiolane (**PhDL**)



PhDL was obtained as a yellow solid after flash column chromatography on silica gel (Et_2O /hexanes 1/10) in 77% yield (0.050 g, 0.025 mmol).

$R_f \sim 0.44$ in EtOAc /hexanes (1/6)

$T_m = 60.1\text{ }^\circ\text{C}$

$^1\text{H NMR}$ (500 MHz, CDCl_3) δ 7.59 (m, 2H), 7.40 (m, 2H), 7.34 (m, 2H), 3.50 (d, $J = 11.5$ Hz, 2H), 3.49 (s, OH), 3.27 (d, $J = 11.5$ Hz, 2H)

$^{13}\text{C NMR}$ (125 MHz, CDCl_3) δ 140.2, 128.7, 120.0, 125.2, 85.3, 52.5

NOE proton assignments: Figure S12

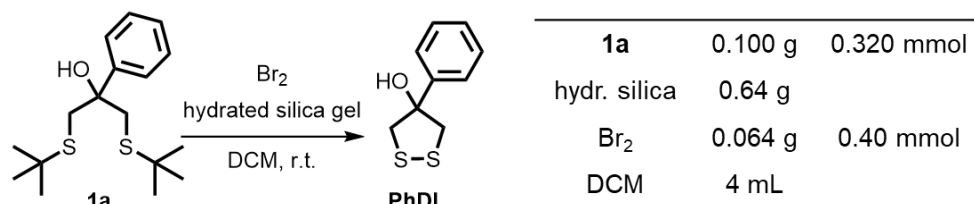
GC-EIMS: calculated 198.0, found 198.0 (HRMS in our hands did not yield sufficient ionization. However, the further functionalized product **2** was found suitable for HRMS.)

UV-vis (λ_{max} , nm; 10 mM in DMSO) 340

Raman (S–S ν_{max} , cm^{-1} ; neat) 496

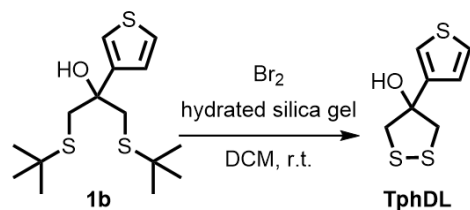
FTIR (ν_{max} , cm^{-1}) 3446, 3091, 3060, 3025, 2933, 2928, 1600, 1494, 1447, 1350, 1208, 1172, 1029, 928, 693

Gram-scale synthesis of 4-hydroxy-4-phenyl-1,2-dithiolane (**PhDL**)



PhDL was obtained as a yellow solid after flash column chromatography on silica gel (Et_2O /hexanes 1/10) in 72% yield (3.74 g, 18.9 mmol).

4-Hydroxy-4-(thiophen-3-yl)-1,2-dithiolane (**TphDL**)



1b	0.100 g	0.314 mmol
hydr. silica	0.62 g	
Br_2	0.075 g	0.47 mmol
DCM	6.3 mL	

TphDL was obtained as a yellow solid after flash column chromatography on silica gel (Et_2O /hexanes 1/10) in 75% yield (0.048 g, 0.024 mmol).

$R_f \sim 0.20$ in EtOAc/hexanes (1/9)

$T_m = 82.5^\circ\text{C}$

$^1\text{H NMR}$ (500 MHz, CDCl_3) δ 7.43 (dd, $J = 3.1, 1.4$ Hz, 1H), 7.36 (dd, $J = 5.06, 3.1$, Hz, 1H), 7.13 (dd, $J = 5.04, 1.4$ Hz, 1H) 3.44 (d, $J = 11.4$ Hz, 2H), 3.27 (d, $J = 11.4$ Hz, 2H)

$^{13}\text{C NMR}$ (125 MHz, CDCl_3) δ 141.4, 126.8, 125.1, 121.6, 84.2, 51.5

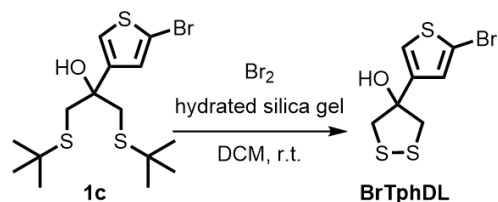
GC-EIMS: calculated 204.0, found 204.0 (HRMS in our hands did not yield sufficient ionization.)

UV-vis (λ_{max} , nm; 10 mM in DMSO) 340

Raman (S–S ν_{max} , cm^{-1} ; neat) 482

FTIR (ν_{max} , cm^{-1}) 3489, 3087, 2977, 2934, 1405, 1326, 1235, 1157, 1035, 851, 789, 725, 681, 632

4-Hydroxy-4-(5-bromothiophen-3-yl)-1,2-dithiolane (**BrTphDL**)



1c	0.250 g	0.629 mmol
hydr. silica	1.3 g	
Br_2	0.131 g	0.818 mmol
DCM	13 mL	

TphDL was obtained as a yellow oil after flash column chromatography on silica gel (Et_2O /hexanes 1/10) in 57% yield (0.102 g, 0.360 mmol).

$R_f \sim 0.30$ in EtOAc/hexanes (1/9)

$^1\text{H NMR}$ (500 MHz, CDCl_3) δ 7.32 (d, $J = 1.6$ Hz, 1H), 7.08 (d, $J = 1.7$, Hz, 1H), 3.41 (s,

OH), 3.38 (d, $J = 11.46$ Hz, 2H), 3.23 (d, $J = 11.44$ Hz, 2H)

^{13}C NMR (125 MHz, CDCl_3) δ 141.9, 128.0, 123.0, 113.5, 83.9, 51.4

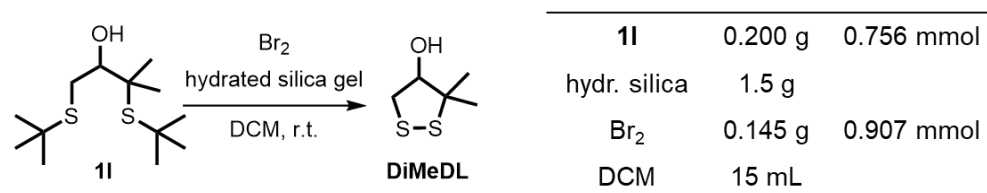
GC-EIMS: calculated 281.9 and 283.9, found 282.0 and 284.0 (HRMS in our hands did not yield sufficient ionization.)

UV-vis (λ_{max} , nm; 10 mM in DMSO) 338

Raman (S–S ν_{max} , cm^{-1} ; neat) 489

FTIR (ν_{max} , cm^{-1}) 3435, 3089, 2926, 2856, 1534, 1415, 1322, 1213, 1133, 1027, 994, 963, 868, 830, 724, 628

3,3-Dimethyl-4-hydroxy-1,2-dithiolane (DiMeDL)



DiMeDL was obtained as a yellow solid after flash column chromatography on silica gel (Et_2O /hexanes 1/3) in 85% yield (0.096 g, 0.64 mmol).

$R_f \sim 0.30$ in EtOAc /hexanes (1/9)

$T_m = 61.2$ °C

^1H NMR (500 MHz, CDCl_3) δ 4.05 (ddd $J = 11.8, 4.0, 1.6$ Hz, 1H), 3.33 (dd, $J = 11.1, 4.0$ Hz, 1H), 3.17 (dd, $J = 11.1, 1.6$ Hz, 2H), 2.32 (d, $J = 11.70$ Hz, OH), 1.49 (s, 3H), 1.43 (s, 3H)

^{13}C NMR (125 MHz, CDCl_3) δ 82.6, 64.9, 43.4, 26.5, 21.4

NOE proton assignments – Figure S13

Crystal structure – Figure S85

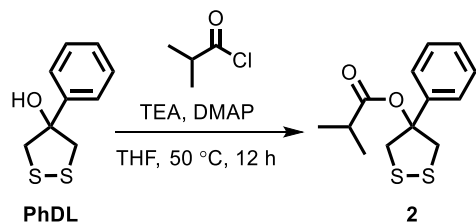
GC-EIMS: calculated 150.0, found 150.1 (HRMS in our hands did not yield sufficient ionization.)

UV-vis (λ_{max} , nm; 10 mM in DMSO) 354

Raman (ν_{\max} , cm^{-1} ; neat) 503, 522, 586

FTIR (ν_{\max} , cm^{-1}) 3273, 2970, 2914, 2854, 1466, 1378, 1311, 1117, 1037, 1002, 863

Synthesis of 4-isobutyryl-4-phenyl-1,2-dithiolane (**2**)



PhDL (0.10 g, 0.50 mmol), TEA (0.20 g, 2.0 mmol), and DMAP (0.025 g, 0.2 mmol) were dissolved in dry THF (3 mL). Under Ar, isobutyryl chloride (0.22 g, 2.0 mmol) was added dropwise. After 1 h of stirring, the reaction mixture was heated to 50 °C and stirred for another 12 h. The reaction mixture was diluted with DCM and washed with 1 M HCl, saturated aqueous NaHCO_3 and brine. After drying over MgSO_4 and evaporation of the solvent, **2** was purified via flash column chromatography on silica gel ($\text{Et}_2\text{O}/\text{hexanes} = 1/10$) to obtain the pure compound in 94% yield (0.13 g, 0.48 mmol).

$R_f \sim 0.51$ in DCM/hexanes (1/1)

$^1\text{H NMR}$ (500 MHz, CDCl_3) δ 7.37–7.27 (m, 5H), 3.75 (d, $J = 12.7$ Hz, 2H), 3.66 (d, $J = 12.7$ Hz, 2H), 2.65 (sept, $J = 6.9$ Hz, 1H), 1.21 (d, $J = 7.0$ Hz, 6H).

$^{13}\text{C NMR}$ (125 MHz, CDCl_3) δ 175.7, 141.0, 128.8, 128.1, 124.5, 92.9, 51.5, 34.5, 19.0.

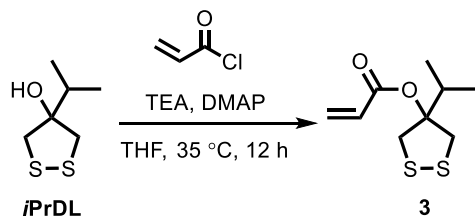
HRMS (ESI-TOF): Calculated for $[\text{M}+\text{Na}]^+$ requires 291.0498; found 291.0498.

UV-vis (λ_{\max} , nm; 10 mM in DMSO) 329

Raman (S–S ν_{\max} , cm^{-1} ; neat) 508

FTIR (ν_{\max} , cm^{-1}) 2973, 2934, 1736, 1144, 695

Synthesis of 4-acrylate-4-isopropyl-1,2-dithiolane (3)



iPrDL (1.14 g, 6.96 mmol), TEA (2.34 g, 23.1 mmol), DMAP (0.353 g, 2.89 mmol), and a small spatula tip of phenothiazine (as radical inhibitor) were dissolved in dry THF (25 mL). Under Ar, acryloyl chloride (2.09 g, 23.1 mmol) was added dropwise. After 1 h of stirring, the reaction mixture was heated to 35 °C and stirred for another 12 h. The reaction mixture was diluted with DCM and washed with 1 M HCl, saturated aqueous NaHCO₃, and brine. After drying over MgSO₄ and evaporation of the solvent, **2** was purified via flash column chromatography on silica gel (Et₂O/hexanes = 1/15) to obtain the compound in 30% yield (0.4550 g, 2.084 mmol) with 50% starting material recovery.

R_f ~ 0.43 in EtOAc/hexanes (1/15)

¹H NMR (500 MHz, CDCl₃) δ 6.38 (dd, *J* = 17.3, 1.5 Hz, 1H), 6.10 (dd, *J* = 17.3, 10.4 Hz, 1H), 5.83 (dd, *J* = 10.4, 1.5 Hz, 1H), 3.53 (d, *J* = 12.9 Hz, 2H), 3.38 (d, *J* = 12.9 Hz, 2H), 3.11 (sept, *J* = 7.0 Hz, 1H), 1.00 (d, *J* = 6.9 Hz, 6H)

¹³C NMR (125 MHz, CDCl₃) δ 165.3, 131.1, 129.3, 99.3, 47.0, 32.1, 18.3

NOE proton assignments: Figure S14

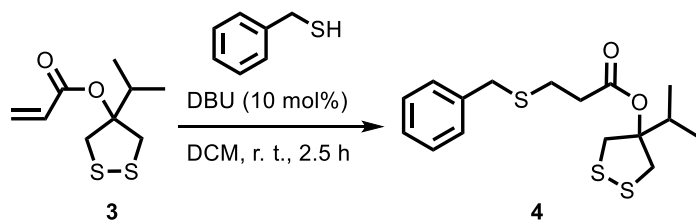
HRMS (ESI-TOF): Calculated for [M+Na]⁺ requires 241.0298; found 241.0319.

UV-vis (λ_{max}, nm; 10 mM in DMSO) 326

Raman (S–S ν_{max}, cm⁻¹; neat) 509

FTIR (ν_{max}, cm⁻¹) 2968, 2879, 1715, 1634, 1466, 1402, 1282, 1198, 1174, 1044, 974, 808

Synthesis of 4-isopropyl-1,2-dithiolan-4-yl 3-(benzylthio)propanoate (**4**)



A solution of **3** (0.050 g, 0.23 mmol) and benzyl mercaptan (0.028 g, 0.23 mmol) in DCM (2.1 mL) was purged under Ar for 10 minutes at 0 °C. Then, a solution of DBU (0.0035 g, 0.023 mmol) dissolved in DCM (0.20 mL) was added and the reaction warmed up to room temperature. After 2.5 h, the reaction was complete, as determined by the complete disappearance of the starting material by TLC. The reaction was diluted with DCM washed with 1 M aqueous HCl, brine, saturated sodium bicarbonate solution, brine, dried over MgSO₄ and passed through a silica plug to give the desired compound in 95% yield (0.0751g, 0.219 mmol).

$R_f \sim 0.21$ in EtOAc/hexanes (1/15)

¹H NMR (500 MHz, CDCl₃) δ 7.32 (m, 5H), 3.76 (s, 2H), 3.49 (d, $J = 12.8$ Hz, 2H), 3.35 (d, $J = 12.8$ Hz, 2H), 3.06 (sept, $J = 6.9$ Hz, 1H), 2.69 (t, $J = 7.2$ Hz, 2H), 2.56 (t, $J = 7.2$, 2H), 1.01 (d, $J = 6.9$ Hz, 6H)

¹³C NMR (125 MHz, CDCl₃) δ 171.1, 138.1, 129.0, 128.7, 127.2, 99.4, 46.8, 36.5, 35.4, 32.1, 26.5, 18.4

HRMS (ESI-TOF): Calculated for [M+H]⁺ requires 343.0852; found 343.0852

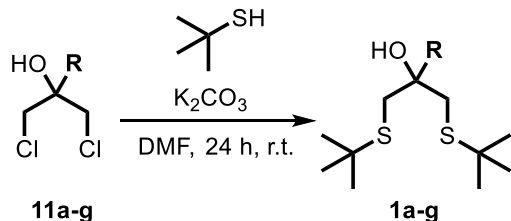
UV-vis (λ_{max} , nm; 10 mM in DMSO) 326

Raman (S–S ν_{max} , cm⁻¹; neat) 513

FTIR (ν_{max} , cm⁻¹) 2986, 2967, 2926, 2876, 1727, 1453, 1409, 1352, 1216, 1135, 984, 978, 698

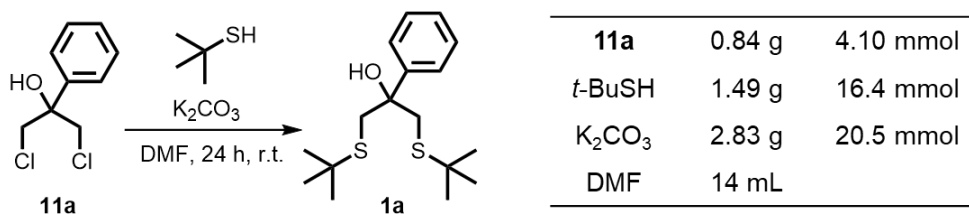
S5. Synthesis of 1,3-*tert*-Butyl Thioether Substrates

General procedure for the synthesis of *tert*-butyl thioethers 1a–g



In a representative procedure, K_2CO_3 (5 equiv) was dispersed in DMF. The total volume of DMF was adjusted to a final 1,3-dichloropropan-2-ol derivative concentration of 0.3 M. The mixture was sparged with Ar and *tert*-butylthiol (4 equiv) was added, followed by the corresponding 1,3-dichloro-2-propanol derivative (1 equiv). The mixture was stirred vigorously for 24 h, diluted with Et_2O , poured into aqueous NaOH (5 wt% in water) and extracted twice with Et_2O . The organic extract was washed with brine, aqueous 1 M HCl, water (3 times), and brine again. The solution was dried with MgSO_4 and pushed through a silica plug. After solvent evaporation, the desired compound was obtained in most cases with good purity without further column chromatography.

1,3-Bis(*tert*-butylthio)-2-phenylpropan-2-ol (**1a**)



1a was obtained as a white solid in 98% yield (1.25 g, 4.0 mmol).

$R_f \sim 0.27$ in EtOAc/hexanes (1/15)

$T_m = 50.2\text{ }^\circ\text{C}$

$^1\text{H NMR}$ (500 MHz, CDCl_3) δ 7.49 (m, 2H), 7.36 (m, 2H), 7.28 (m, 1H), 3.44 (b, OH), 3.18

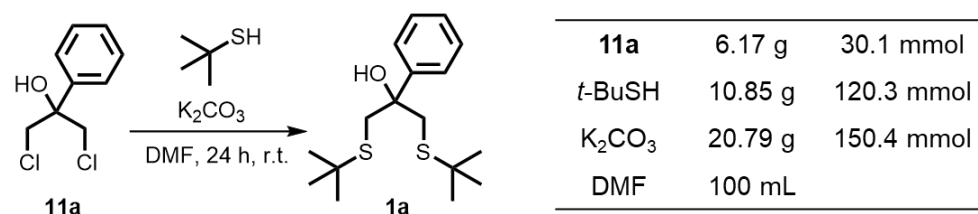
(d, $J = 12.4$ Hz, 2H), 3.06 (d, $J = 12.4$ Hz, 2H), 1.31 (s, 18H)

^{13}C NMR (125 MHz, CDCl_3) δ 144.9, 128.3, 127.4, 125.5, 74.3, 42.6, 40.8, 31.0

FTIR (ν_{max} , cm^{-1}) 3473, 3061, 2990, 2961, 2926, 2863, 1459, 1365, 1340, 1161, 1057, 1030, 735, 697

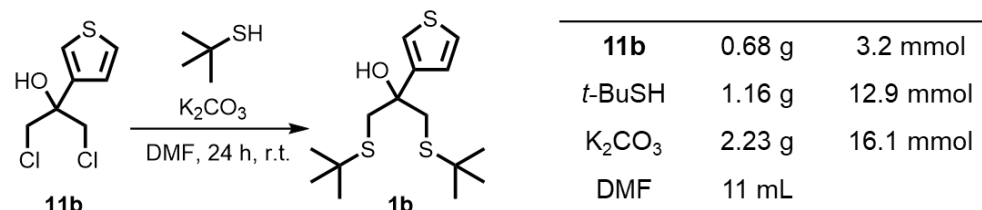
Note: The splitting of the methylene protons into a doublet is most likely due to intramolecular hydrogen bonding, strongly favoring one conformer, as it has been reported for β -hydroxy thioderivatives.²¹ Corroborating this hypothesis is the collapse of the two doublets into one singlet in the hydrogen-bonding solvent $\text{DMSO-}d_6$ shown with compound **11c** (Figure S15). This phenomenon has been observed for all 1,3-bis-tert-butyl thioethers and 1,3-dihalide substrates reported herein.

Gram-scale synthesis of 1,3-Bis(*tert*-butylthio)-2-phenylpropan-2-ol (**1a**)



In a gram-scale synthesis, **2e** was obtained as a white solid in 92% yield (8.62 g, 27.6 mmol).

1,3-Bis(*tert*-butylthio)-2-(thiophen-3-yl)propan-2-ol (**1b**)



1b was obtained as a white solid after flash column chromatography on silica gel (EtOAc/hexanes 1/9) in 74% yield (0.76 g, 2.4 mmol).

$R_f \sim 0.36$ in EtOAc/hexanes (1/9)

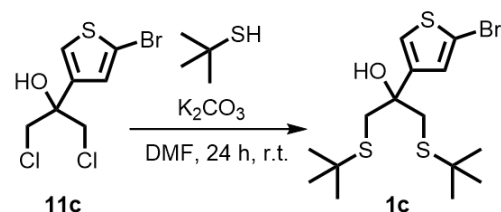
$T_m = 54.8 \text{ }^\circ\text{C}$

$^1\text{H NMR}$ (500 MHz, CDCl_3) δ 7.27 (m, 2H), 7.08 (dd, $J = 4.2, 2.2$ Hz, 1H), 3.48 (s, OH), 3.11 (d, $J = 12.4$ Hz, 2H), 3.03 (d, $J = 12.4$ Hz, 2H), 1.30 (s, 18H)

$^{13}\text{C NMR}$ (125 MHz, CDCl_3) δ 146.9, 125.9, 125.8, 121.4, 73.4, 42.7, 40.6, 31.1

FTIR (ν_{max} , cm^{-1}) 3454, 3102, 2959, 2924, 2862, 1459, 1364, 1341, 1160, 1058, 859, 800, 738, 650

1,3-Bis(*tert*-butylthio)-2-(5-bromothiophen-3-yl)propan-2-ol (**1c**)



11c	0.72 g	2.5 mmol
<i>t</i> -BuSH	0.90 g	9.9 mmol
K_2CO_3	1.71 g	12.3 mmol
DMF	8.2 mL	

1c was obtained as a white solid after flash column chromatography on silica gel (EtOAc/hexanes 1/12) in 73% yield (0.74 g, 1.9 mmol).

$R_f \sim 0.28$ in EtOAc/hexanes (1/12)

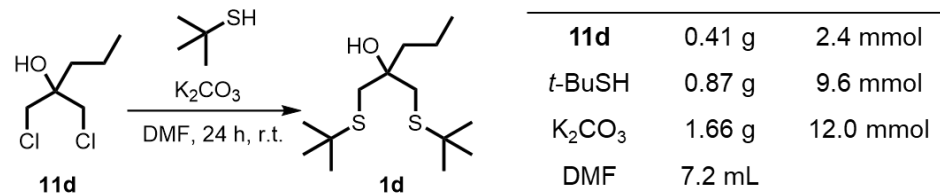
$T_m = 66.3 \text{ }^\circ\text{C}$

$^1\text{H NMR}$ (500 MHz, CDCl_3) δ 7.15 (d, $J = 1.5$ Hz, 1H), 7.03 (d, $J = 1.6$ Hz, 1H), 3.46 (s, OH), 3.04 (d, $J = 12.5$ Hz, 2H), 2.97 (d, $J = 12.5$ Hz, 2H), 1.29 (s, 18H)

$^{13}\text{C NMR}$ (125 MHz, CDCl_3) δ 147.2, 128.6, 122.9, 112.5, 73.2, 42.8, 40.3, 31.1

FTIR (ν_{max} , cm^{-1}) 3486, 3085, 2957, 2920, 2861, 1458, 1414, 1364, 1330, 1161, 1056, 973, 848, 741, 652

1,3-Bis(*tert*-butylthio)-2-*n*-propylpropan-2-ol (**1d**)



1d was obtained as a liquid in 94% yield (0.627 g, 2.25 mmol).

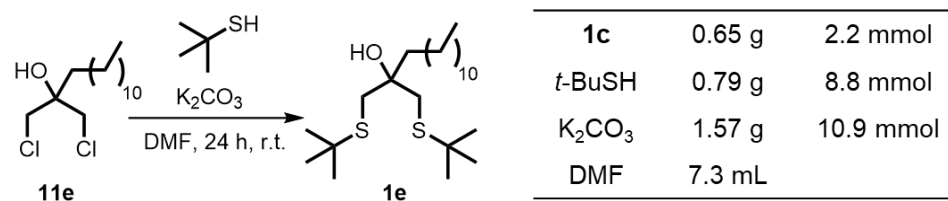
R_f ~ 0.35 in EtOAc/hexanes (1/15)

¹H NMR (500 MHz, CDCl₃) δ 2.81 (d, *J* = 12.1 Hz, 2H), 2.80 (s, OH), 2.62 (d, *J* = 12.1 Hz, 2H), 1.54 (m, 2H), 1.43 (m, 2H), 1.32 (s, 18H), 0.93 (t, *J* = 7.2 Hz, 3H)

¹³C NMR (125 MHz, CDCl₃) δ 72.7, 42.4, 41.5, 37.9, 31.1, 16.9, 14.6

FTIR (ν_{\max} , cm⁻¹) 3548, 3457, 2923, 2853, 1466, 1437, 1359, 1261, 1152, 1070, 800, 755, 733

1,3-Bis(*tert*-butylthio)-2-*n*-dodecylpropan-2-ol (**1e**)



1e was obtained as a liquid after flash column chromatography on silica gel (DCM/hexanes = 1/7 gradient to 1/1) in 98% yield (0.867 g, 2.14 mmol).

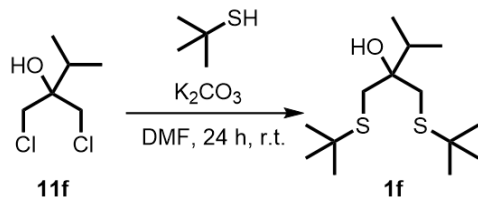
R_f ~ 0.50 in EtOAc/hexanes (1/9)

¹H NMR (500 MHz, CDCl₃) δ 2.80 (d, *J* = 12.0 Hz, 2H), 2.79 (s, OH), 2.62 (d, *J* = 12.1 Hz, 2H), 1.55 (m, 2H), 1.37 (m, 2H), 1.32 (s, 18H), 1.27 (b, 18H), 0.88 (t, *J* = 6.9 Hz, 3H)

¹³C NMR (125 MHz, CDCl₃) δ 72.7, 42.4, 39.2, 37.9, 32.1, 31.1, 30.2, 29.9, 29.79, 29.75, 29.7, 29.5, 23.6, 22.8, 14.26

FTIR (ν_{\max} , cm⁻¹) 3474, 2923, 2853, 1459, 1364, 1162

1,3-Bis(*tert*-butylthio)-2-isopropylpropan-2-ol (**1f**)



11f	0.26 g	1.5 mmol
<i>t</i> -BuSH	0.55 g	6.1 mmol
K ₂ CO ₃	1.1 g	7.6 mmol
DMF	5 mL	

1f was obtained as a liquid in 99% yield (0.42 g, 1.5 mmol).

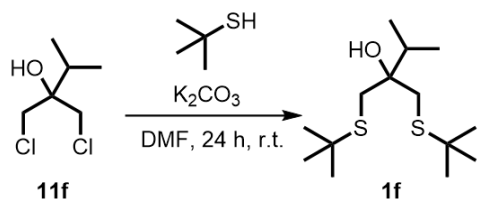
R_f ~ 0.23 in DCM/hexanes (1/1)

¹H NMR (500 MHz, CDCl₃) δ 2.82 (d, *J* = 12.3 Hz, 2H), 2.73 (s, OH), 2.71 (d, *J* = 12.3 Hz, 2H), 1.92 (sept, *J* = 6.9 Hz, 1H), 1.32 (s, 18H), 0.98 (d, *J* = 6.9 Hz, 6H)

¹³C NMR (125 MHz, CDCl₃) δ 74.2, 42.4, 36.0, 34.9, 31.1, 17.2

FTIR (*v*_{max}, cm⁻¹) 3480, 2961, 2900, 1459, 1364, 1161, 991

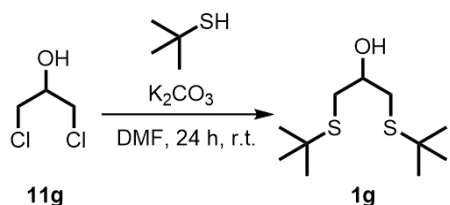
Gram-scale synthesis of 1,3-Bis(*tert*-butylthio)-2-isopropylpropan-2-ol (**1f**)



11f	4.24 g	24.8 mmol
<i>t</i> -BuSH	6.71 g	74.4 mmol
K ₂ CO ₃	13.7 g	99.1 mmol
DMF	85 mL	

In a gram-scale synthesis, **1f** was obtained as a liquid after flash column chromatography on silica gel (DCM/hexanes 1/1) in 93% yield (6.42 g, 23.1 mmol).

1,3-Bis(*tert*-butylthio)propan-2-ol (**1g**)



11g	0.50 g	3.9 mmol
<i>t</i> -BuSH	1.41 g	15.5 mmol
K ₂ CO ₃	2.68 g	19.4 mmol
DMF	12.9 mL	

1g was obtained as a liquid (solidifies at 4 °C) in 99% yield (0.917 g, 3.90 mmol).

R_f ~ 0.39 in EtOAc/hexanes (1/7)

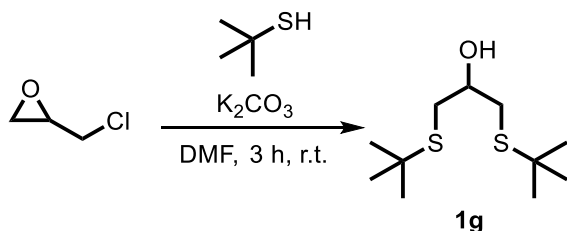
¹H NMR (500 MHz, CDCl₃) δ 3.80 (tt, *J* = 7.2, 5.2 Hz, 1H), 2.79 (dd, *J* = 12.8, 5.2 Hz, 2H), 2.68 (dd, *J* = 12.8, 7.2 Hz, 2H) 1.64 (m, 2H), 1.33 (s, 18H)

¹³C NMR (125 MHz, CDCl₃) δ 69.9, 42.7, 35.3, 31.2

FTIR (ν_{max} , cm⁻¹) 3412, 2961, 2900, 2864, 1459, 1364, 1161, 1032

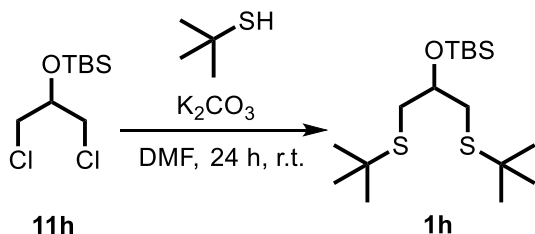
*The spectroscopic data agreed with a previous report.*²³

Alternative route to 1,3-Bis(*tert*-butylthio)propan-2-ol (**1g**)



K₂CO₃ (2.68 g, 12.4 mmol) was dispersed in DMF (13 mL). The mixture was sparged with Ar and *tert*-butylthiol (1.41 g, 15.5 mmol) was added, followed by epichlorohydrin (0.36 g, 3.9 mmol). The mixture was stirred vigorously for 3 h, diluted with Et₂O, poured into aqueous NaOH (5 wt% in water) and extracted twice with Et₂O. The organic extract was washed with brine, aqueous 1 M HCl, water (3 times), and brine again. The solution was dried with MgSO₄ and pushed through a silica plug. **1g** was obtained in 99% yield (0.92 g, 3.9 mmol).

1,3-Bis(*tert*-butylthio)-2-(*tert*-butyldimethylsiloxy)propane (**1h**)



K₂CO₃ (0.284 g, 2.06 mmol) was dispersed in DMF (1.4 mL). The mixture was sparged with Ar and *tert*-butylthiol (0.149 g, 1.64 mmol) was added, followed by **11h** (0.100 g,

0.411 mmol). The mixture was stirred vigorously for 24 h, diluted with Et₂O, poured into water and extracted twice with Et₂O. The organic extract was washed with water (3 times) and brine. The solution was dried with MgSO₄ and pushed through a silica plug. **1h** was obtained as a liquid after flash column chromatography on silica gel (DCM/hexanes 1/15) in 96% yield (0.138 g, 0.393 mmol). (*Note: The same reaction conditions with the TMS-protected substrate resulted in substantial deprotection*)

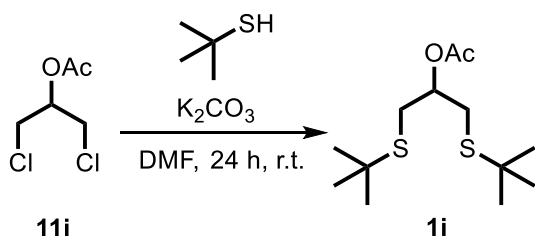
$R_f \sim 0.46$ in EtOAc/hexanes (1/30)

¹H NMR (500 MHz, CDCl₃) δ 3.89 (tt, $J = 6.4, 5.4$ Hz, 1H), 2.81 (dd, $J = 12.6, 6.4$ Hz, 2H), 2.61 (dd, $J = 12.6, 5.4$ Hz, 2H) (m, 2H), 1.31 (s, 18H), 0.90 (s, 9H), 0.11 (s, 6H)

¹³C NMR (125 MHz, CDCl₃) δ 73.0, 42.2, 35.1, 31.2, 26.1, 18.3, -4.2

FTIR (ν_{\max} , cm⁻¹) 2957, 2928, 2858, 1460, 1364, 1254, 1162, 1083, 1054, 912, 835, 774

1,3-Bis(*tert*-butylthio)-2-acetoxypropane (**1i**)



K₂CO₃ (1.01 g, 7.31 mmol) was dispersed in DMF (4.9 mL). The mixture was sparged with Ar and *tert*-butylthiol (0.531 g, 5.85 mmol) was added, followed by **11i** (0.250 g, 1.46 mmol). The mixture was stirred vigorously for 24 h, diluted with Et₂O, poured into aqueous NaOH (5 wt% in water) and extracted twice with Et₂O. The organic extract was washed with brine, aqueous 1 M HCl, water (3 times), and brine again. The solution was dried with MgSO₄ and pushed through a silica plug. **1i** was obtained as a liquid in 86% yield (0.350 g, 1.26 mmol).

$R_f \sim 0.47$ in EtOAc/hexanes (1/7)

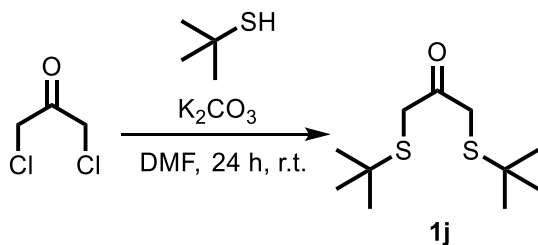
¹H NMR (500 MHz, CDCl₃) δ 5.01 (p, $J = 6.2$ Hz, 1H), 2.86 (dd, $J = 13.3, 6.3$ Hz, 2H),

2.77 (dd, $J = 13.3, 6.0$ Hz, 2H), 2.07 (s, 3H), 1.33 (s, 18H)

^{13}C NMR (125 MHz, CDCl_3) δ 170.0, 71.9, 42.5, 20.9

FTIR (ν_{max} , cm^{-1}) 2960, 2900, 2863, 1739, 1460, 1366, 1234, 1162, 1022

1,3-Bis(*tert*-butylthio)acetone (**1j**)



K_2CO_3 (2.72 g, 19.7 mmol) was dispersed in DMF (13.1 mL). The mixture was sparged with Ar and *tert*-butylthiol (1.43 g, 15.8 mmol) was added, followed by 1,3-dichloroacetone (0.50 g, 3.9 mmol). The mixture was stirred vigorously for 24 h, diluted with Et_2O , poured into aqueous NaOH (5 wt% in water) and extracted twice with Et_2O . The organic extract was washed with brine, aqueous 1 M HCl, water (3 times), and brine again. The solution was dried with MgSO_4 and pushed through a silica plug. **1j** was obtained as a liquid in 66% yield (0.61 g, 2.6 mmol).

$R_f \sim 0.54$ in EtOAc/hexanes (1/9)

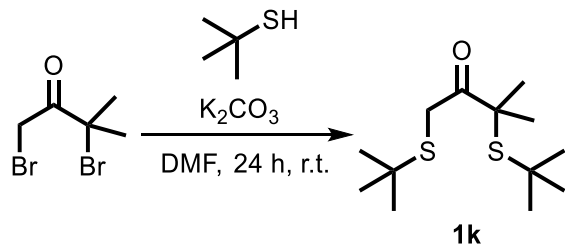
^1H NMR (500 MHz, CDCl_3) δ 3.55 (s, 4H), 1.32 (s, 18H)

^{13}C NMR (125 MHz, CDCl_3) δ 204.9, 43.7, 37.2, 30.9

FTIR (ν_{max} , cm^{-1}) 2962, 2901, 2865, 1705, 1459, 1392, 1365, 1248, 1161, 1068

*The compound has been reported before, albeit without spectroscopic data.*²⁴

1,3-Bis(*tert*-butylthio)-3-methylbutan-2-one (**1k**)



K_2CO_3 (2.83 g, 20.5 mmol) was dispersed in DMF (13.7 mL). The mixture was sparged with Ar and *tert*-butylthiol (1.49 g, 16.4 mmol) was added, followed by 1,3-dibromo-3-methylbutan-2-one (1.00 g, 4.10 mmol). The mixture was stirred vigorously for 24 h, diluted with Et_2O , poured into water and extracted twice with Et_2O . The organic extract was washed with water (3 times) and brine. The solution was dried with $MgSO_4$ and pushed through a silica plug. **1k** was obtained as a solid after flash column chromatography on silica gel (DCM/hexanes 1/17 gradient to 1/10) in 63% yield (0.68 g, 2.6 mmol).

$R_f \sim 0.25$ in DCM/hexanes (1/17)

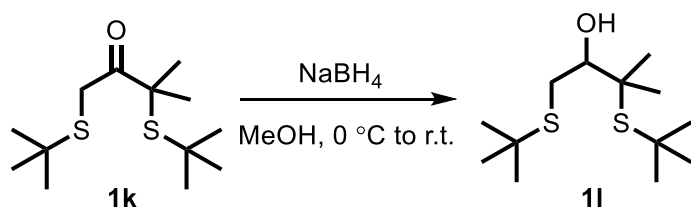
$T_m = 56.0\text{ }^\circ C$

1H NMR (500 MHz, $CDCl_3$) δ 3.90 (s, 2H), 1.52 (s, 6H), 1.35 (s, 9H), 1.31 (s, 9H)

^{13}C NMR (125 MHz, $CDCl_3$) δ 207.0, 55.3, 47.0, 42.7, 33.7, 32.4, 30.9, 26.8

FTIR (ν_{max} , cm^{-1}) 2961, 2922, 2894, 2861, 1696, 1456, 1366, 1155, 1050

1,3-Bis(*tert*-butylthio)-3-methylbutan-2-ol (**1l**)



$NaBH_4$ (0.044 g, 1.16 mmol) was added to a solution of **1k** (0.608 g, 2.32 mmol) in MeOH (10 mL) at $0\text{ }^\circ C$. After 2 h, the reaction was diluted with DCM and washed with aqueous

1 M HCl, water and brine, followed by drying with MgSO₄. After flash column chromatography on silica gel (EtOAc/hexanes = 1/20), **11** was obtained as a colorless oil in 67% yield (0.413 g, 1.56 mmol).

R_f ~ 0.34 in EtOAc/hexanes (1/20)

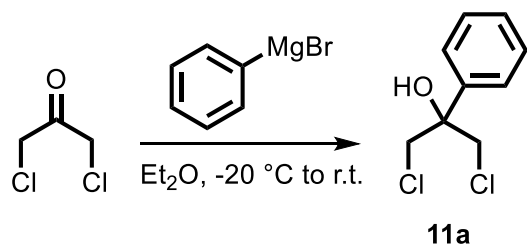
¹H NMR (500 MHz, CDCl₃) δ 3.73 (ddd, *J* = 10.0, 2.3, 2.2 Hz, 1H), 3.09 (dd, *J* = 2.1, 1.0 Hz, OH), 2.95 (ddd, *J* = 12.6, 2.4, 1.0 Hz, 1H), 2.59 (dd, *J* = 12.6, 10.0 Hz, 1H), 1.49 (s, 3H), 1.44 (s, 9H), 1.36 (s, 3H), 1.35 (s, 9H)

¹³C NMR (125 MHz, CDCl₃) δ 76.3, 54.6, 46.8, 42.5, 33.5, 31.19, 31.16, 26.7, 25.8

FTIR (ν_{max}, cm⁻¹) 3473, 2962, 2899, 2865, 1459, 1363, 1161, 1116, 1063, 984

S6. Starting Material Synthesis

Synthesis of 1,3-dichloro-2-phenylpropan-2-ol (**11a**)



Mg turnings (0.460 g, 18.9 mmol) were placed into a flame-dried three-neck round bottom flask, equipped with an addition funnel and a reflux condenser under Ar atmosphere. Et₂O (5 mL) was added, followed by ~25% of the total bromobenzene amount (2.97 g, 18.9 mmol). The reaction mixture was gently heated until the Grignard reaction started, upon which the remaining bromobenzene was added dropwise in Et₂O (13 mL), maintaining a smooth reflux of the reaction mixture. After the complete addition, the mixture was refluxed for 1 h and cooled to -20 °C in a NaCl/ice bath. 1,3-Dichloroacetone (2.00 g, 15.8 mmol) in dry Et₂O (20 mL) was added dropwise. Upon complete addition, the mixture warmed up to room temperature over 4 h. The reaction was quenched with saturated

aqueous NH_4Cl and extracted twice with Et_2O . The combined organic extracts were washed with brine and dried over MgSO_4 . Upon evaporation of the solvent, the product was purified via flash column chromatography on silica gel ($\text{DCM}/\text{hexanes} = 1/1$). **11a** was obtained as a colorless liquid in 90% yield (2.90 g, 14.17 mmol).

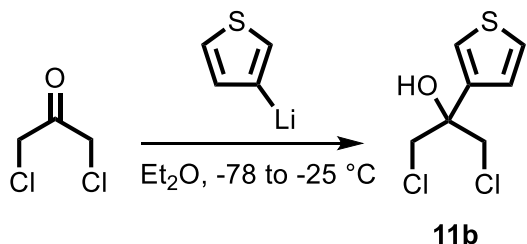
$R_f \sim 0.32$ in $\text{DCM}/\text{hexanes} (1/1)$

$^1\text{H NMR}$ (500 MHz, CDCl_3) δ 7.50 (m, 2H), 7.41 (m, 2H), 7.36 (m, 1H), 3.98 (d, $J = 11.6$ Hz, 2H), 3.93 (d, $J = 11.6$ Hz, 2H), 2.89 (s, OH)

$^{13}\text{C NMR}$ (125 MHz, CDCl_3) δ 140.2, 128.7, 128.5, 125.8, 75.6, 50.8

FTIR (ν_{max} , cm^{-1}) 3540, 3469, 3063, 3031, 2961, 1496, 1449, 1357, 1251, 1176, 1070, 1032, 774, 725, 696, 593

Synthesis of 1,3-dichloro-2-(thiophen-3-yl)propan-2-ol (**11b**)



$n\text{-BuLi}$ (2.5 M in hexanes, 2.70 ml, 6.75 mmol) was added to 3-bromothiophene (1.00 g, 6.14 mmol) in Et_2O (15 mL) at -78 °C under Ar. After 2 h, still at -78 °C, 1,3-dichloroacetone (0.858 g, 6.75 mmol) in Et_2O (13 mL) was added dropwise. After 4 h at -78 °C, the mixture slowly warmed up to -25 °C, upon which we quenched the reaction with saturated aqueous NH_4Cl and extracted twice with Et_2O . The combined organic extracts were washed with brine and dried over MgSO_4 . Upon evaporation of the solvent, the product was purified via flash column chromatography on silica gel ($\text{DCM}/\text{hexanes} = 1/1$). **11b** was obtained as a liquid in 70% yield (0.90 g, 4.3 mmol).

$R_f \sim 0.32$ in $\text{EtOAc}/\text{hexanes} (1/9)$

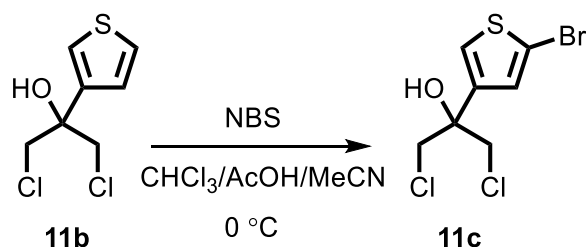
$^1\text{H NMR}$ (500 MHz, CDCl_3) δ 7.41 (dd, $J = 3.1, 1.4$ Hz, 1H), 7.35 (dd, $J = 5.1, 3.1$ Hz, 1H),

7.14 (dd, $J = 5.1, 1.4$ Hz, 1H), 3.95 (d, $J = 11.4$ Hz, 2H), 3.89 (d, $J = 11.4$ Hz, 2H), 2.90 (b, OH)

$^{13}\text{C NMR}$ (125 MHz, CDCl_3) δ 140.2, 128.7, 128.5, 125.8, 75.6, 50.8

FTIR (ν_{max} , cm^{-1}) 3534, 3457, 3110, 2962, 1431, 1338, 1260, 1162, 1087, 1054, 865, 790, 733, 641, 595

Synthesis of 1,3-dichloro-2-(5-bromothiophen-3-yl)propan-2-ol (**11c**)



11b (0.920 g, 4.36 mmol) was dissolved in CHCl_3 (4.0 mL) and acetic acid (AcOH; 1.8 mL). *N*-Bromosuccinimide (NBS; 0.854 g, 4.79 mmol) was added at $0\text{ }^\circ\text{C}$, followed by acetonitrile (MeCN; 0.75 mL). After stirring for 7 h at $0\text{ }^\circ\text{C}$, the mixture was diluted with Et_2O , washed with aqueous $\text{Na}_2\text{S}_2\text{O}_3$ and brine. The solution was dried over MgSO_4 and the solvent was evaporated. The product was purified via flash column chromatography on silica gel (EtOAc/hexanes = 1/9). **11c** was obtained as a liquid in 58% yield (0.73 g, 2.5 mmol).

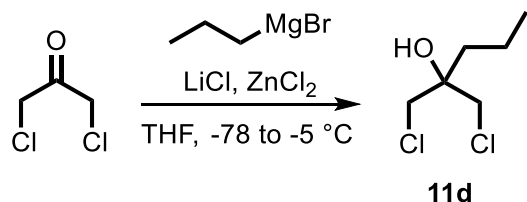
$R_f \sim 0.23$ in EtOAc/hexanes (1/9)

$^1\text{H NMR}$ (500 MHz, CDCl_3) δ 7.30 (d, $J = 1.8$ Hz, 1H), 7.19 (d, $J = 1.8$ Hz, 1H), 4.29 (d, $J = 11.7$ Hz, 2H), 4.20 (d, $J = 11.7$ Hz, 2H)

$^{13}\text{C NMR}$ (125 MHz, CDCl_3) δ 140.4, 129.8, 124.9, 113.8, 62.7, 49.4

FTIR (ν_{max} , cm^{-1}) 3107, 2954, 2921, 2852, 1420, 1195, 1163, 981, 941, 874, 828, 740, 650, 609

1,3-Dichloro-2-*n*-propylpropan-2-ol (**11d**)



The Synthesis of **11d** was accomplished via a modified protocol of Hatano *et al.*²⁵⁻²⁶ LiCl (0.429 g, 9.76 mmol) was placed in a flame-dried Schlenk flask and dried with a heat gun under vacuum. Pre-dried Mg turnings (0.255 g, 10.5 mmol) and THF (2 mL) were added under Ar, followed by ~25% of the total 1-bromopropane amount (1.20 g, 9.27 mmol) to start the Grignard reaction. The remaining 1-bromopropane was added dropwise in THF (4 mL) over 30 min. After the reaction was stirred for another 10 min, it was placed in an oil bath at 45 °C for 20 min. ZnCl₂ (0.205 g, 1.50 mmol) was melt-dried with a heat gun under vacuum in a two-neck round bottom flask. After cooling to room temperature, the Grignard solution was added to the dry ZnCl₂, stirred for 15 min, and placed in a dry ice/acetone bath at -78 °C. 1,3-Dichloroacetone (0.953 g, 7.51 mmol) in THF (6 mL) was added dropwise, and the mixture was left to stir at -78 °C. After 5 h, we stopped replenishing dry ice and the reaction slowly warmed up in the cooling bath to -5 °C over 8 h. The resulting mixture was quenched with saturated aqueous NH₄Cl and extracted twice with Et₂O. The combined organic extracts were washed with brine and dried over MgSO₄. Upon evaporation of the solvent, the product was purified via flash column chromatography on silica gel (EtOAc/hexanes = 1/9). **11d** was obtained as a colorless liquid in 42% yield (0.540 g, 3.16 mmol). (*Note: the main impurity in this reaction was identified as 1,3-dichloro-2-propanol, presumably from an undesired hydride addition to 1,3-dichloroacetone.*)

R_f ~ 0.31 in EtOAc/hexanes (1/9); product stains very faintly with KMnO₄

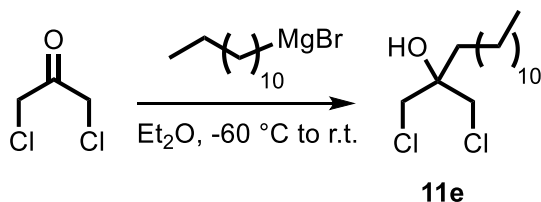
¹H NMR (500 MHz, CDCl₃) δ 3.66 (d, *J* = 11.2 Hz, 2H), 3.58 (d, *J* = 11.2 Hz, 2H), 2.26 (s,

OH), 1.64 (m, 2H), 1.45 (m, 2H), 0.97 (t, $J = 7.3$ Hz, 3H)

^{13}C NMR (125 MHz, CDCl_3) δ 73.8, 48.4, 37.2, 16.1, 14.4

FTIR (ν_{max} , cm^{-1}) 3533, 3443, 2962, 2875, 1436, 1159, 1018, 799, 756, 737

1,3-Dichloro-2-*n*-dodecylpropan-2-ol (**11e**)



The procedure for the synthesis of **11e** was adapted from Pugia *et al.*²⁷ Mg turnings (0.230 g, 9.45 mmol) were placed into a flame-dried three-neck round bottom flask, equipped with an addition funnel and a reflux condenser under Ar atmosphere. Et₂O (3 mL) was added, followed by ~25% of the total 1-bromododecane amount (2.36 g, 9.45 mmol). The reaction mixture was gently heated until the Grignard reaction started, upon which the remaining 1-bromododecane was added dropwise in Et₂O (7 mL), maintaining a smooth reflux of the reaction mixture. After the complete addition, the mixture was refluxed for 1 h and cooled to -60 °C in a CHCl_3 /liquid N_2 slush bath. 1,3-Dichloroacetone (1.00 g, 7.88 mmol) in dry Et₂O (10 mL) was added dropwise. Upon complete addition, the mixture warmed up to room temperature over 6 h. The reaction was quenched with saturated aqueous NH_4Cl and extracted twice with Et₂O. The combined organic extracts were washed with brine and dried over MgSO_4 . Upon evaporation of the solvent, the product was purified via flash column chromatography on silica gel (EtOAc/hexanes = 1/11). **11e** was obtained as a colorless liquid (solidifies at 4 °C) in 41% yield (0.960 g, 3.23 mmol).

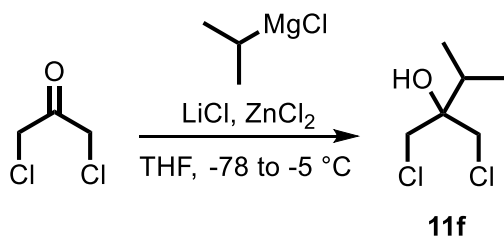
$R_f \sim 0.41$ in EtOAc/hexanes (1/9)

^1H NMR (500 MHz, CDCl_3) δ 3.66 (d, $J = 11.2$ Hz, 2H), 3.58 (d, $J = 11.2$ Hz, 2H), 2.26 (s, OH), 1.65 (m, 2H), 1.40 (m, 2H), 1.28 (b, 18H), 0.88 (t, $J = 6.9$ Hz, 3H)

^{13}C NMR (125 MHz, CDCl_3) δ 73.9, 48.5, 35.1, 32.1, 30.0, 29.8, 29.8, 29.8, 29.7, 29.6, 22.9, 22.8, 14.3

FTIR (ν_{max} , cm^{-1}) 3477, 2959, 2928, 2871, 1459, 1364, 1162, 999

1,3-Dichloro-2-isopropylpropan-2-ol (11f)



The Synthesis of **11f** was accomplished via a modified protocol of Hatano *et al.*²⁵⁻²⁶ LiCl (2.53 g, 59.7 mmol) was placed in a flame-dried Schlenk flask and dried with a heat gun under vacuum. Pre-dried Mg turnings (1.59 g, 65.6 mmol), a small grain of I_2 and THF (20 mL) were added under Ar, followed by ~25% of the total 2-chloropropane amount (4.69 g, 59.7 mmol) to start the Grignard reaction. The remaining 2-chloropropane was added dropwise in THF (40 mL) for 60 min. After the reaction was stirred for another 10 min, it was placed in an oil bath at 45 °C for 20 min. ZnCl_2 (0.581 g, 4.26 mmol) was melt-dried with a heat gun under vacuum in a two-neck round bottom flask. After cooling to room temperature, the Grignard solution -78 °C. 1,3-Dichloroacetone (5.41 g, 42.6 mmol) in THF (12 mL) was added dropwise, and the mixture was left to stir at -78 °C. After 5 h, we stopped replenishing dry ice and the reaction slowly warmed up in the cooling bath to -5 °C over 8 h. The resulting mixture was quenched with saturated aqueous NH_4Cl and extracted twice with Et_2O . The combined organic extracts were washed with brine and dried over MgSO_4 . Upon evaporation of the solvent, the product was purified via flash column chromatography on silica gel ($\text{EtOAc}/\text{hexanes} = 1/9$). **11f** was obtained as a colorless liquid in 58% yield (4.24 g, 24.8 mmol).

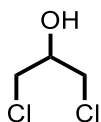
$R_f \sim 0.42$ in EtOAc/hexanes (1/9); product stains very faintly with KMnO_4

$^1\text{H NMR}$ (500 MHz, CDCl_3) δ 3.72 (s, 4H), 2.15 (m, 2H), 1.01 (d, $J = 6.9$ Hz, 6H)

$^{13}\text{C NMR}$ (125 MHz, CDCl_3) δ 75.0, 47.6, 31.4, 16.6

FTIR (ν_{max} , cm^{-1}) 3551, 3479, 2971, 2883, 1470, 1438, 1369, 1173, 1005, 836, 772, 738, 707

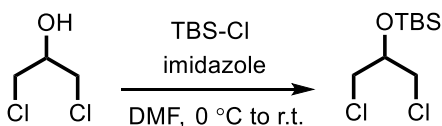
1,3-Dichloropropan-2-ol (11g)



11g

11g is commercially available and was purchased from Acros Organics.

Synthesis of 1,3-dichloro-2-(tert-butyldimethylsiloxy)propane (11h)



11g

11h

11h was synthesized according to Axenrod *et al.*²⁸ After flash column chromatography on silica gel (EtOAc/hexanes = 1/12), we obtained the product as a colorless liquid in 78% yield (0.73 g, 3.0 mmol).

$R_f \sim 0.82$ in EtOAc/hexanes (1/12)

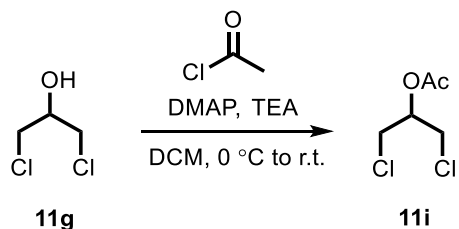
$^1\text{H NMR}$ (500 MHz, CDCl_3) δ 4.03 (p, $J = 5.6$ Hz, 1H), 3.62 (dd, $J = 11.3, 5.6$ Hz, 2H), 3.56 (dd, $J = 11.3, 5.0$ Hz, 2H), 0.90 (s, 9H), 0.12 (s, 6H)

$^{13}\text{C NMR}$ (125 MHz, CDCl_3) δ 72.4, 46.0, 25.8, 18.2, -4.6

FTIR (ν_{max} , cm^{-1}) 2955, 2930, 2858, 1472, 1253, 1108, 1077, 932, 835, 776

*The spectroscopic data matched the original report.*²⁸

Synthesis of 1,3-dichloro-2-acetoxypropane



1,3-Dichloro-2-propanol (1.00 g, 7.75 mmol), triethylamine (TEA; 1.57 g, 15.5 mmol), and 4-(dimethylamino)pyridine (DMAP; 0.189 g, 1.55 mmol) were combined in DCM (38 mL) under Ar. At 0 °C, acetyl chloride (1.22 g, 15.5 mmol) was added dropwise. The reaction was left to warm up to room temperature over 10 h. Then, the mixture was diluted with DCM, and washed with aqueous 1 M HCl, saturated aqueous NaHCO₃, and brine. The organic extract was dried over MgSO₄ and the solvent was evaporated. The product was purified via flash column chromatography on silica gel (EtOAc/hexanes = 1/9). 1,3-Dichloro-2-acetoxypropane was obtained as a colorless liquid in 80% yield (1.06 g, 6.20 mmol).

$R_f \sim 0.43$ in EtOAc/hexanes (1/7)

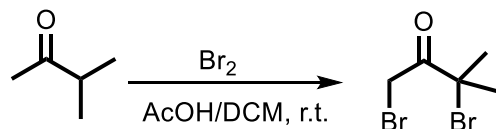
¹H NMR (500 MHz, CDCl₃) δ 5.18 (p, $J = 5.2$ Hz, 1H), 3.75 (m, 4H), 2.13 (s, 3H)

¹³C NMR (125 MHz, CDCl₃) δ 170.0, 71.9, 42.5, 20.9

FTIR (ν_{\max} , cm⁻¹) 2970, 1743, 1432, 1373, 1210, 1036, 935, 872, 758, 705

The spectroscopic data agreed with a previous report.²⁹

Synthesis of 1,3-dibromo-3-methylbutan-2-one



Br₂ (37.1 g, 232 mmol) in DCM (60 mL) was added to a mixture of 3-methyl-2-butanone (10.0 g, 116 mmol) and AcOH (1 mL) at room temperature (water bath) over 4 h. The

reaction was left to stir overnight and worked up by washing with aqueous $\text{Na}_2\text{S}_2\text{O}_3$ and brine. We obtained 1,3-dibromo-3-methylbutan-2-one as a liquid after distillation under reduced pressure (the product distilled over at an oil bath temperature of $80\text{ }^\circ\text{C}$) in 66% yield (18.5 g, 76.1 mmol).

$^1\text{H NMR}$ (500 MHz, CDCl_3) δ 4.44 (s, 2H), 1.94 (s, 6H)

$^{13}\text{C NMR}$ (125 MHz, CDCl_3) δ 196.8, 62.7, 30.0, 29.9

FTIR (ν_{max} , cm^{-1}) 2978, 2931, 1724, 1455, 1372, 1104, 1046

*The spectroscopic data agreed with a previous report.*³⁰

S7. NMR Spectra and Additional Characterizations

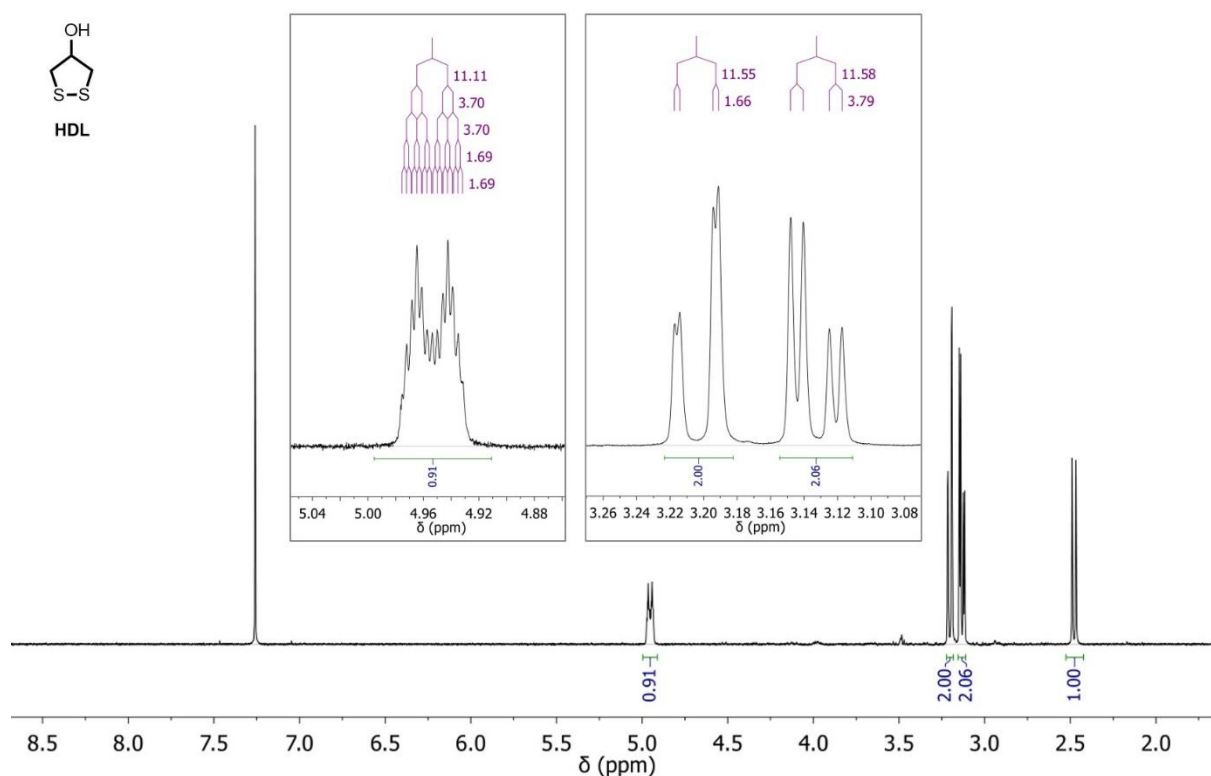


Figure S16. $^1\text{H NMR}$ spectrum of **HDL** in CDCl_3 .

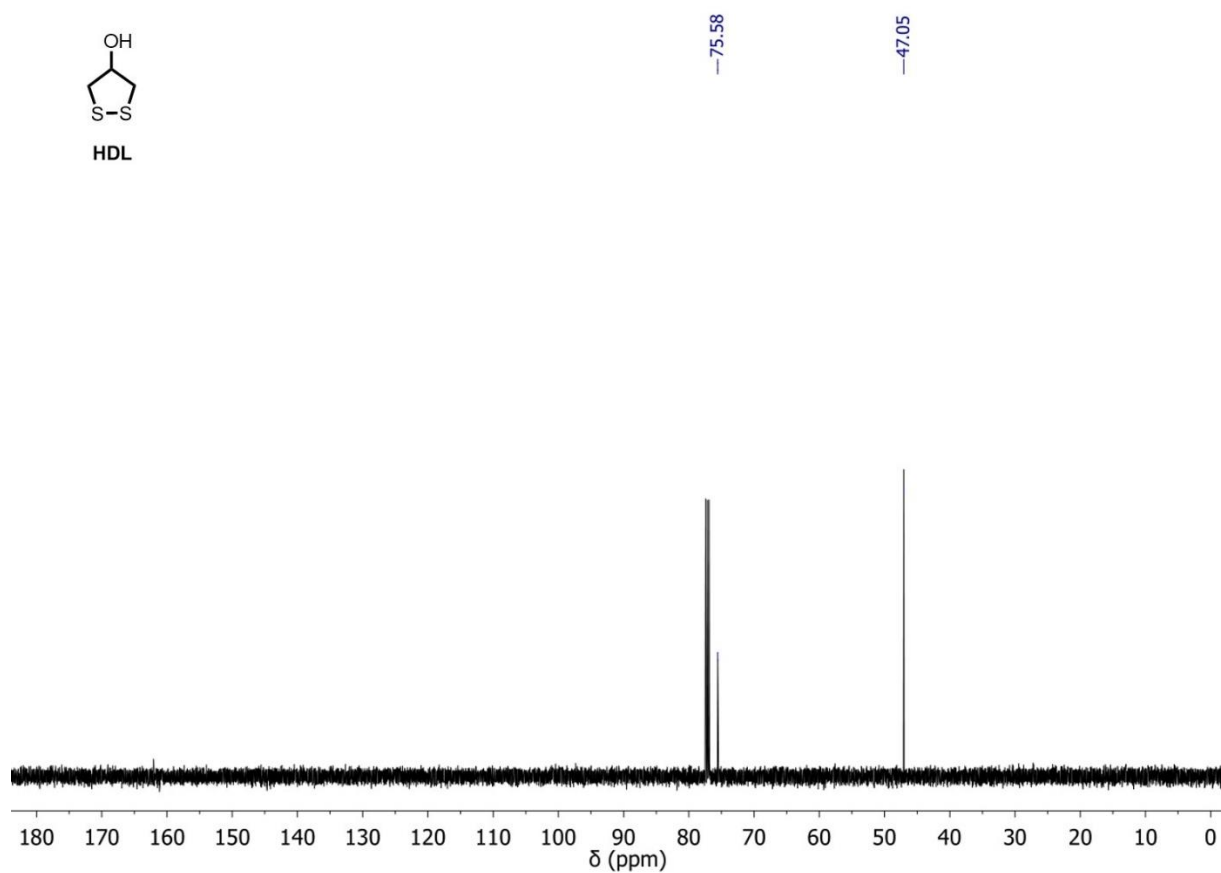


Figure S17. ^{13}C NMR spectrum of **HDL** in CDCl_3 .

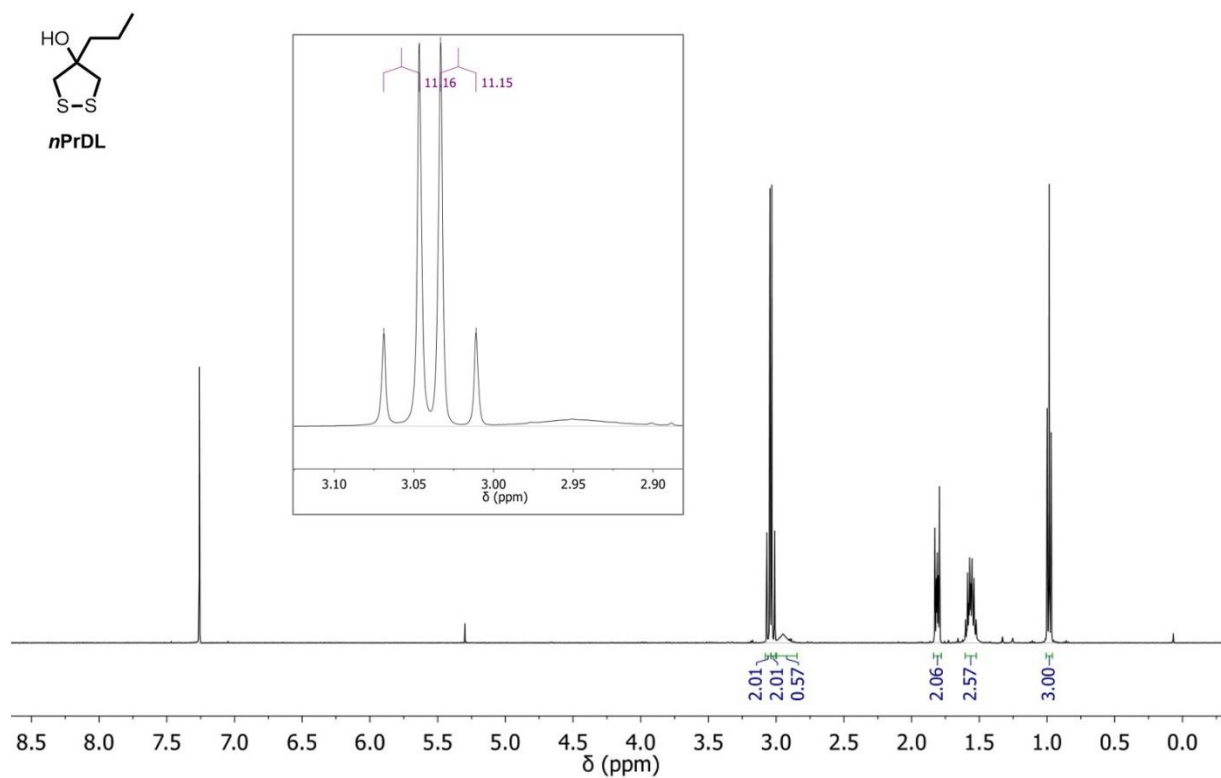


Figure S18. ^1H NMR spectrum of **nPrDL** in CDCl_3 .

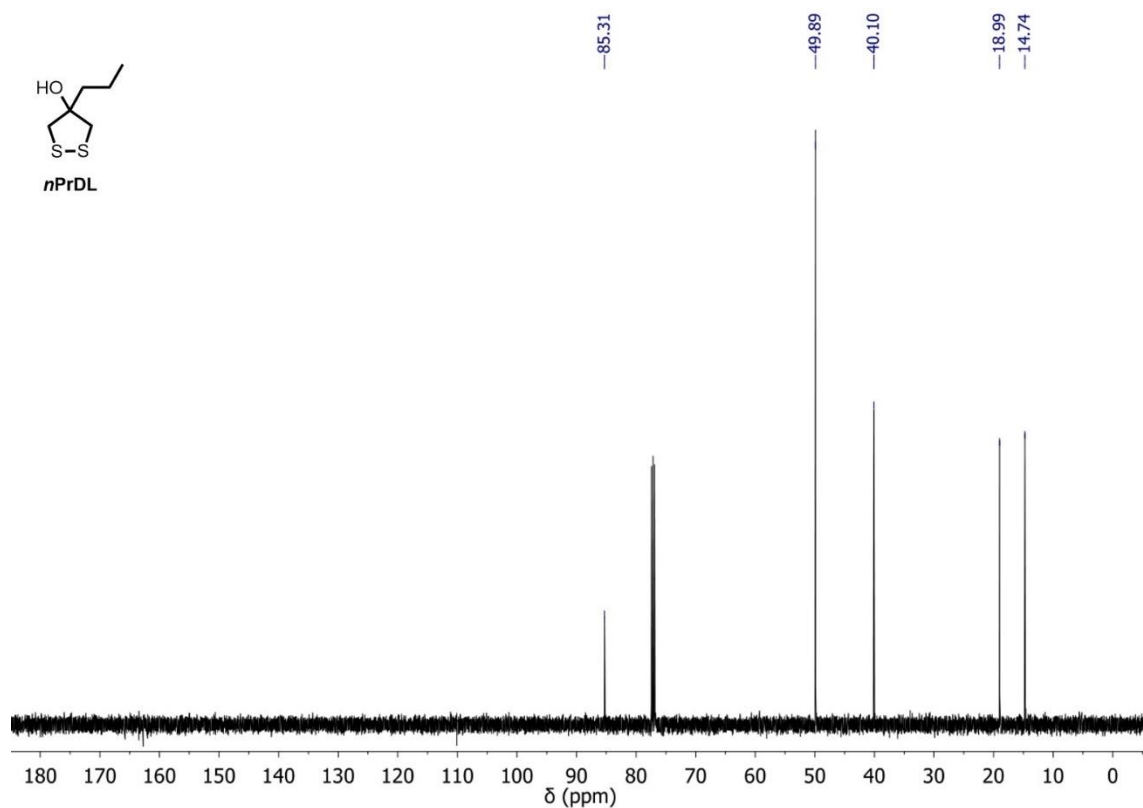


Figure S19. ^{13}C NMR spectrum of *nPrDL* in CDCl_3 .

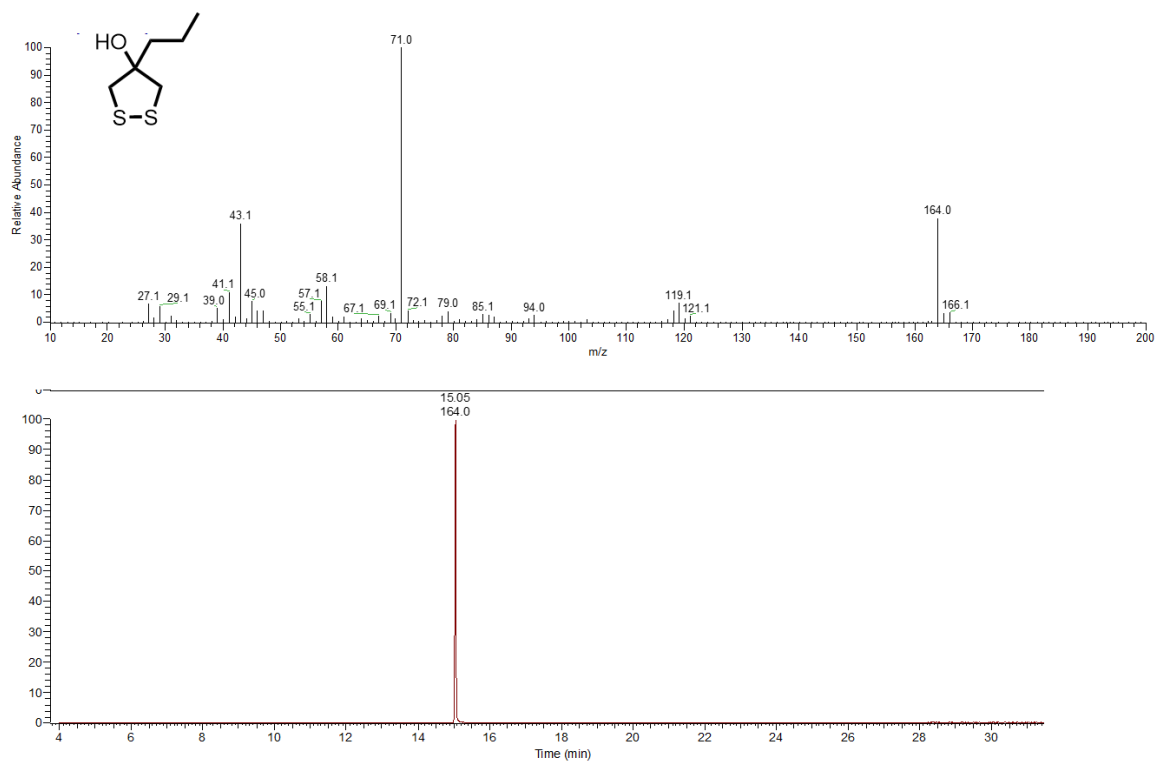
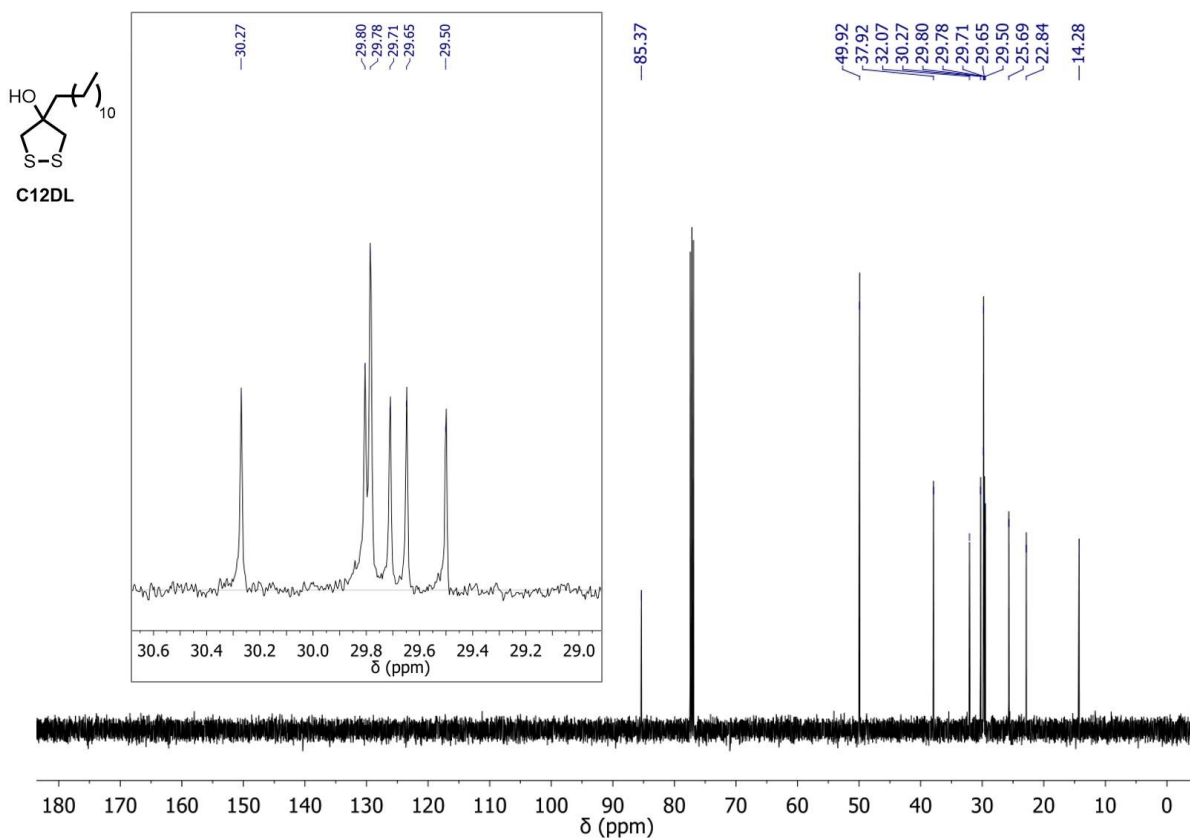
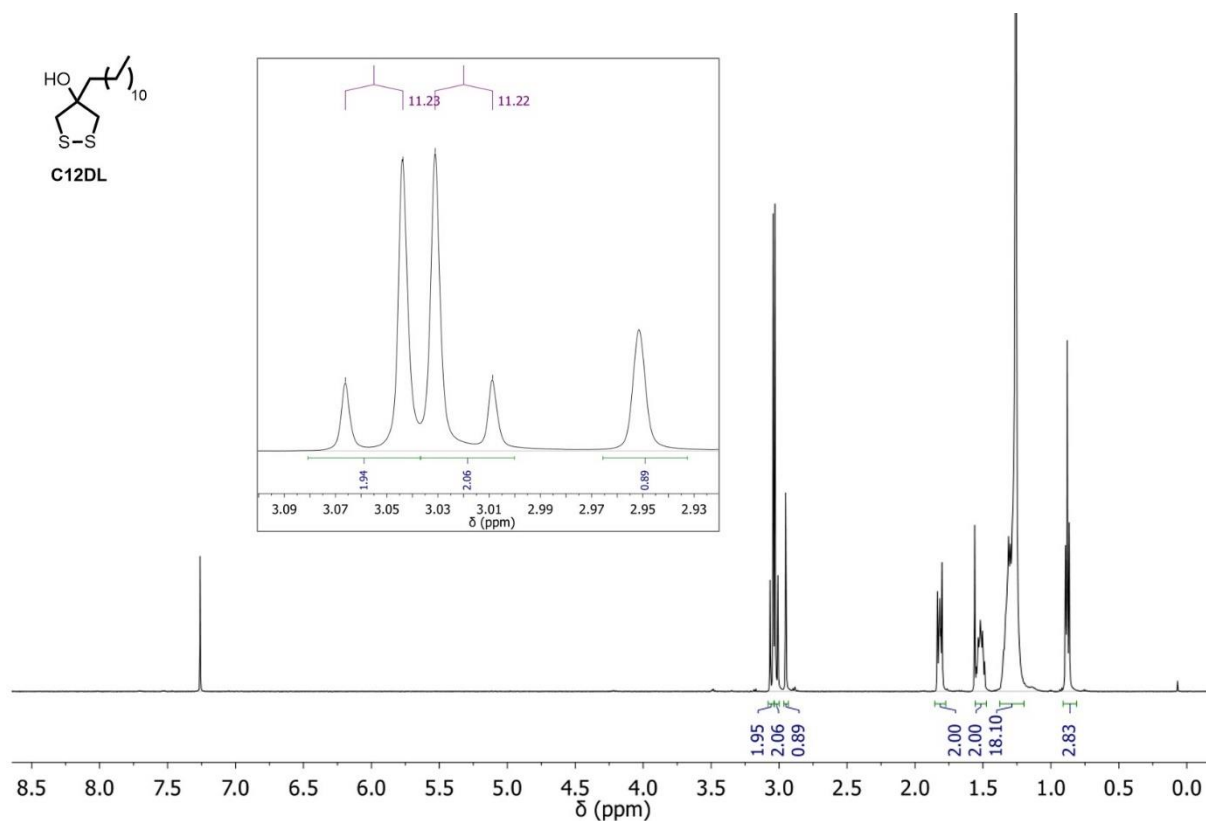


Figure S20. Mass spectrum (top) of the single peak at 15.05 min and corresponding gas chromatogram (bottom) of *nPrDL*.



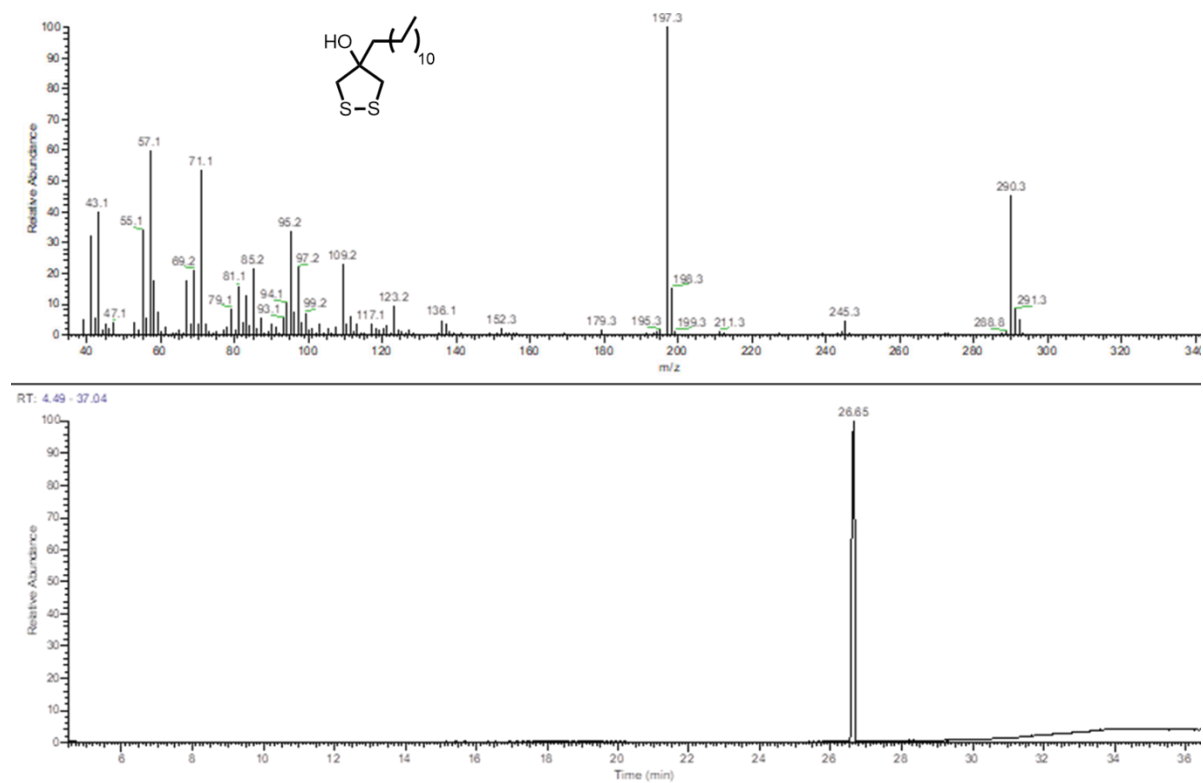


Figure S23. Mass spectrum (top) of the single peak at 26.65 min and corresponding gas chromatogram (bottom) of **C12DL**.

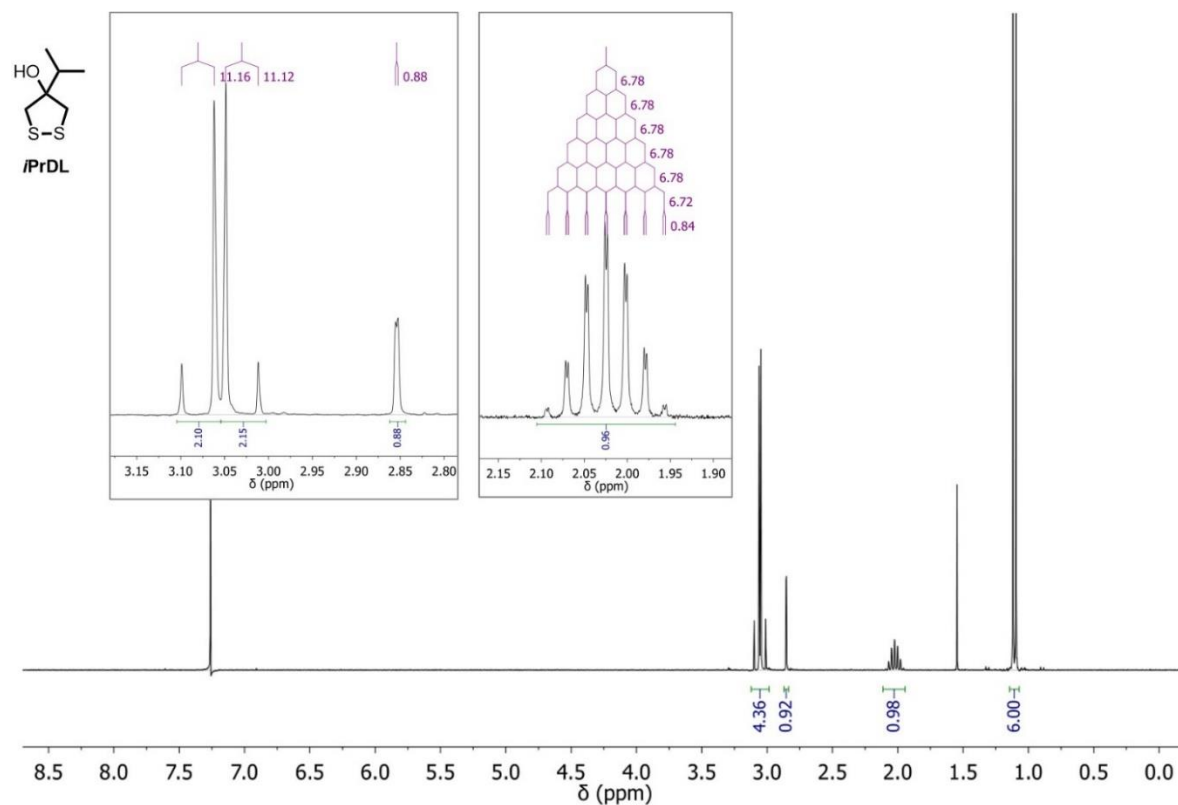


Figure S24. ^1H NMR spectrum of **iPrDL** in CDCl_3 .

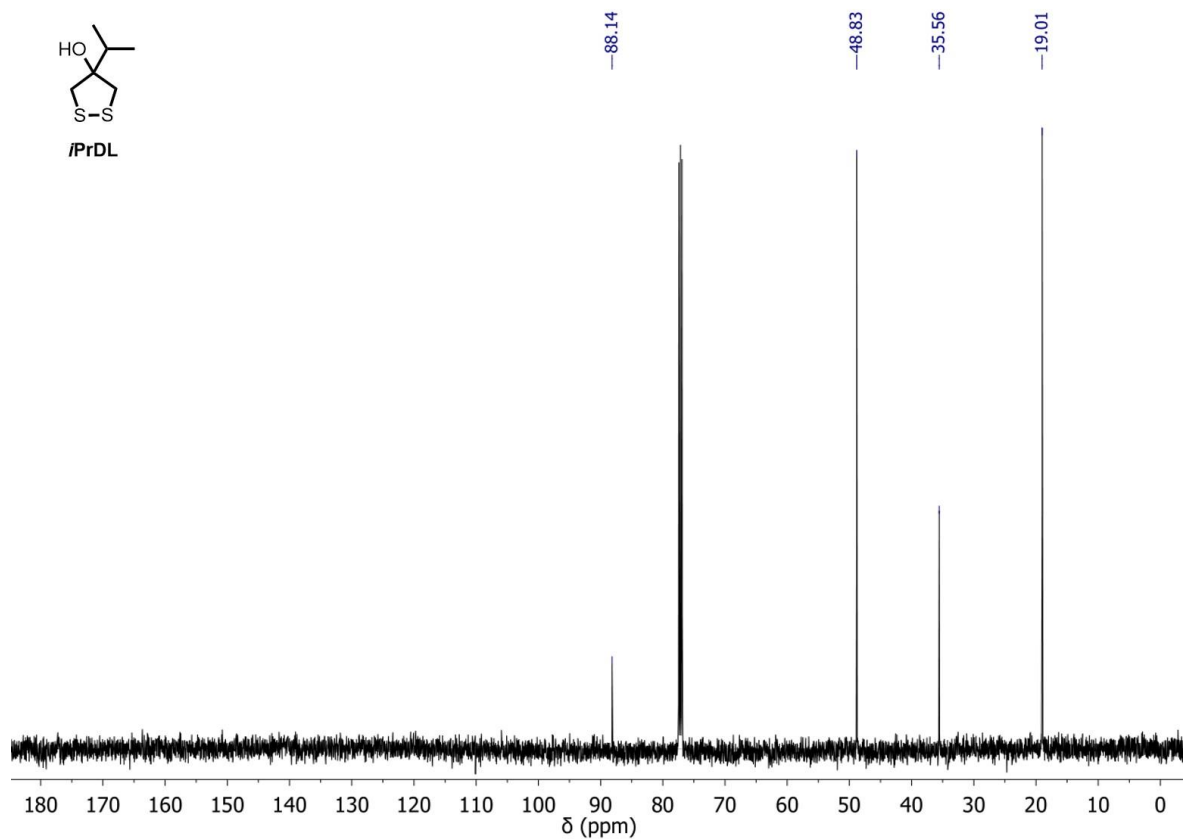


Figure S25. ^{13}C NMR spectrum of *iPrDL* in CDCl_3 .

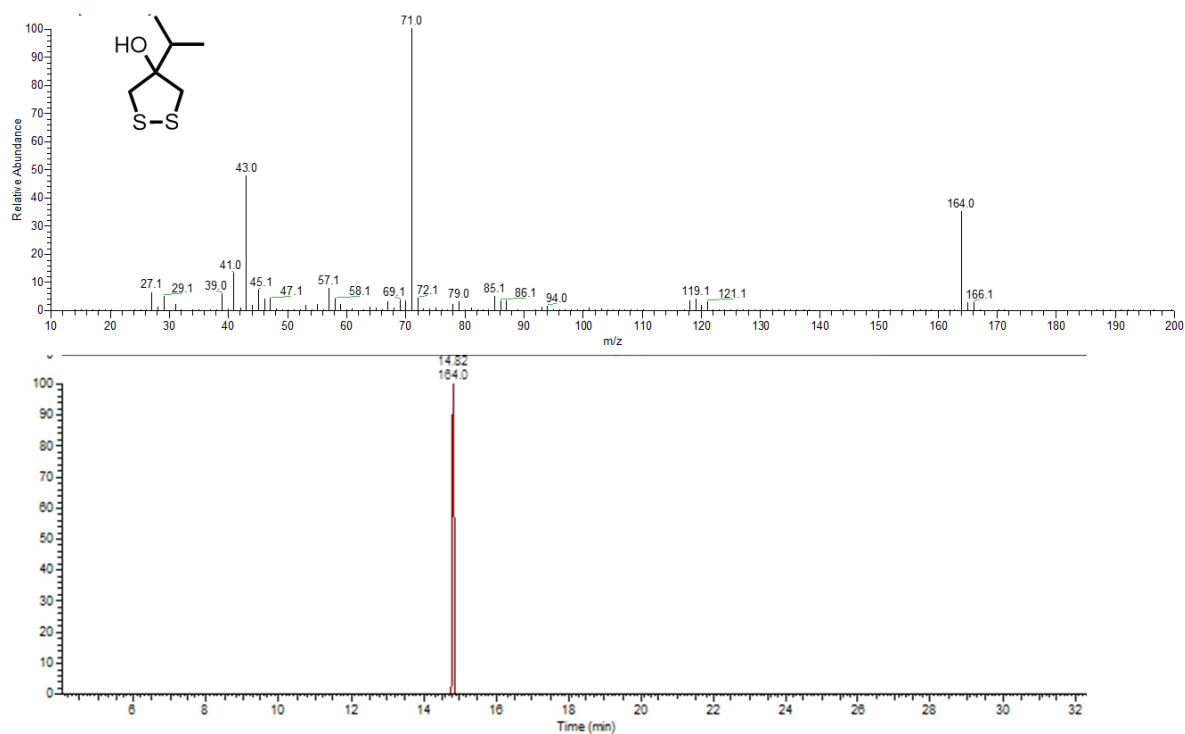
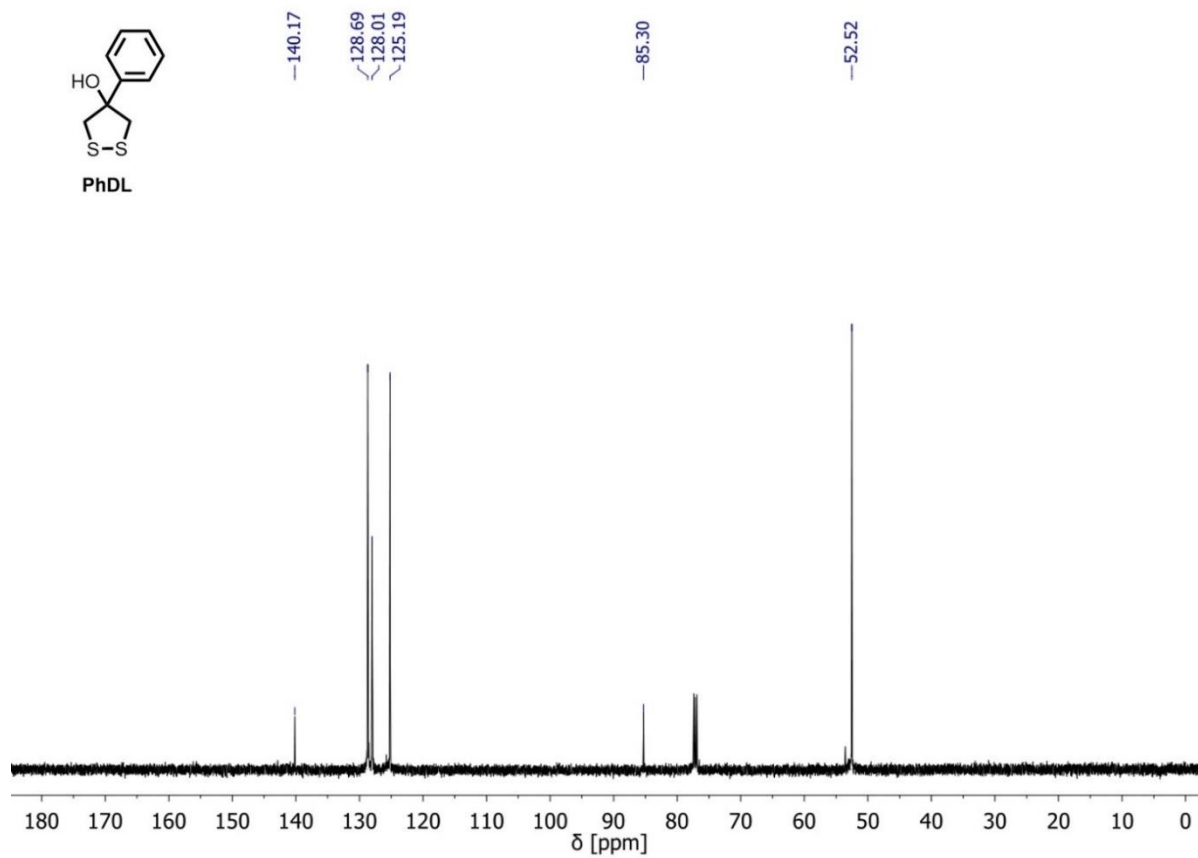
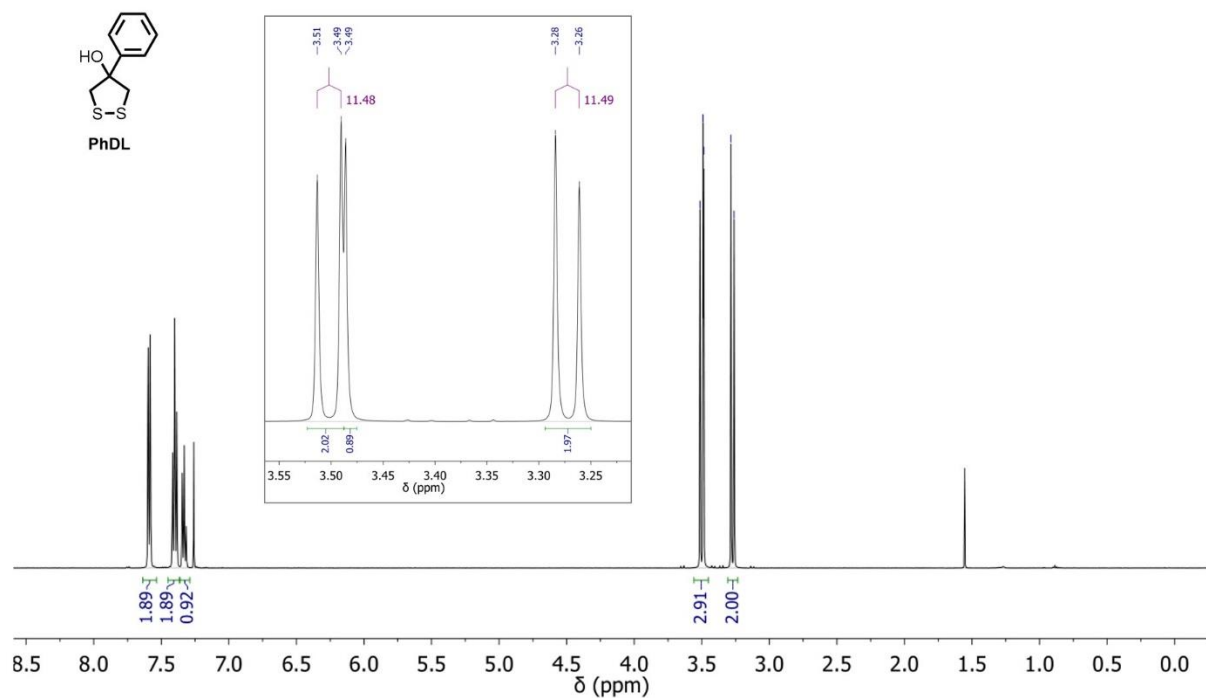


Figure S26. Mass spectrum (top) of the single peak at 14.82 min and corresponding gas chromatogram (bottom) of *iPrDL*.



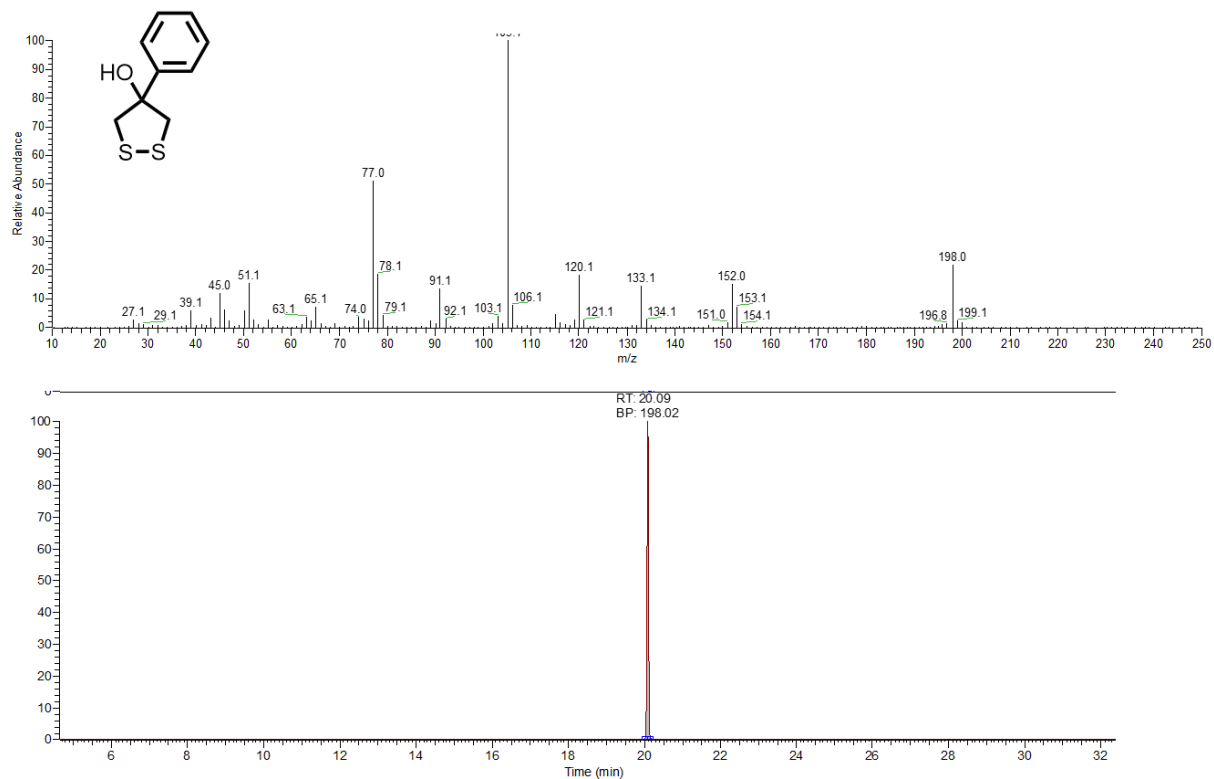


Figure S29. Mass spectrum (top) of the single peak at 20.09 min and corresponding gas chromatogram (bottom) of **PhDL**.

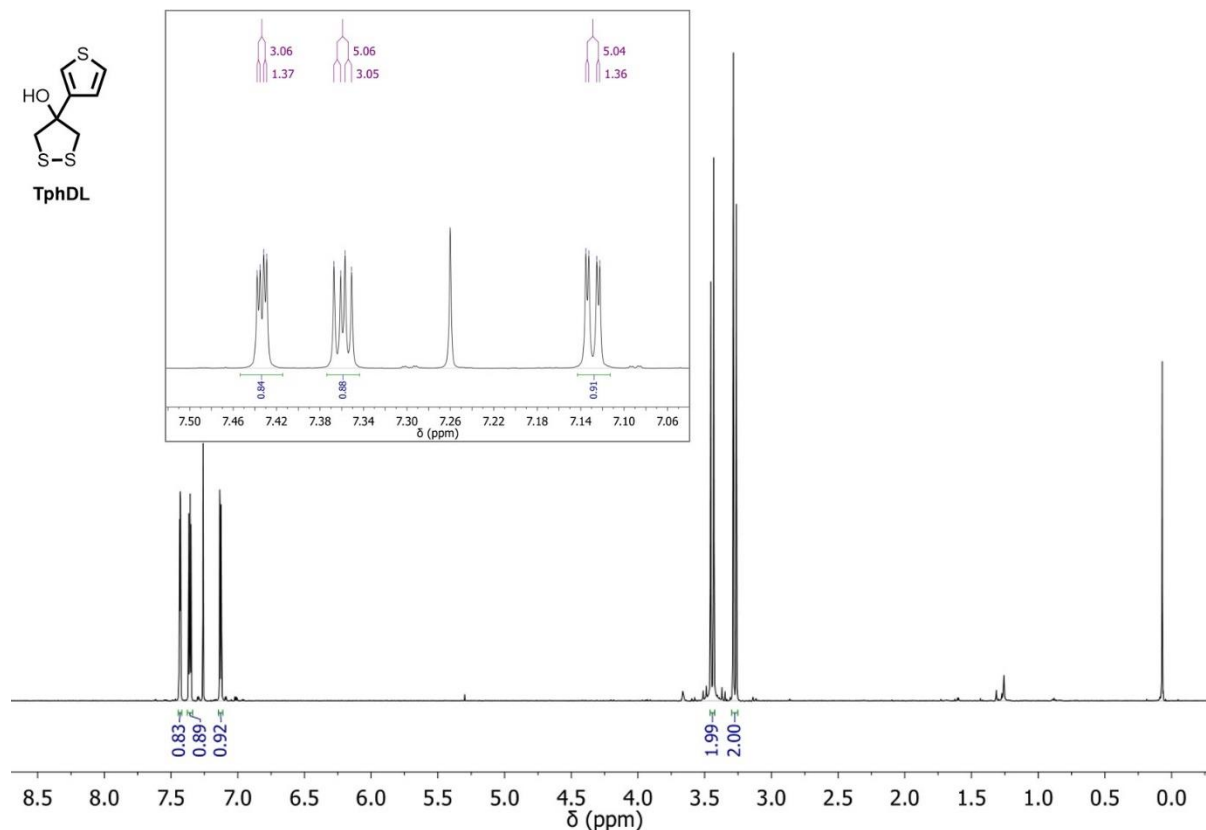


Figure S30. ¹H NMR spectrum of **TphDL** in CDCl₃.

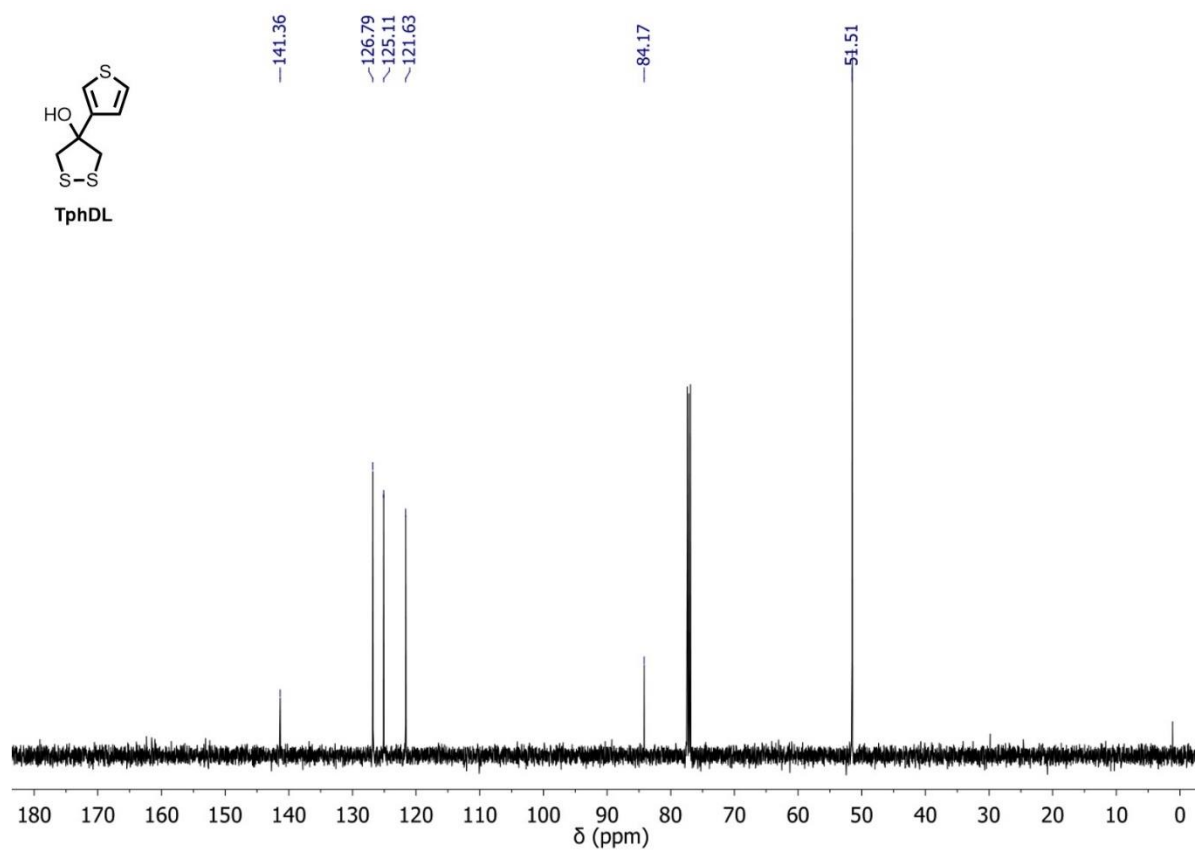


Figure S31. ^{13}C NMR spectrum of TphDL in CDCl_3 .

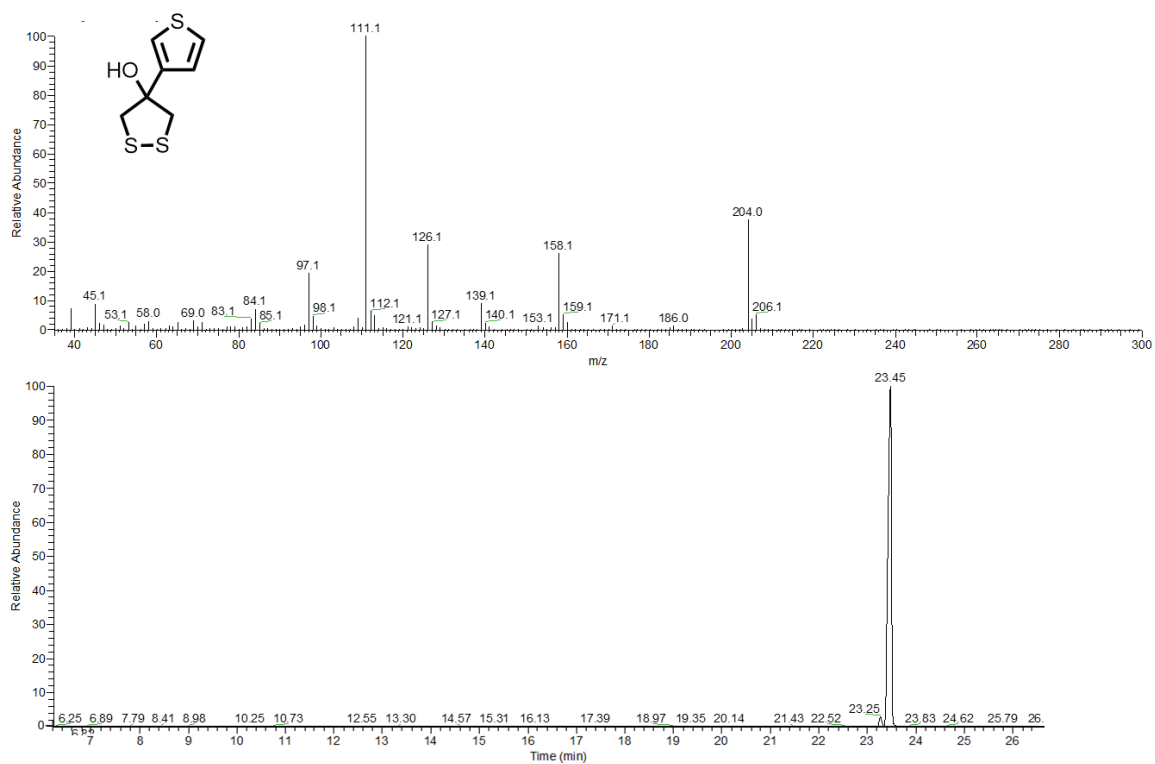


Figure S32. Mass spectrum (top) of the single peak at 23.45 min and corresponding gas chromatogram (bottom) of TphDL.

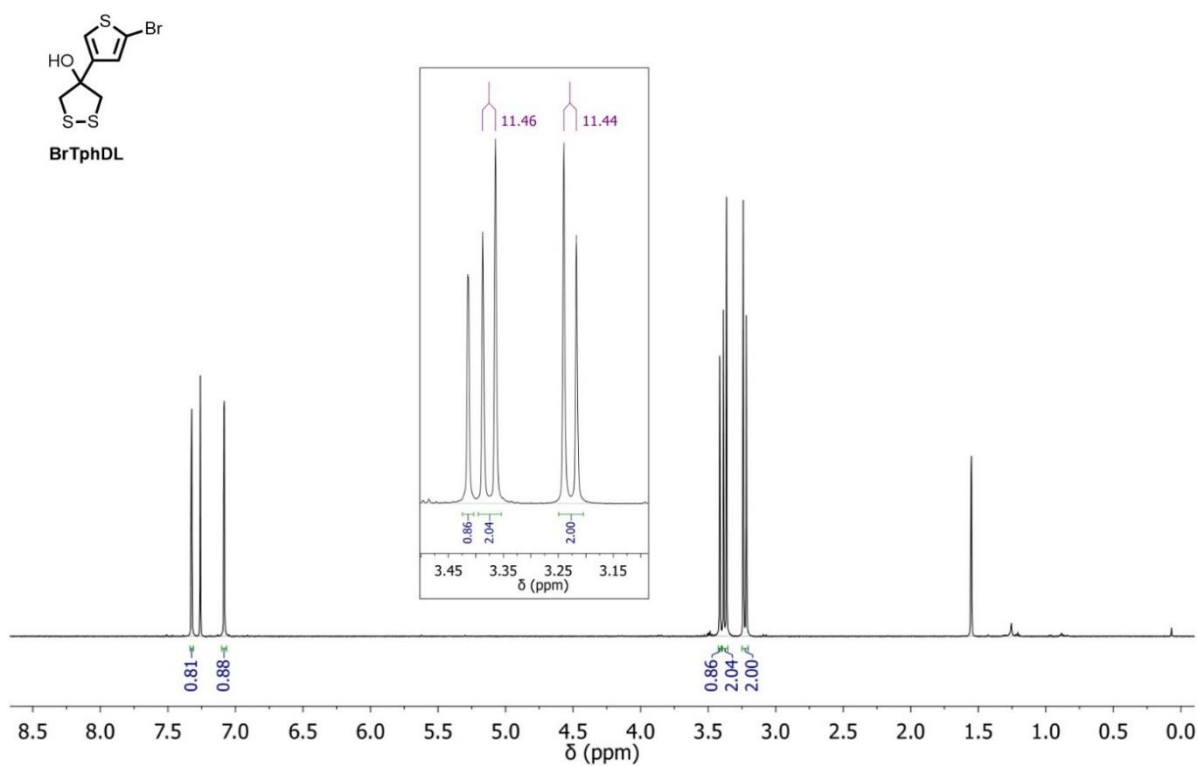


Figure S33. ^1H NMR spectrum of **BrTphDL** in CDCl_3 .

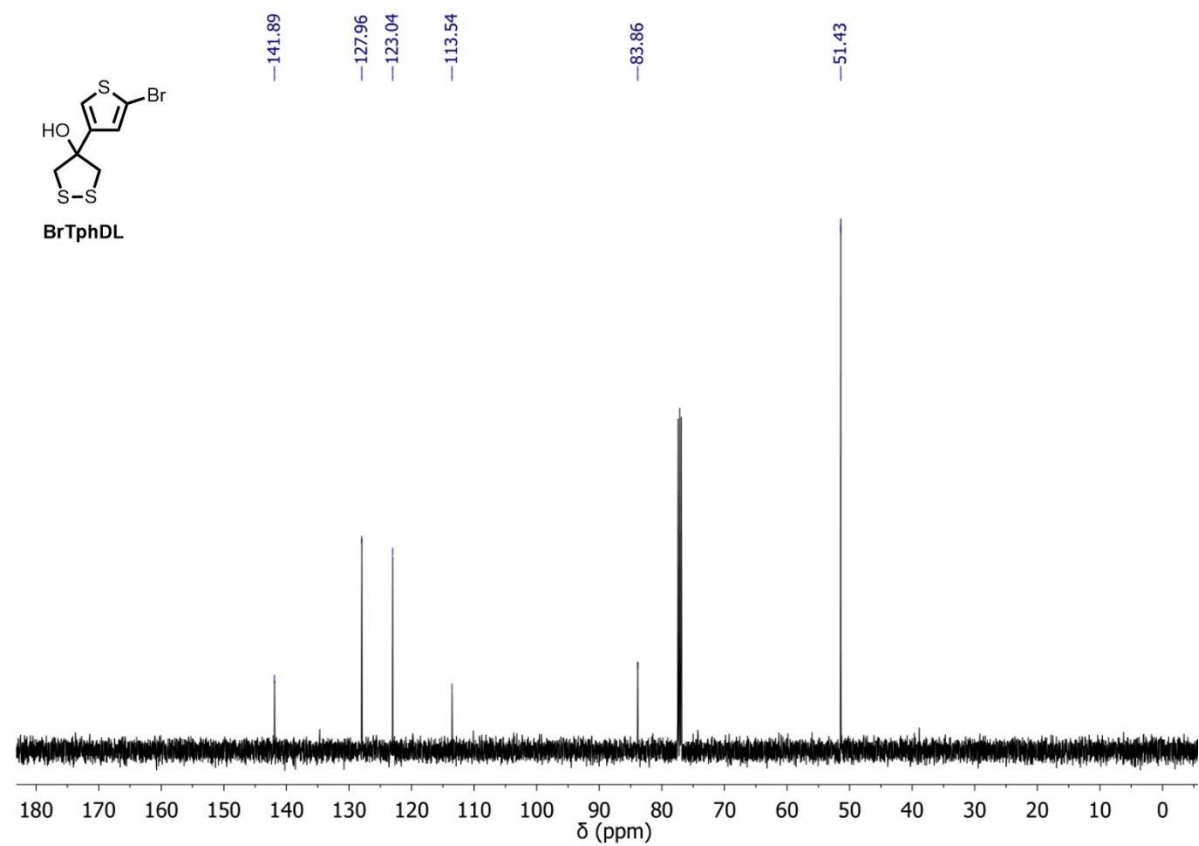


Figure S34. ^{13}C NMR spectrum of **BrTphDL** in CDCl_3 .

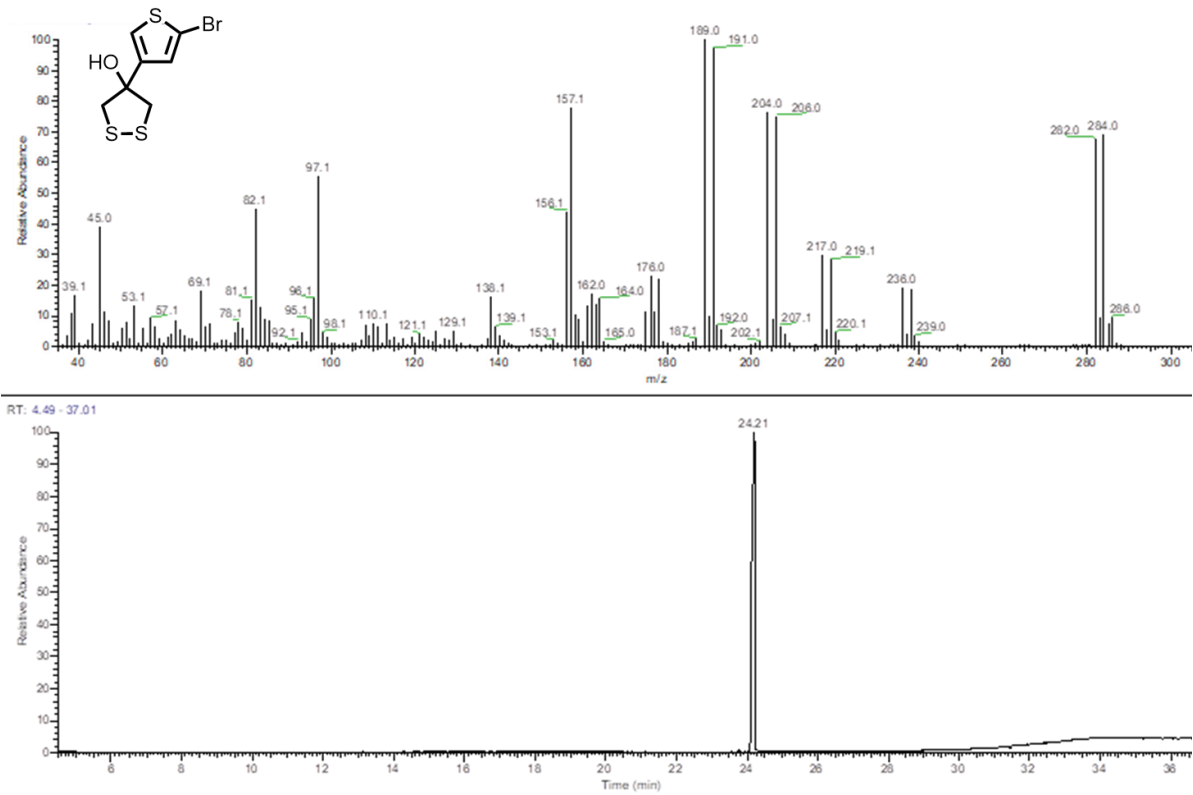


Figure S35. Mass spectrum (top) of the single peak at 24.21 min and corresponding gas chromatogram (bottom) of BrTphDL.

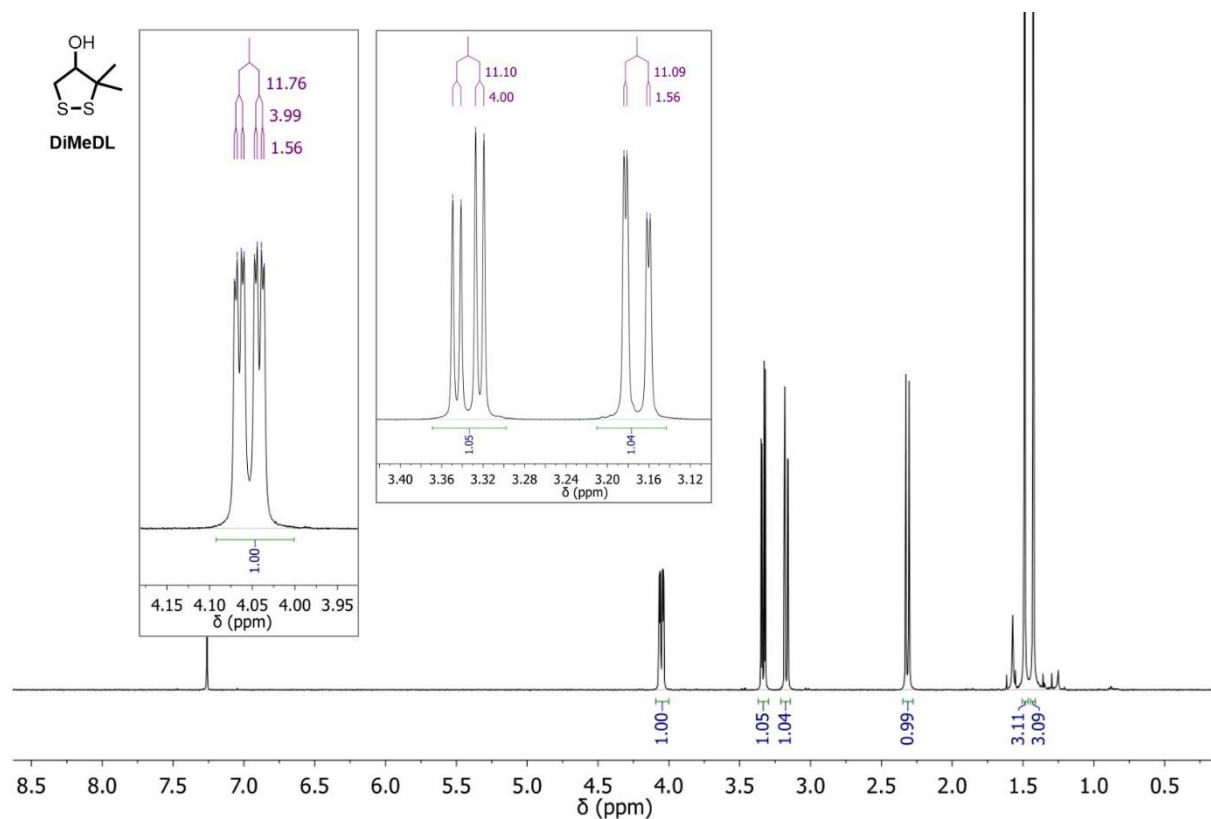


Figure S36. ^1H NMR spectrum of DiMeDL in CDCl_3 .

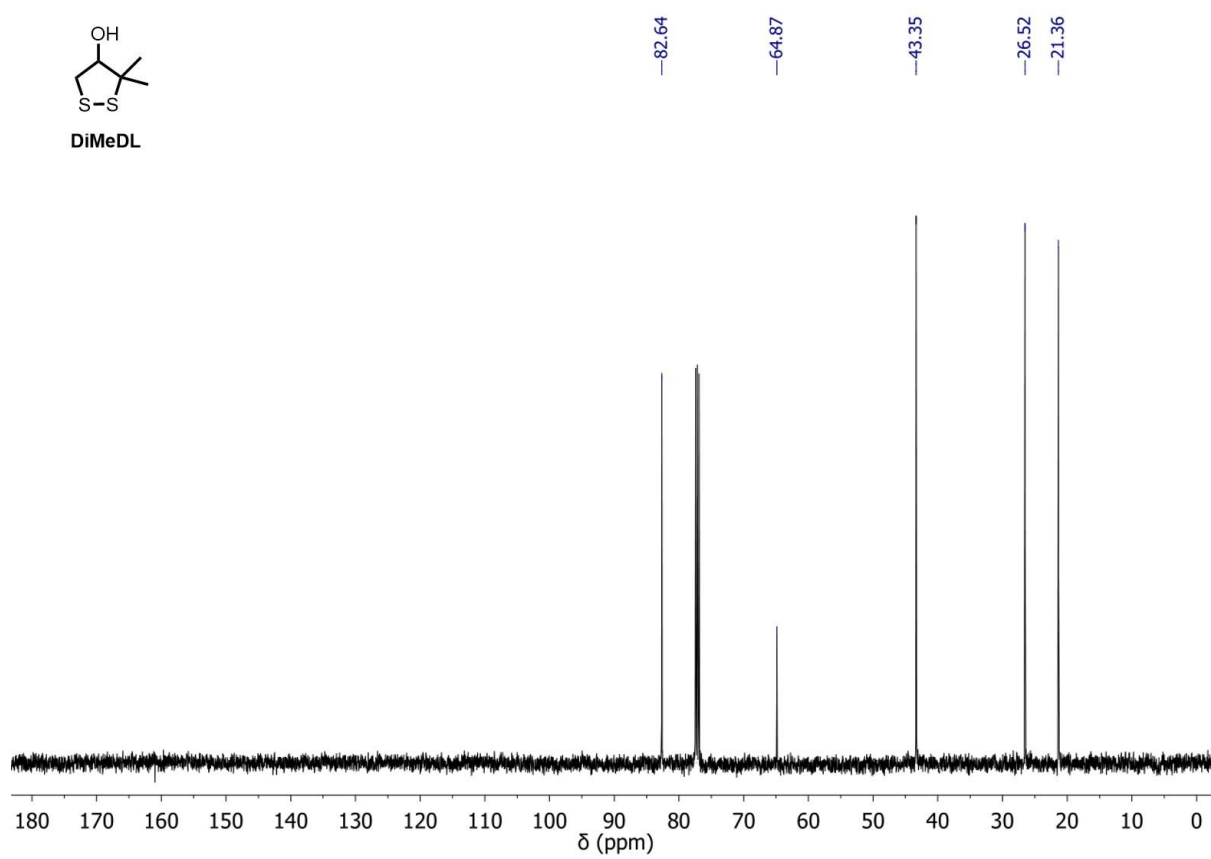
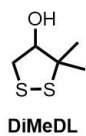


Figure S37. ¹³C NMR spectrum of DiMeDL in CDCl₃.

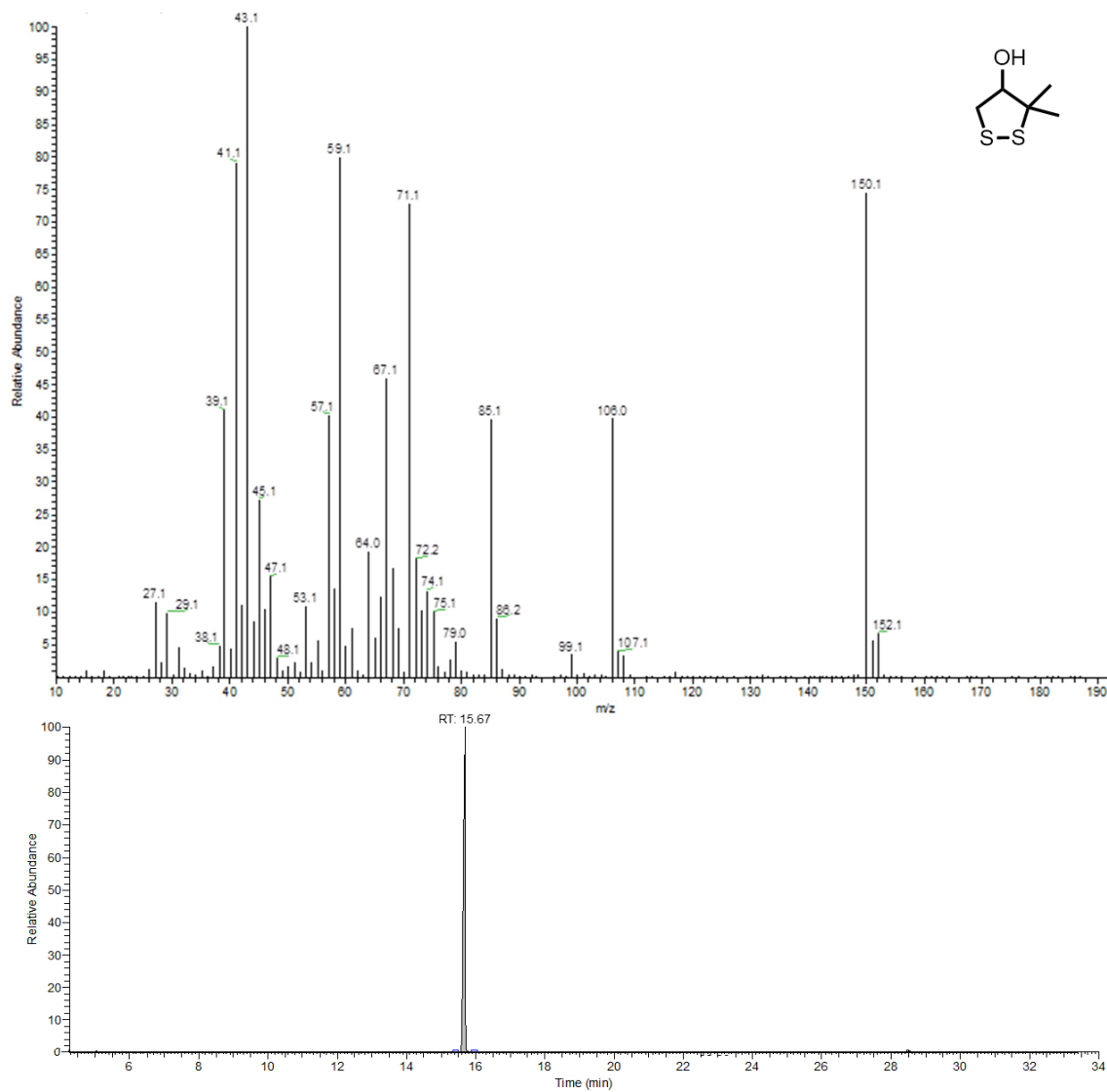


Figure S38. Mass spectrum (top) of the single peak at 15.67 min and corresponding gas chromatogram (bottom) of **DiMeDL**.

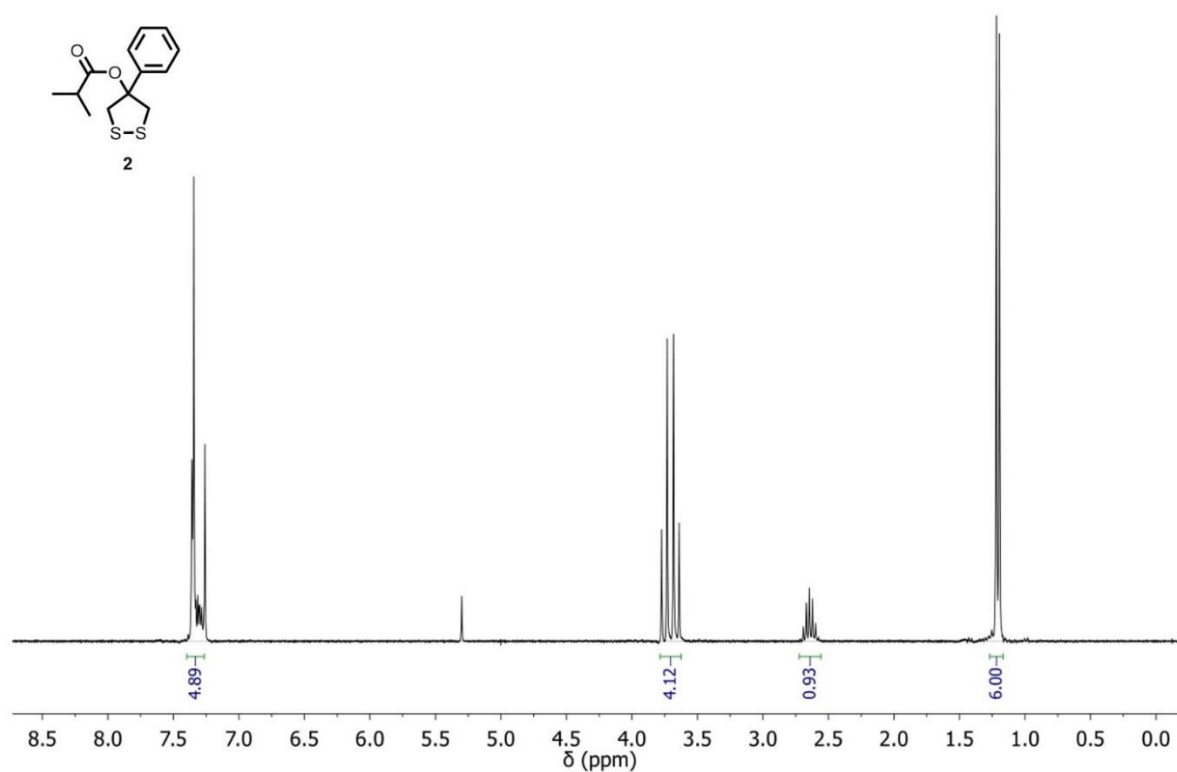


Figure S39. ¹H NMR spectrum of **2** in CDCl₃.

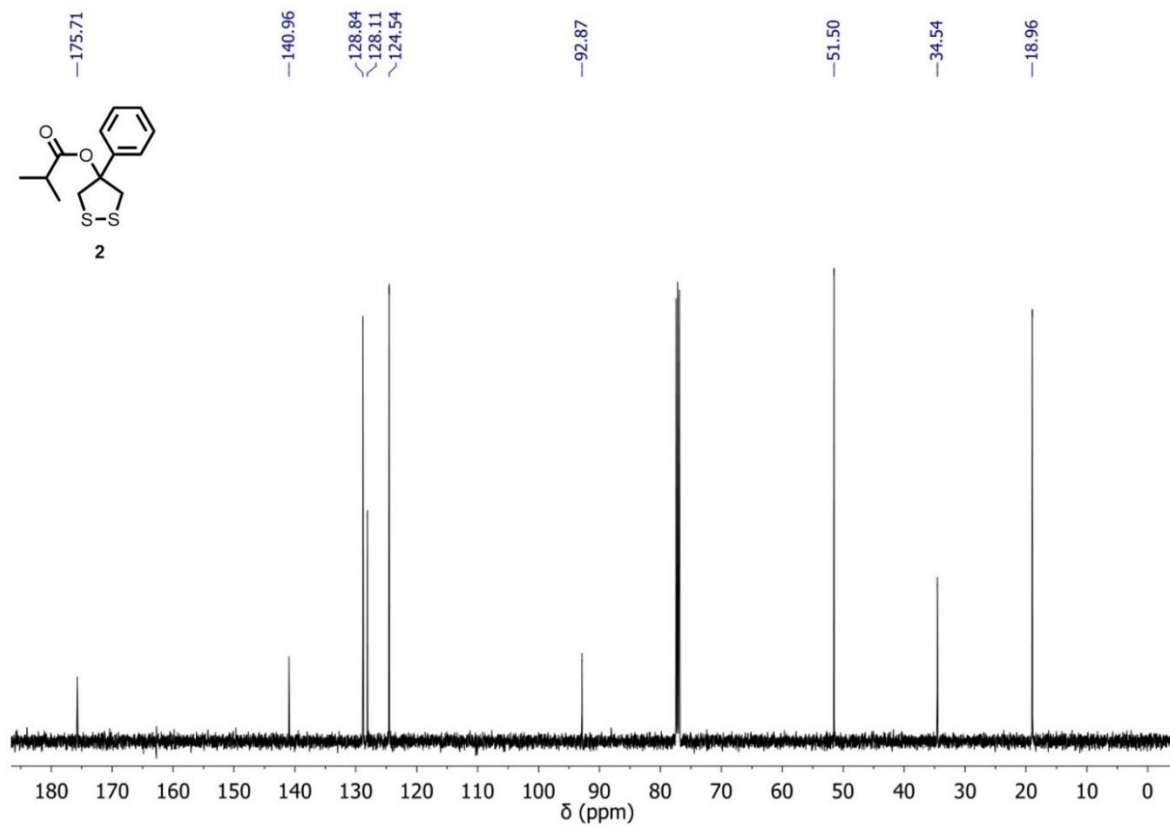


Figure S40. ¹³C NMR spectrum of **2** in CDCl₃.

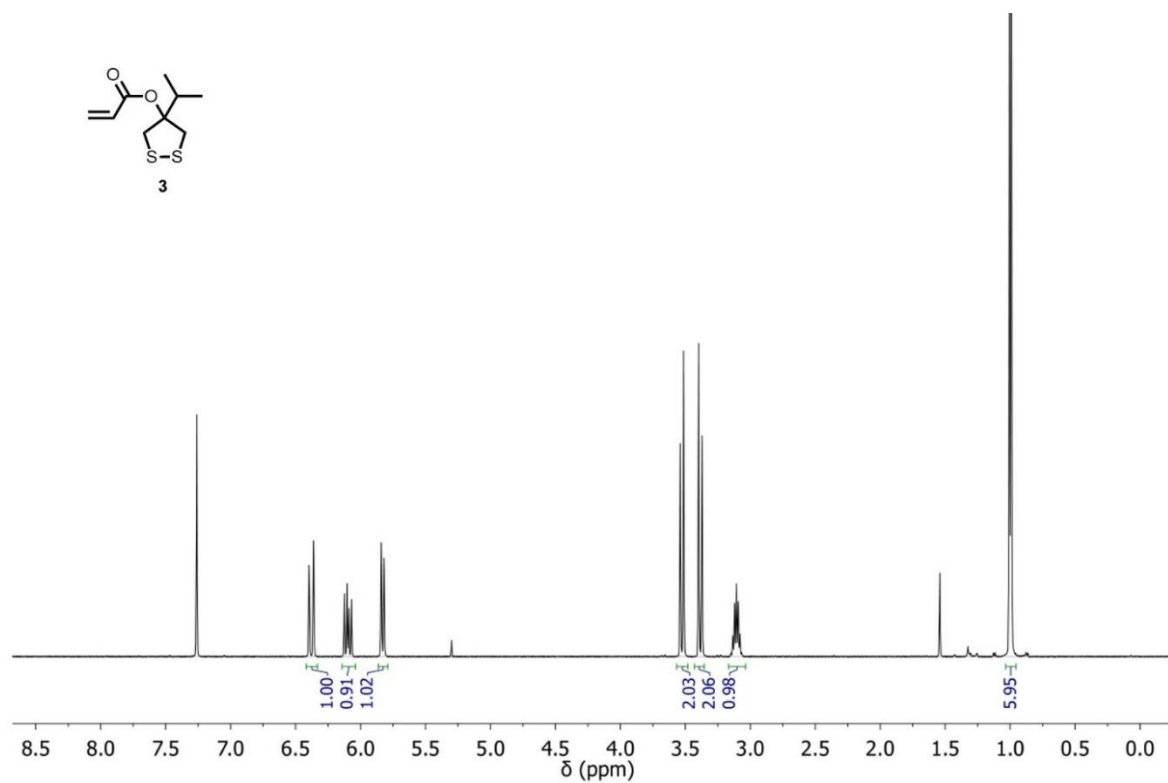


Figure S41. ¹H NMR spectrum of **3** in CDCl₃.

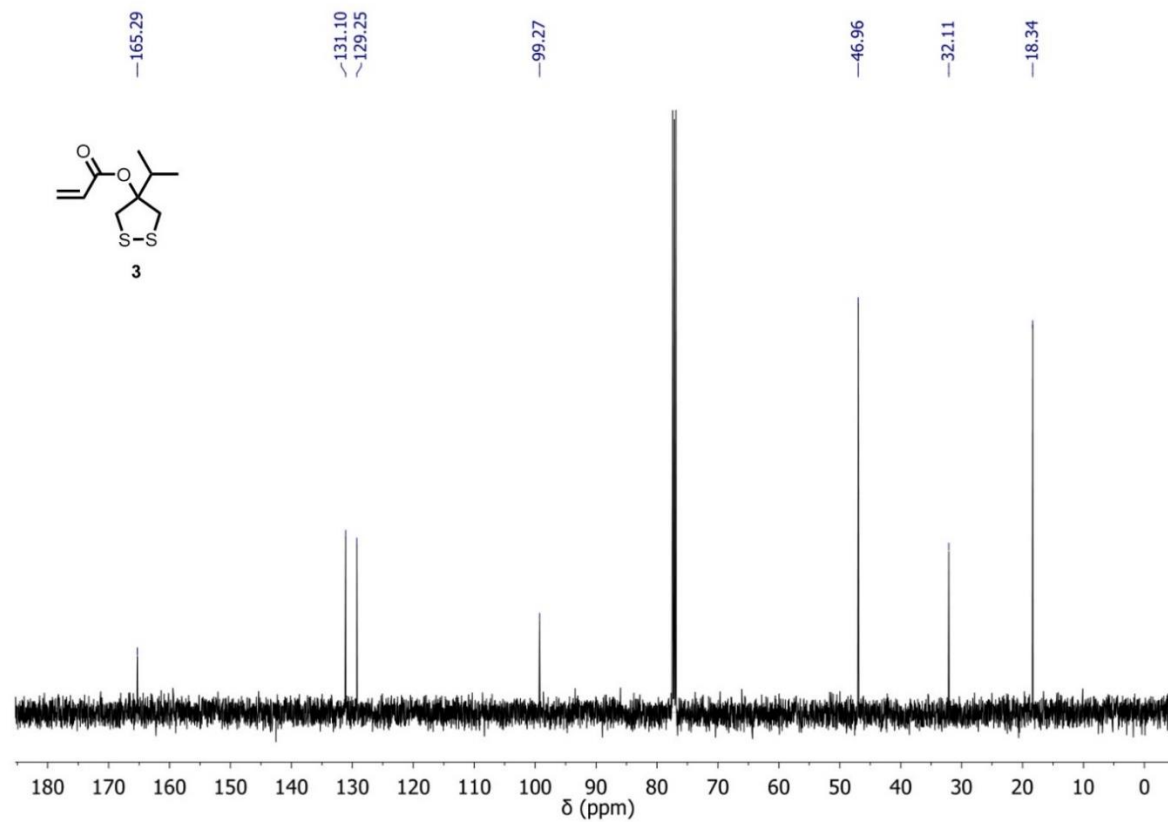


Figure S42. ¹³C NMR spectrum of **3** in CDCl₃.

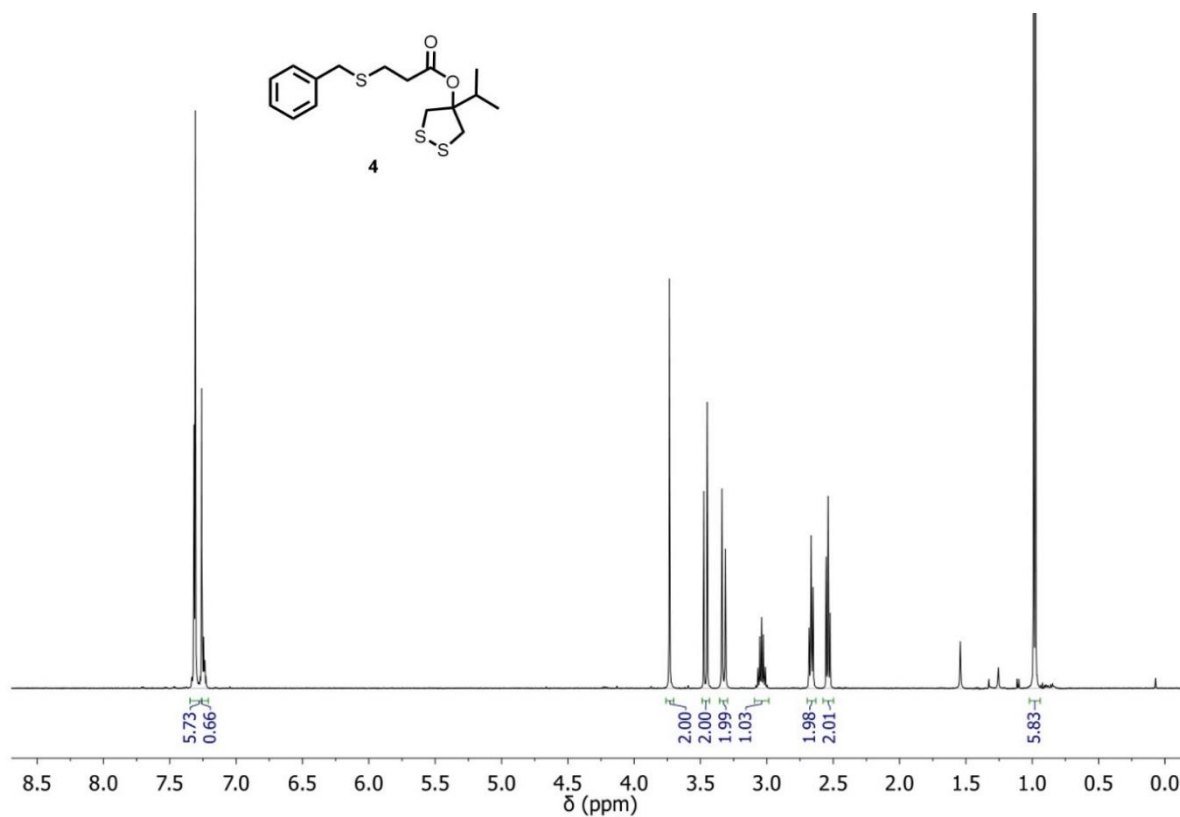


Figure S43. ¹H NMR spectrum of **4** in CDCl₃.

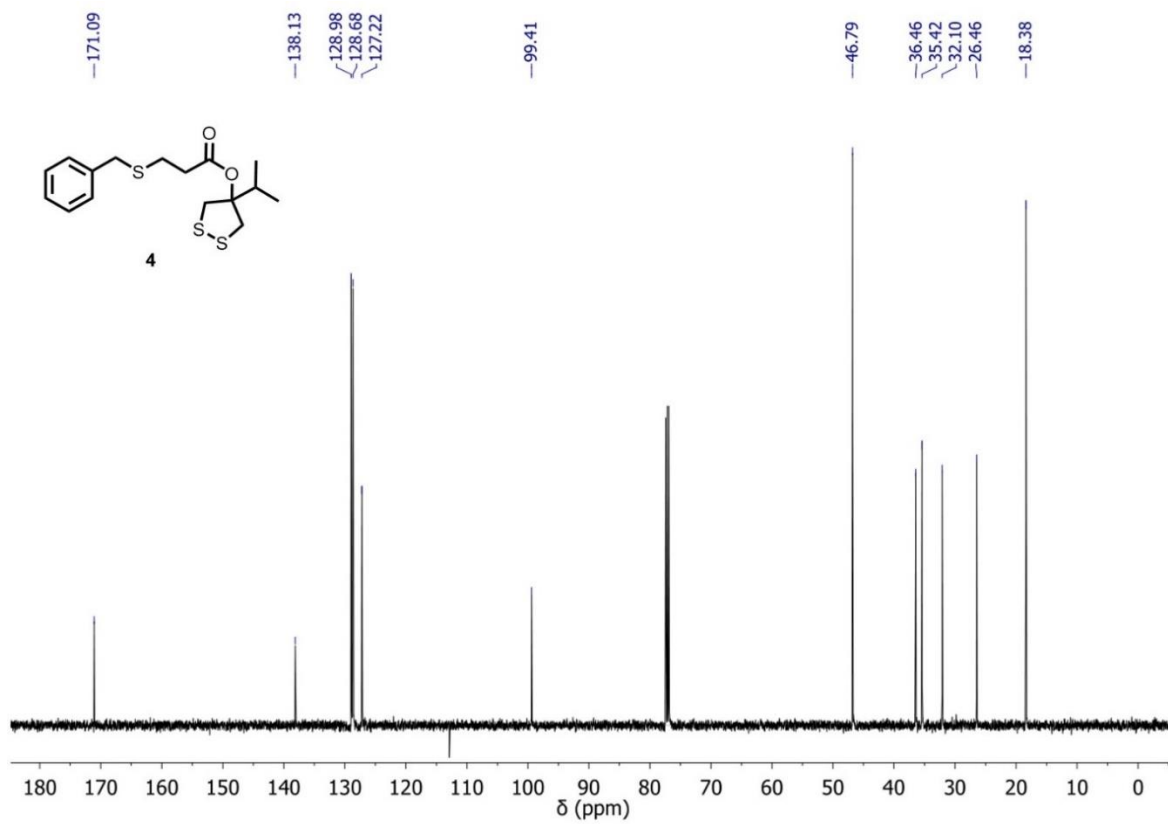


Figure S44. ¹³C NMR spectrum of **4** in CDCl₃.

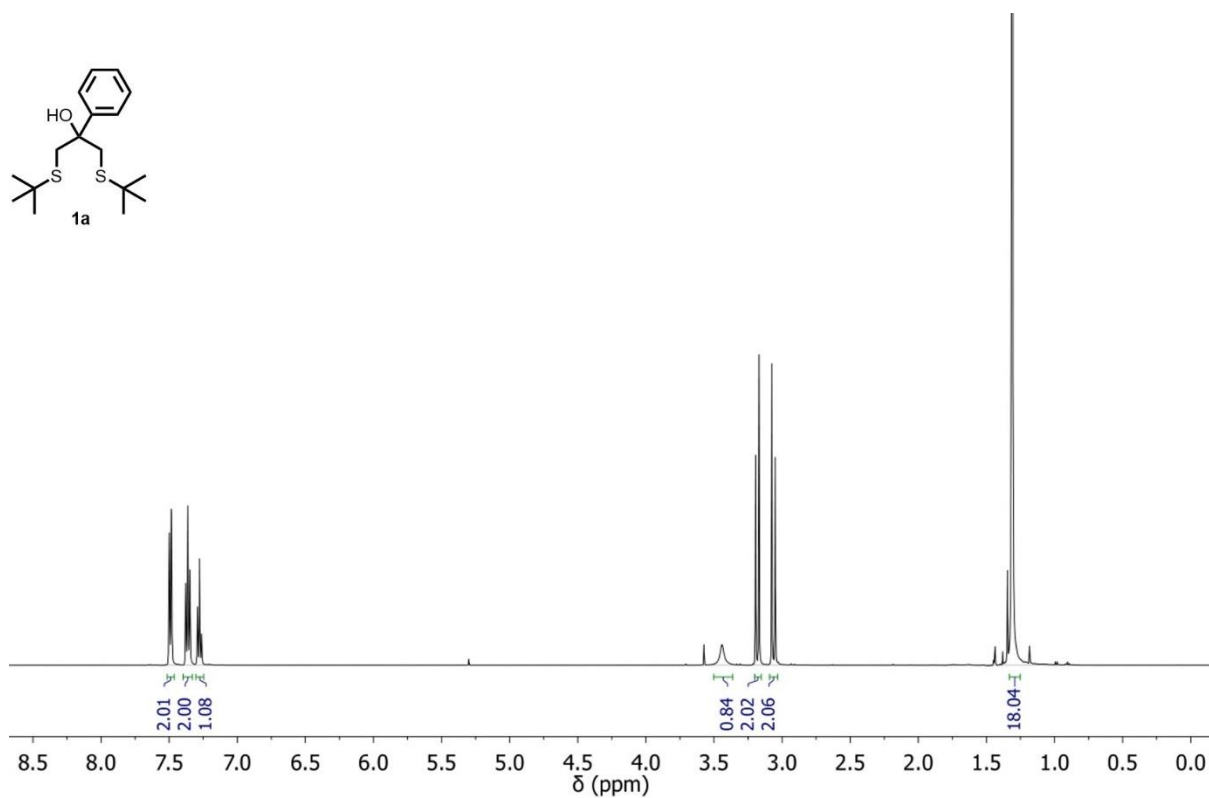


Figure S45. ¹H NMR spectrum of **1a** in CDCl₃.

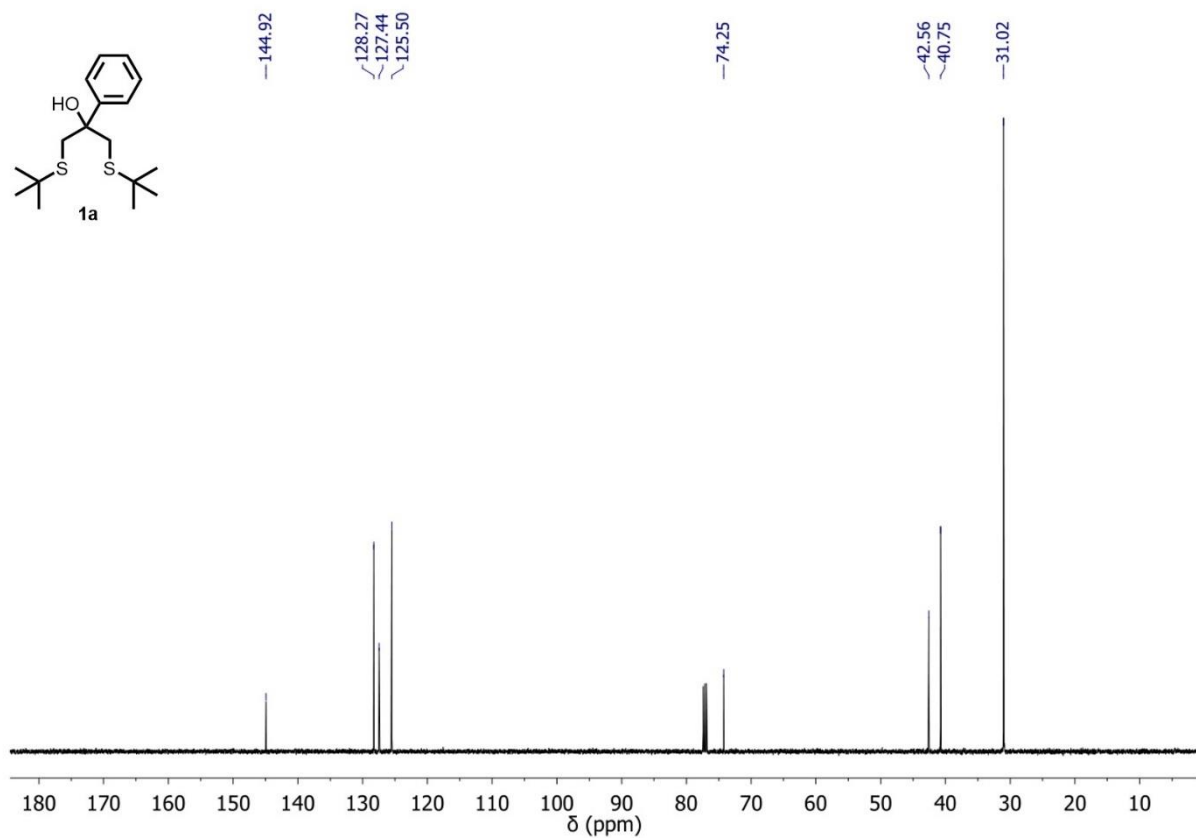
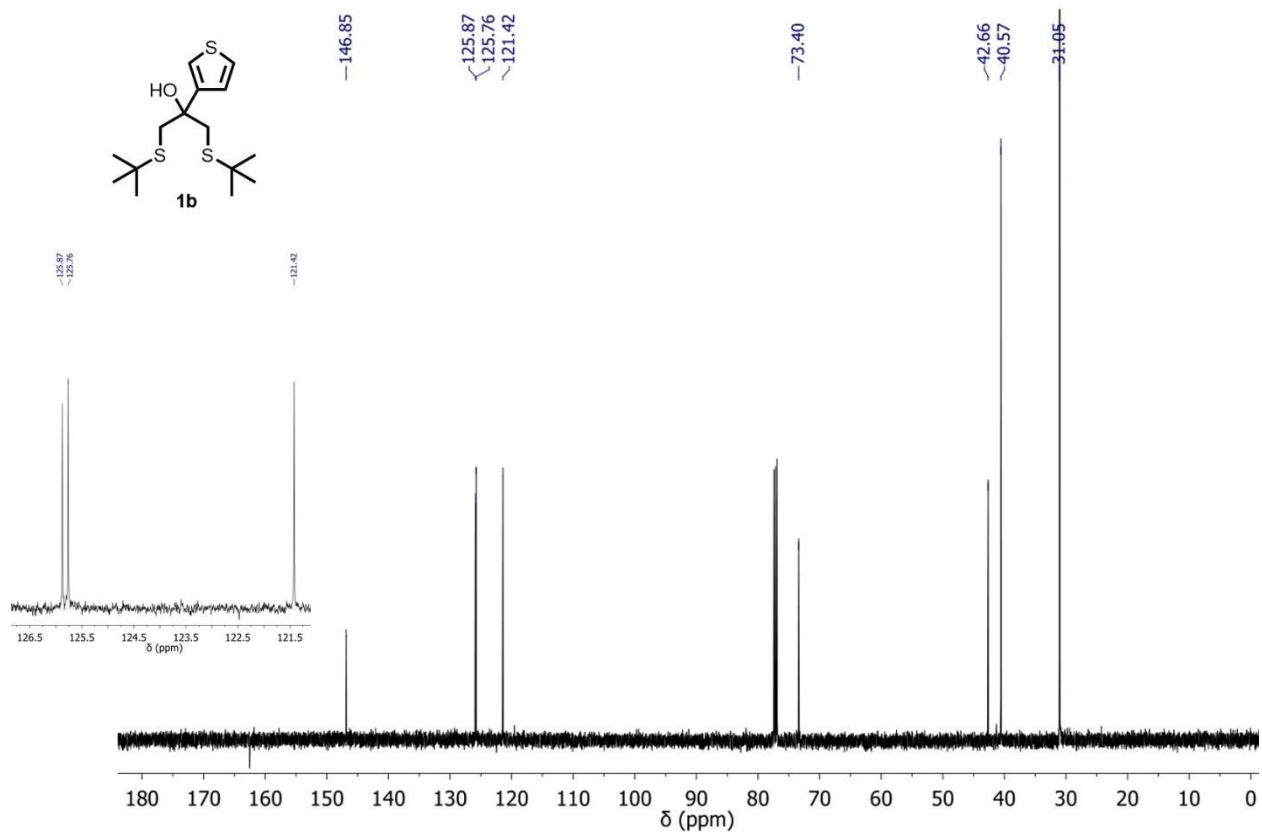
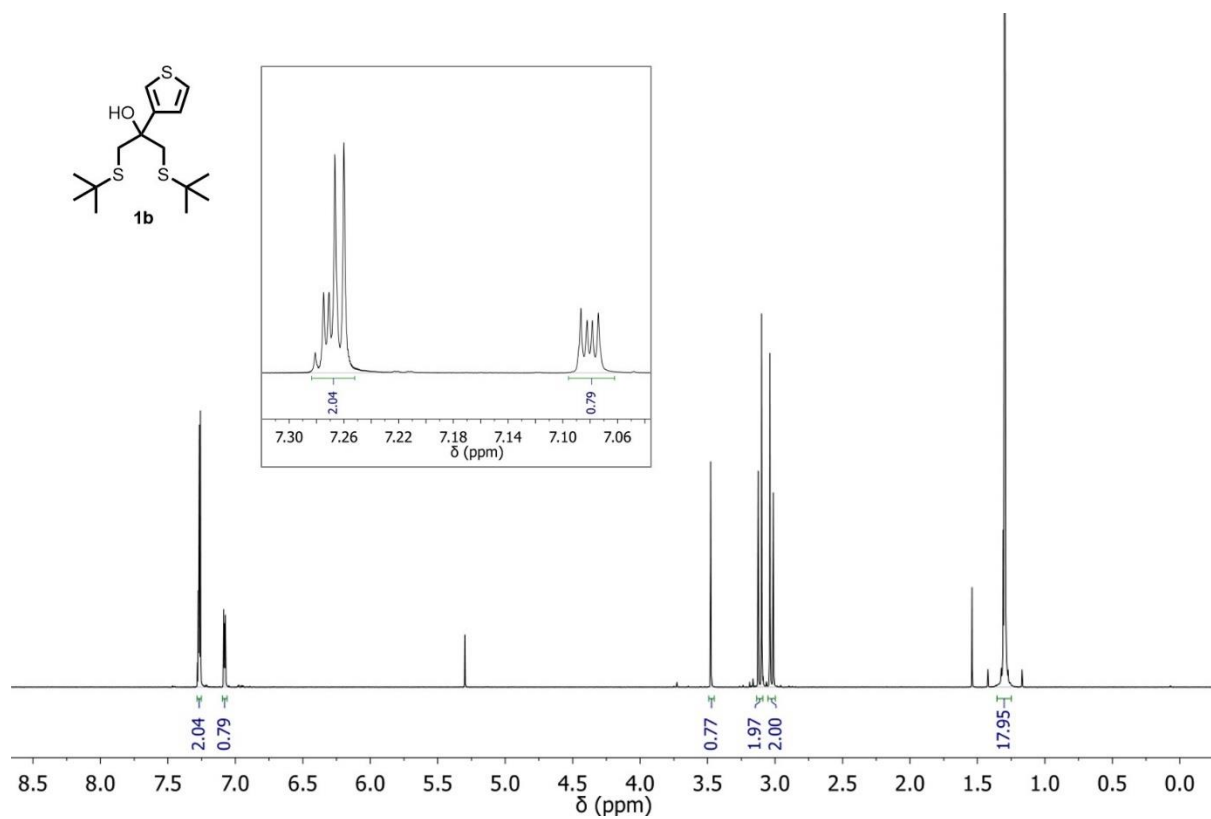


Figure S46. ¹³C NMR spectrum of **1a** in CDCl₃.



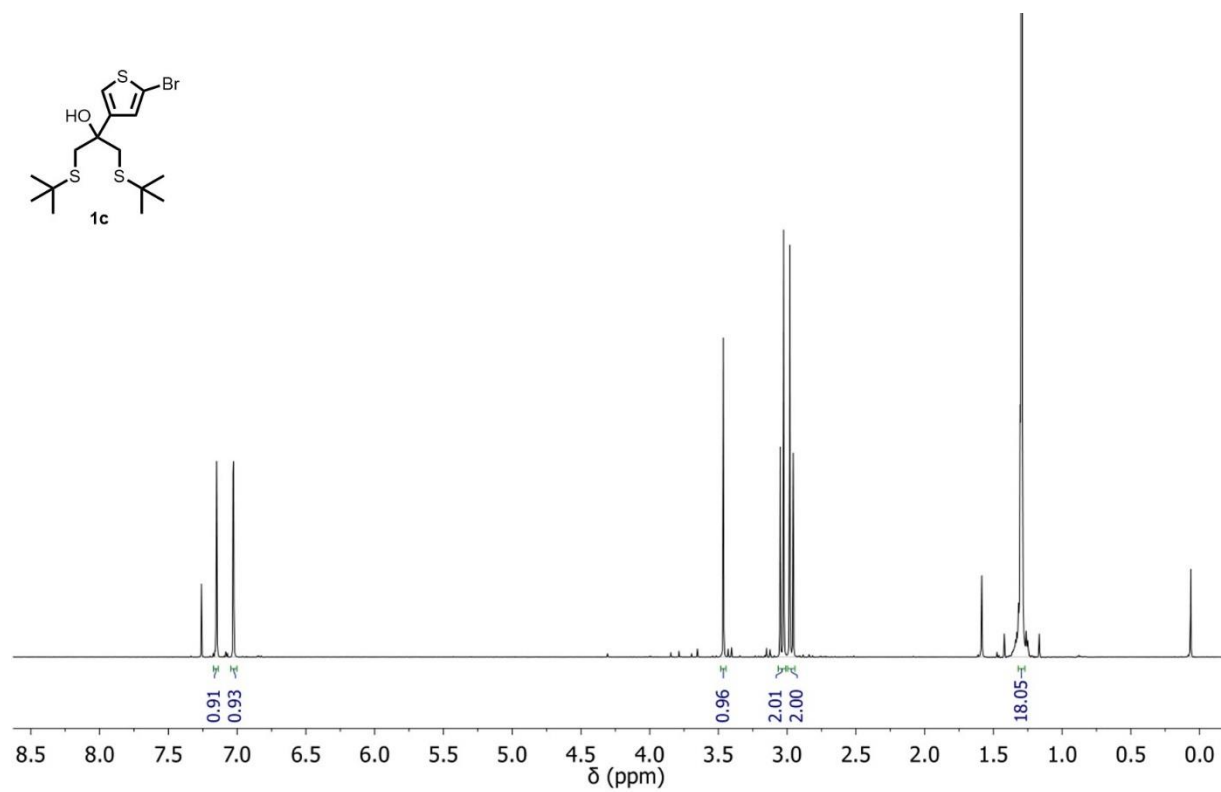


Figure S49. ¹H NMR spectrum of **1c** in CDCl₃.

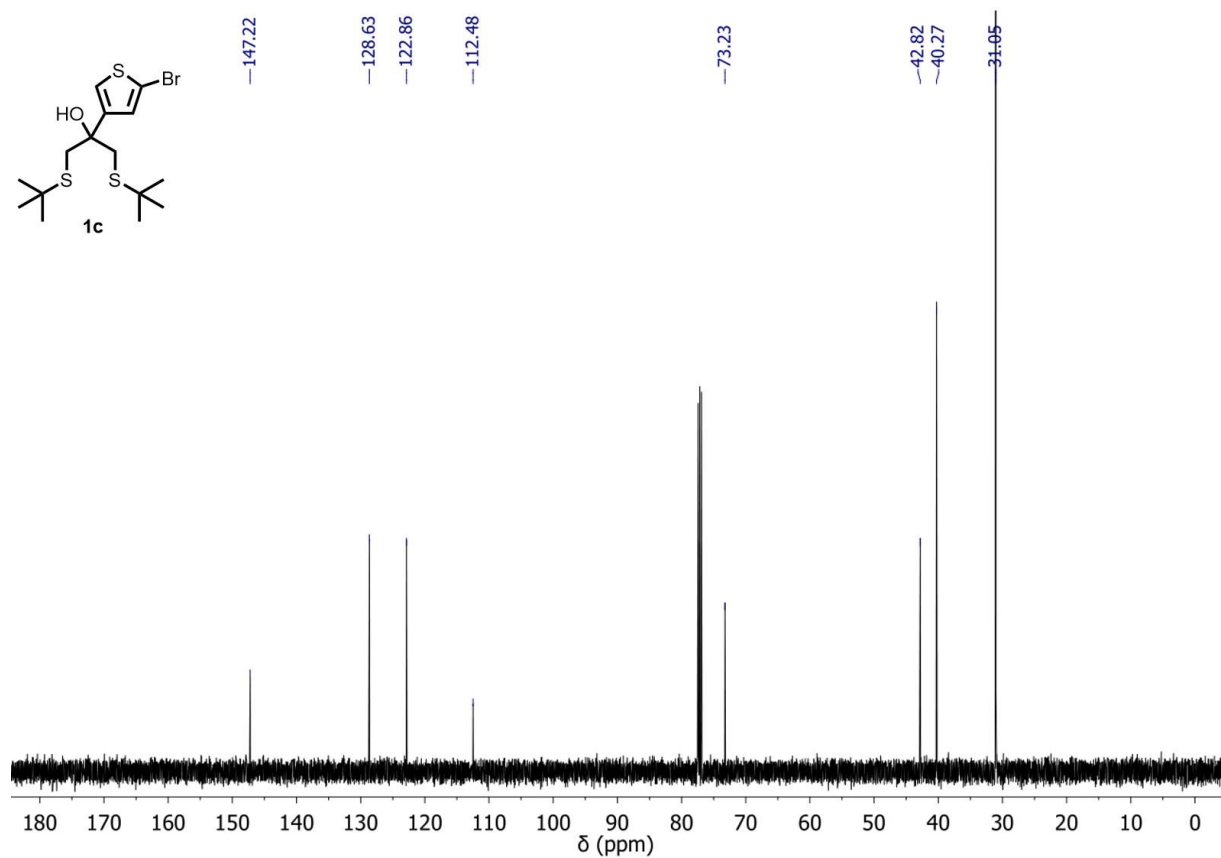


Figure S50. ¹³C NMR spectrum of **1c** in CDCl₃.

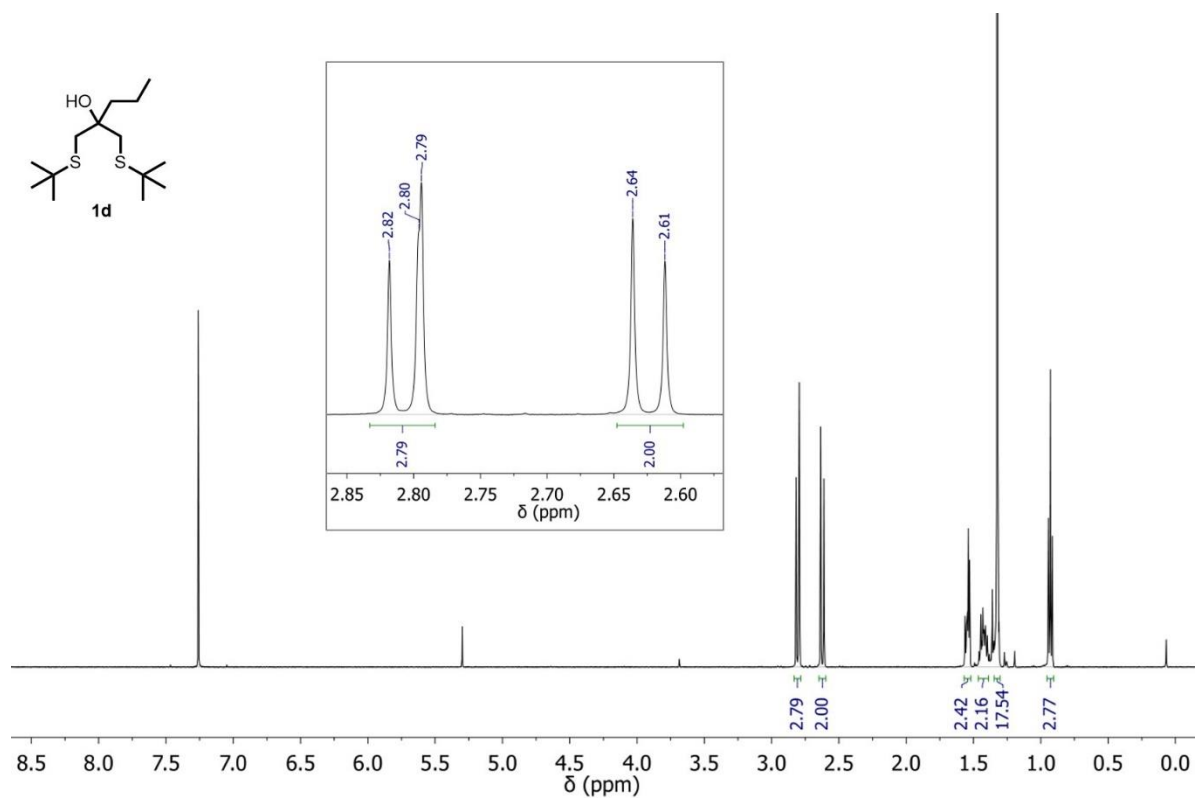


Figure S51. ¹H NMR spectrum of **1d** in CDCl₃.

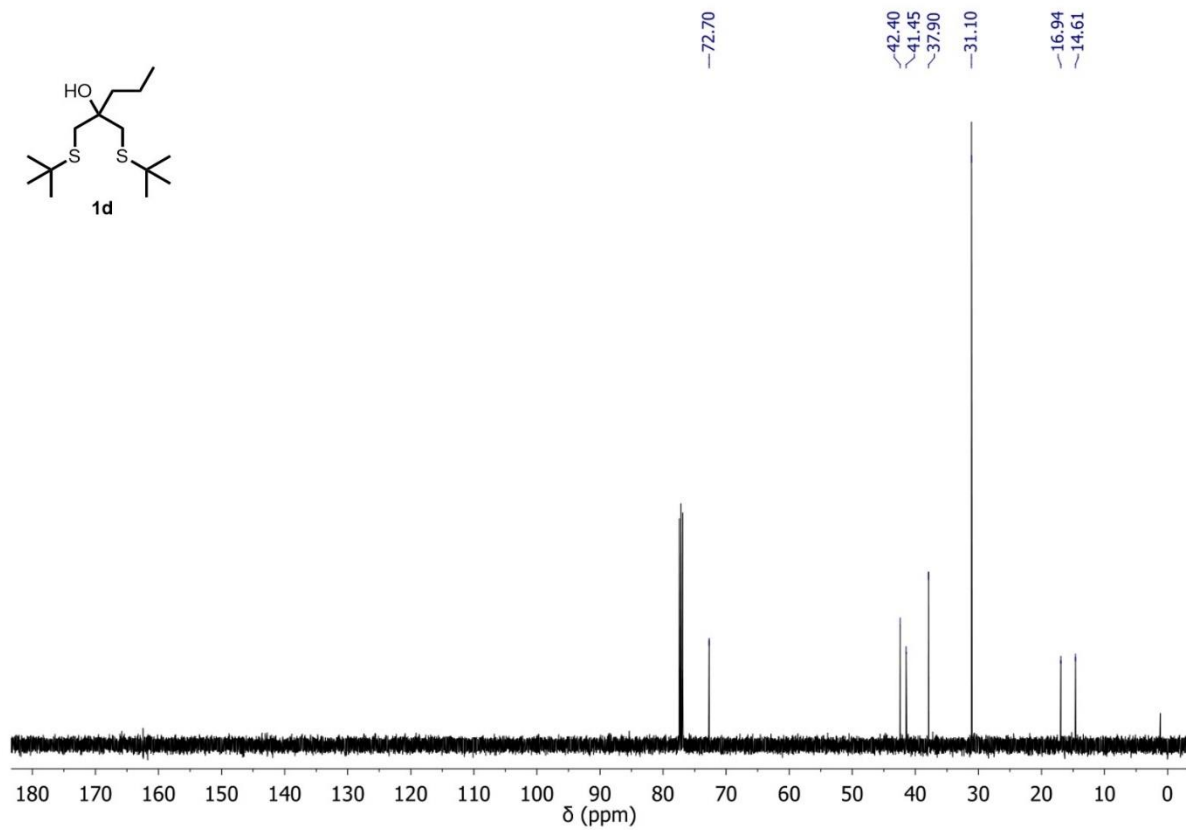


Figure S52. ¹³C NMR spectrum of **1d** in CDCl₃.

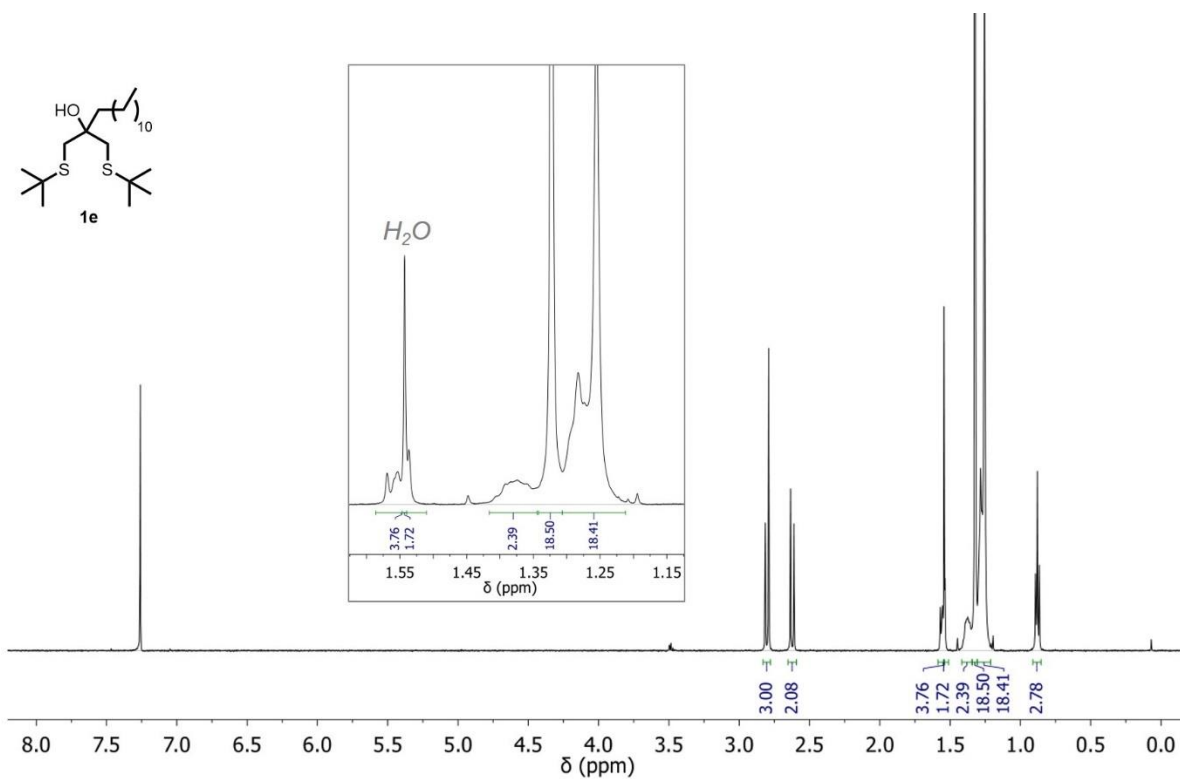


Figure S53. ^1H NMR spectrum of **1e** in CDCl_3 .

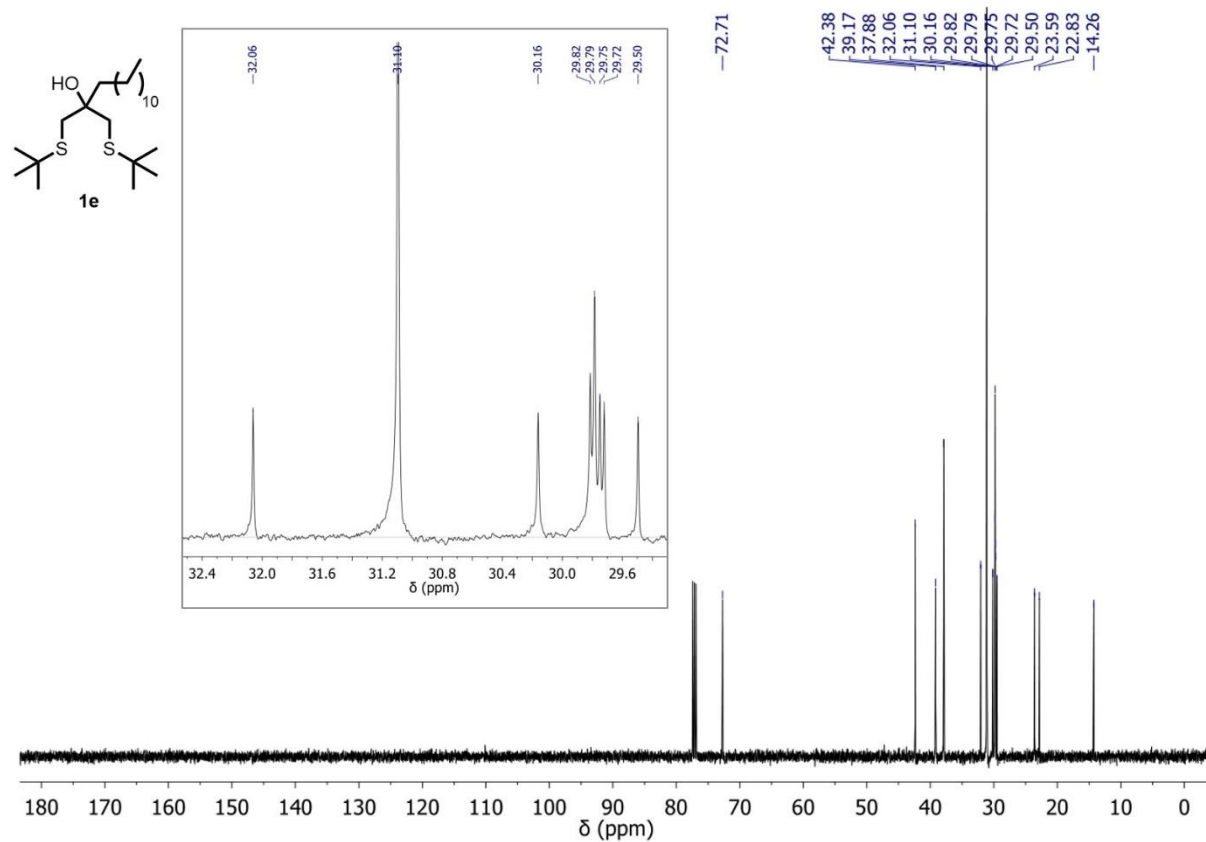


Figure S54. ^{13}C NMR spectrum of **1e** in CDCl_3 .

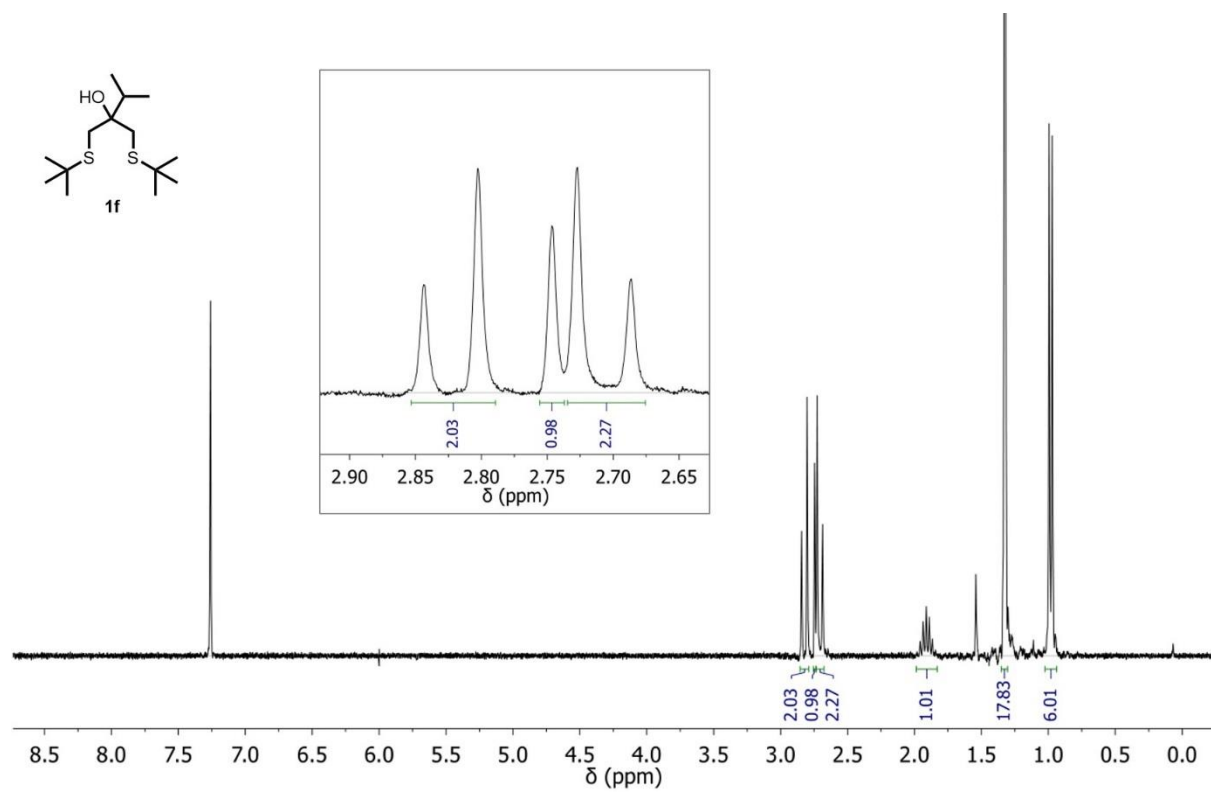


Figure S55. ¹H NMR spectrum of **1f** in CDCl₃.

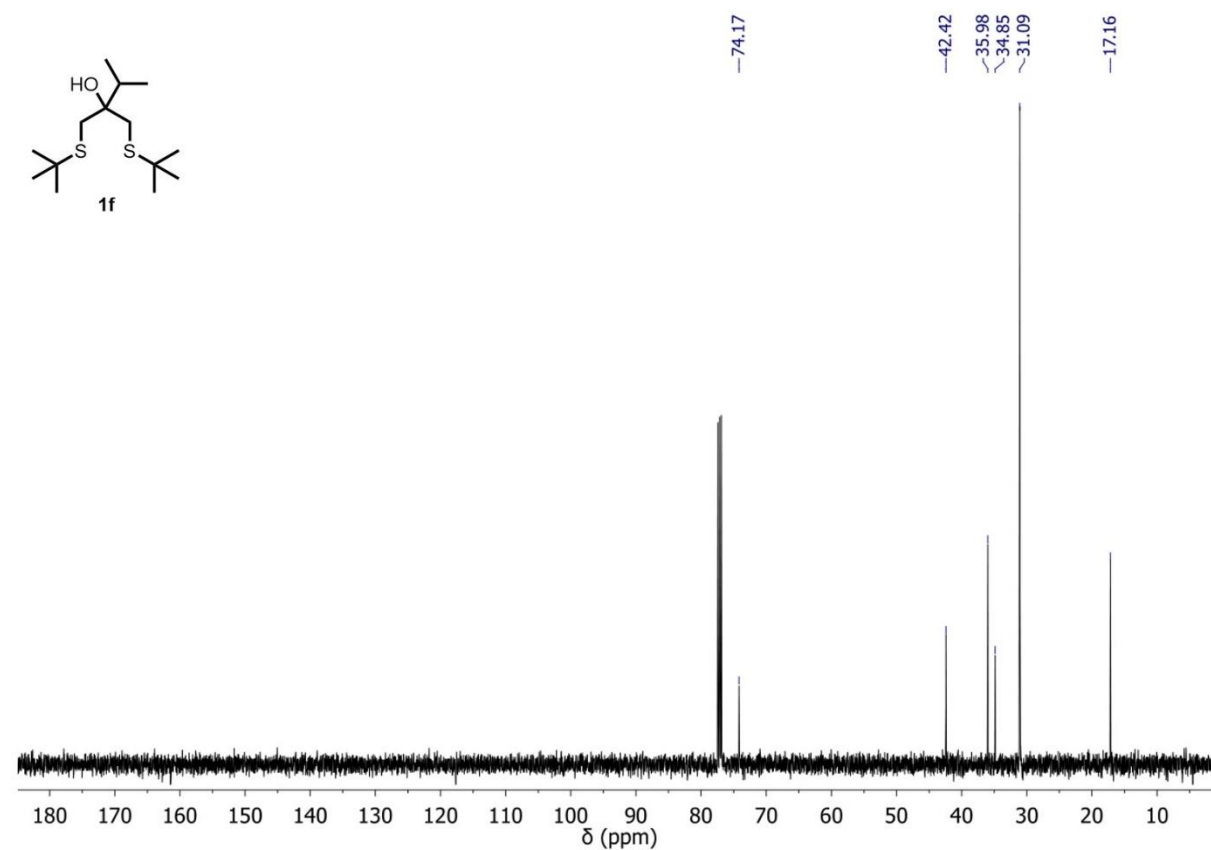


Figure S56. ¹³C NMR spectrum of **1f** in CDCl₃.

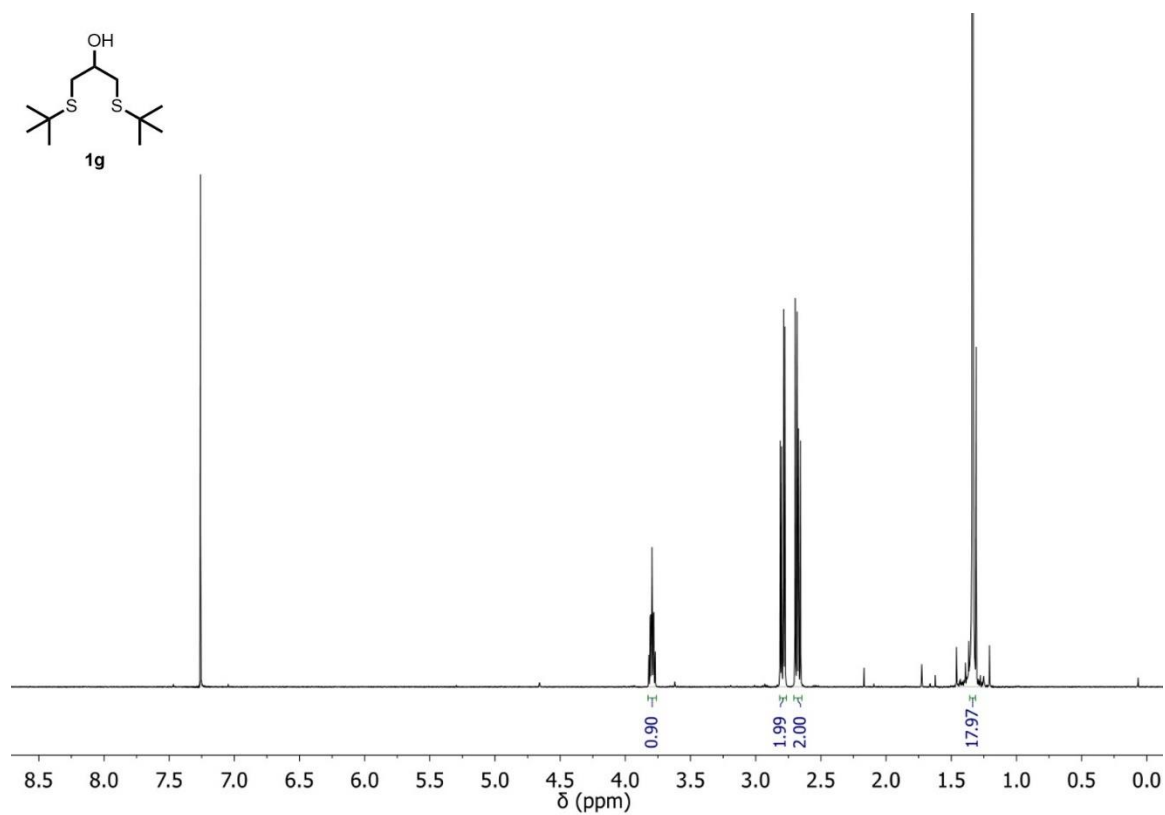


Figure S57. ¹H NMR spectrum of **1g** in CDCl₃.

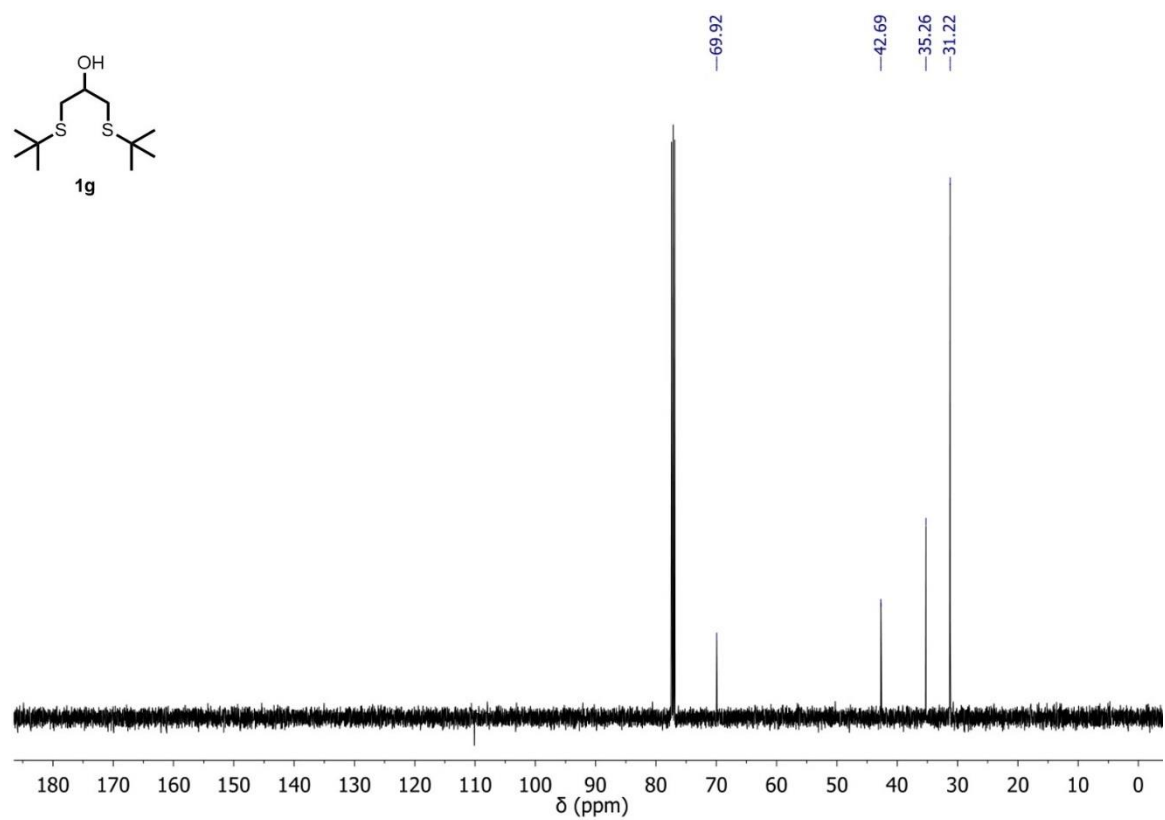


Figure S58. ¹³C NMR spectrum of **1g** in CDCl₃.

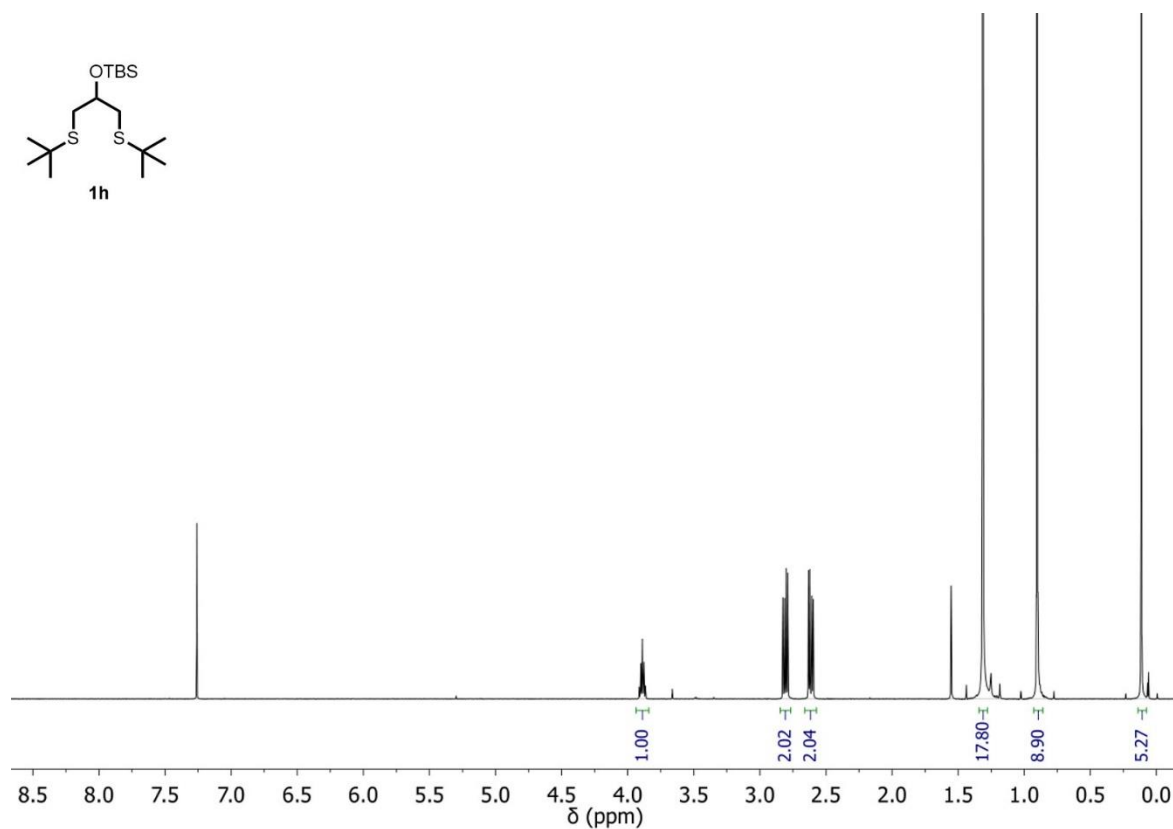


Figure S59. ¹H NMR spectrum of **1h** in CDCl₃.

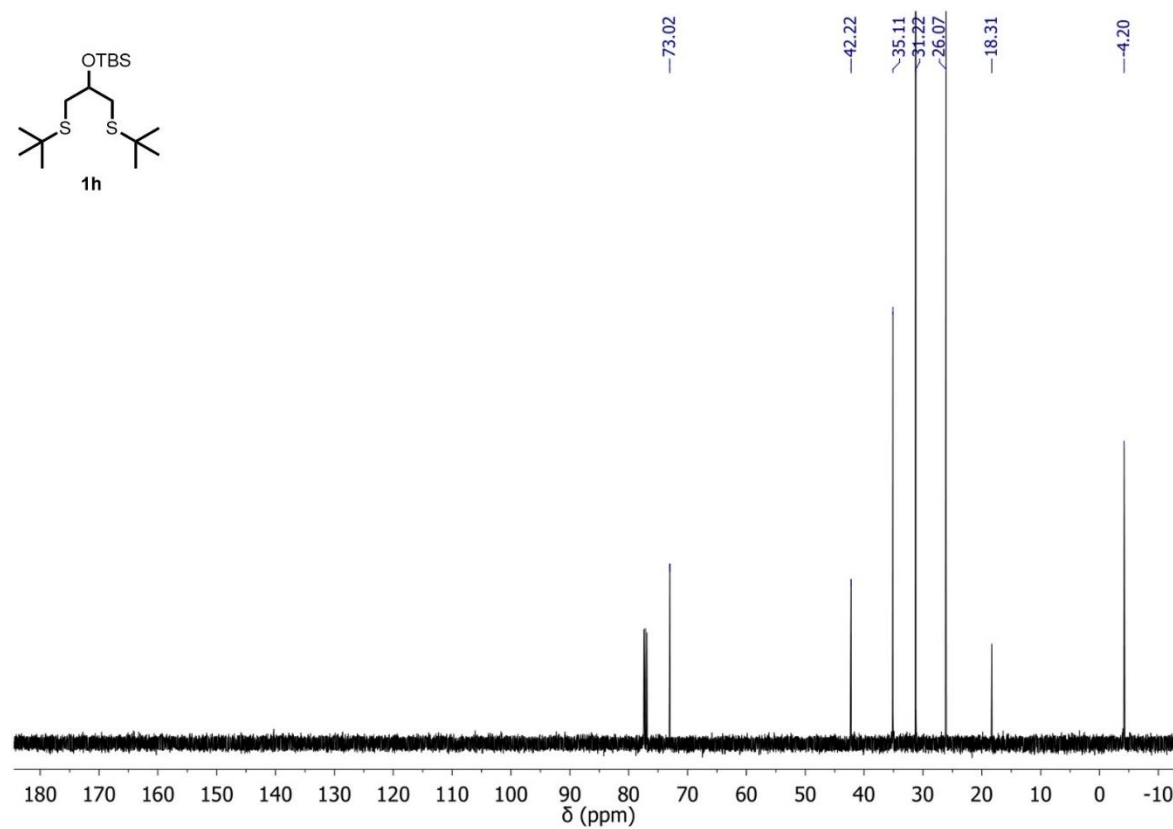


Figure S60. ¹³C NMR spectrum of **1h** in CDCl₃.

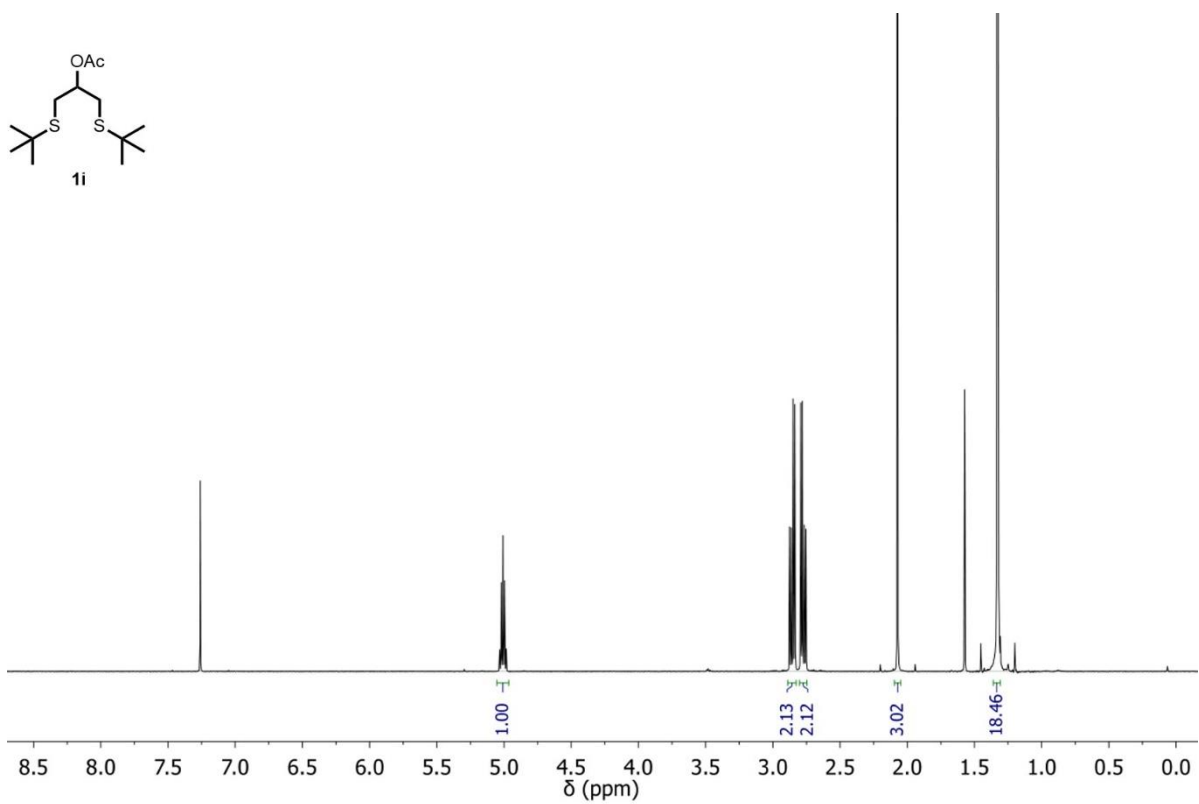


Figure S61. ¹H NMR spectrum of **1i** in CDCl₃.

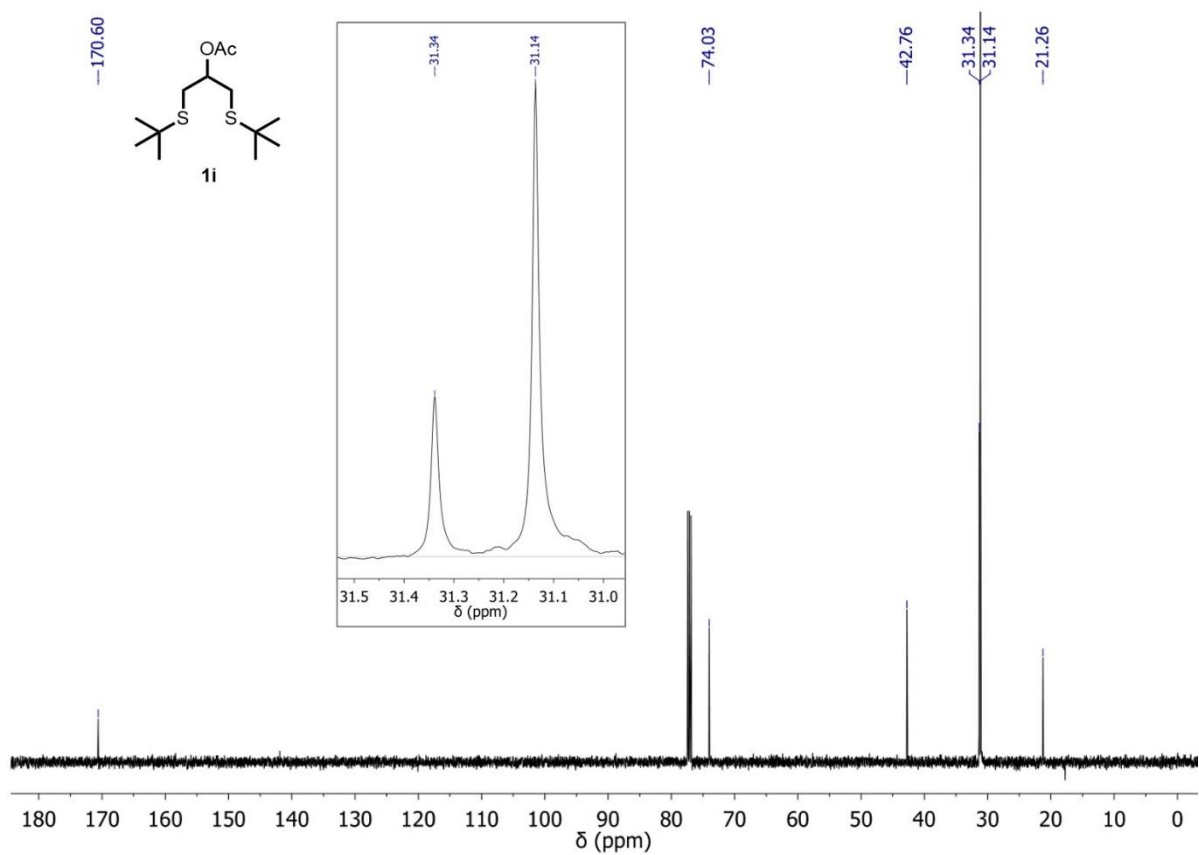


Figure S62. ¹³C NMR spectrum of **1i** in CDCl₃.

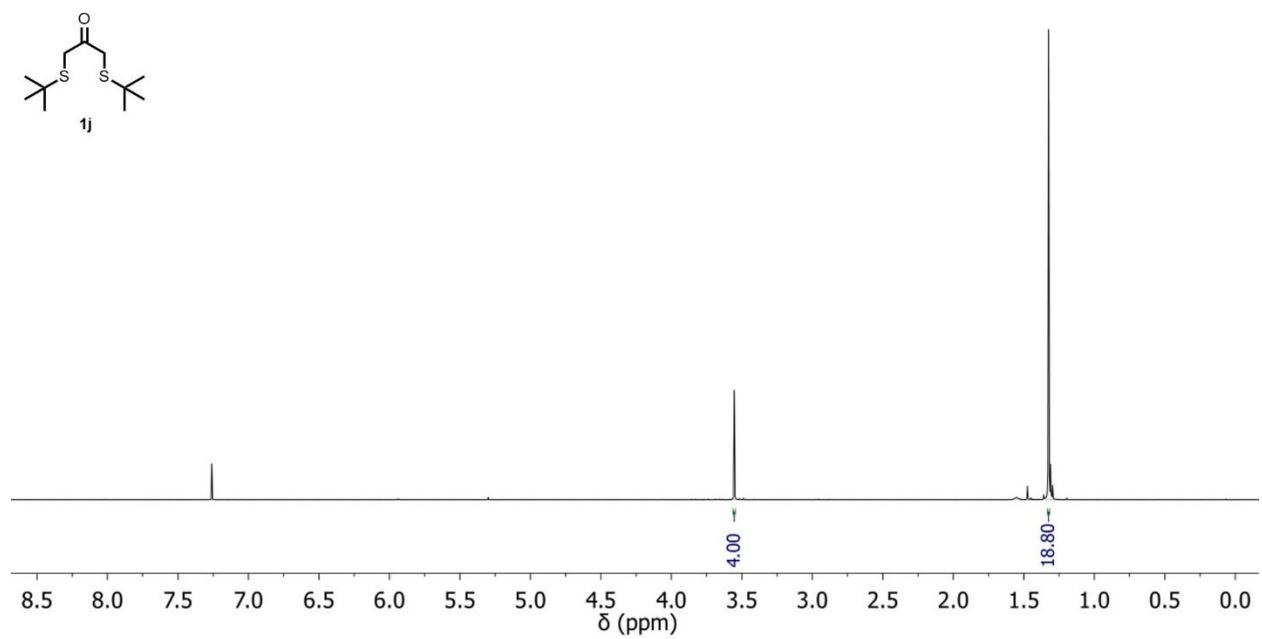


Figure S63. ^1H NMR spectrum of **1j** in CDCl_3 .

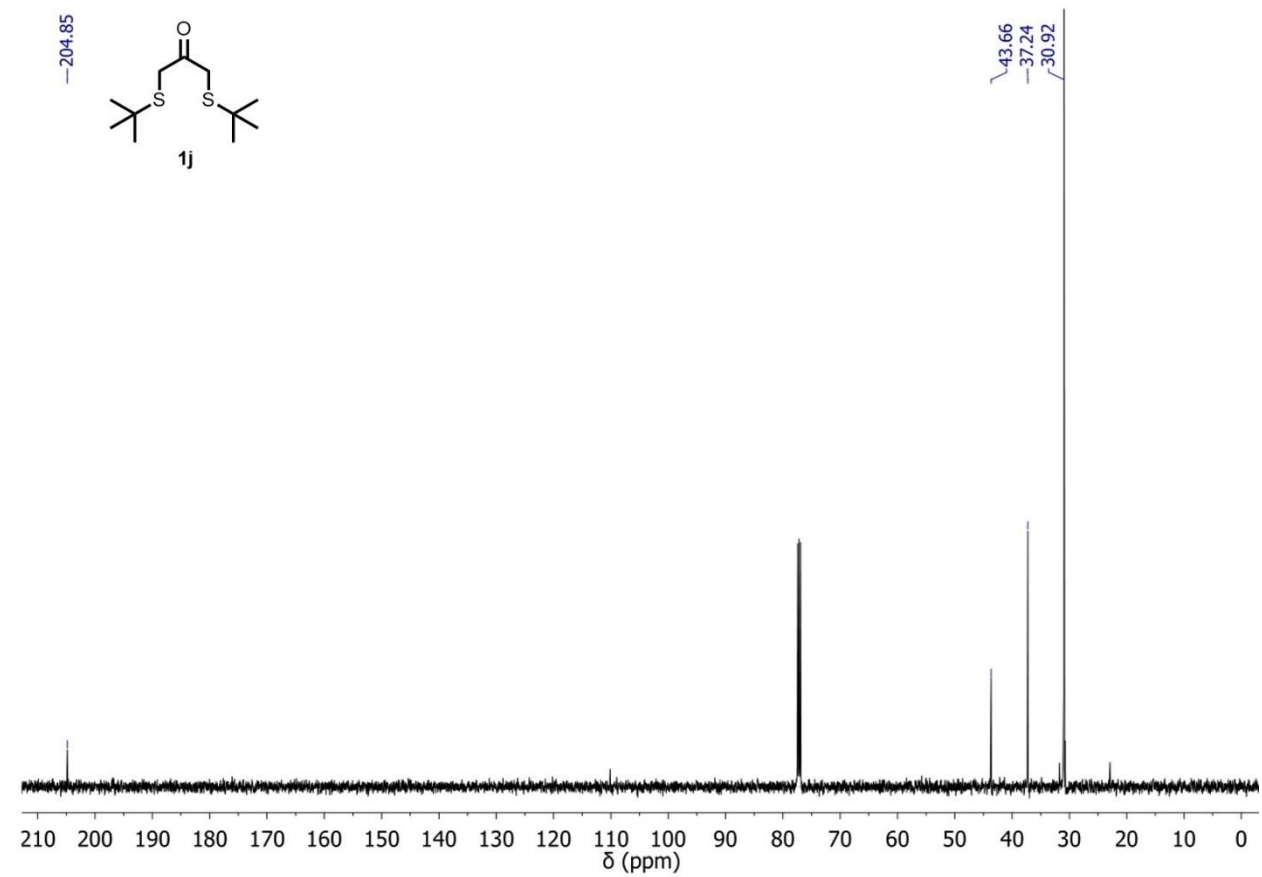


Figure S64. ^{13}C NMR spectrum of **1j** in CDCl_3 .

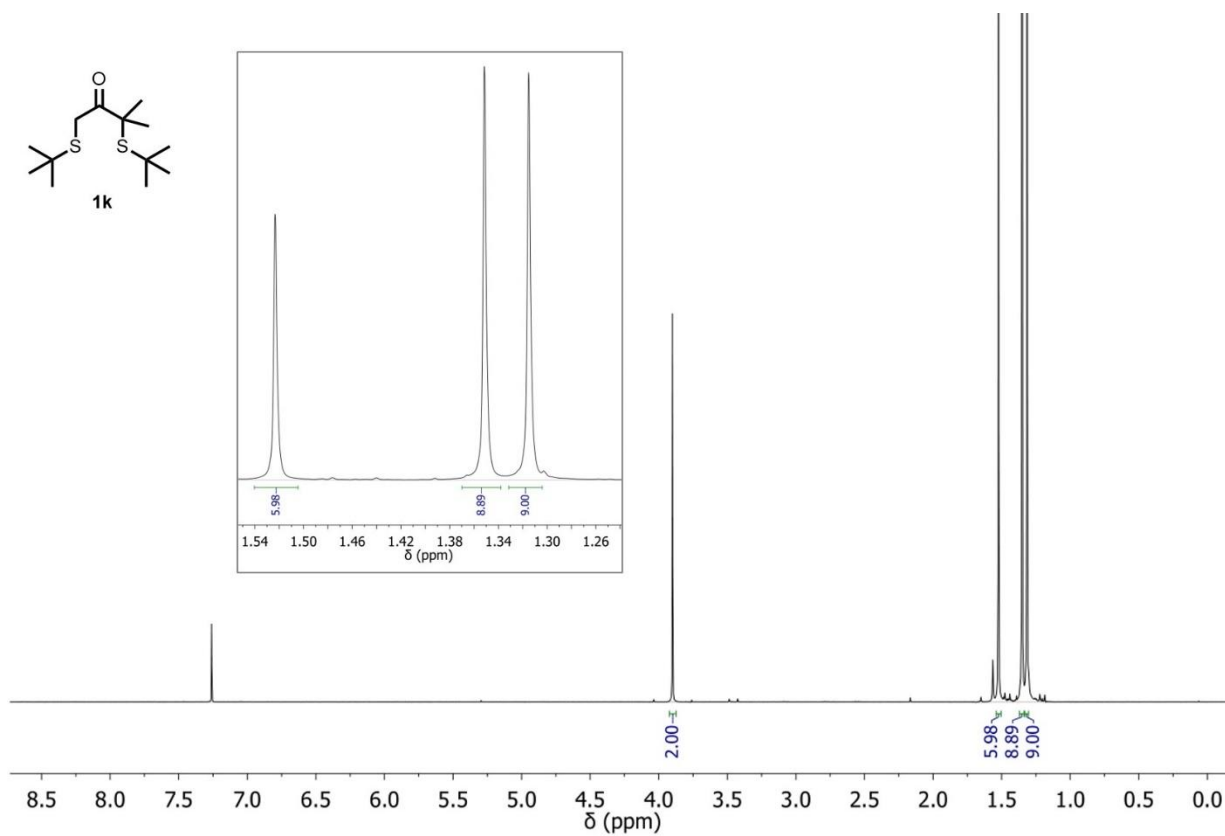


Figure S65. ¹H NMR spectrum of **1k** in CDCl₃.

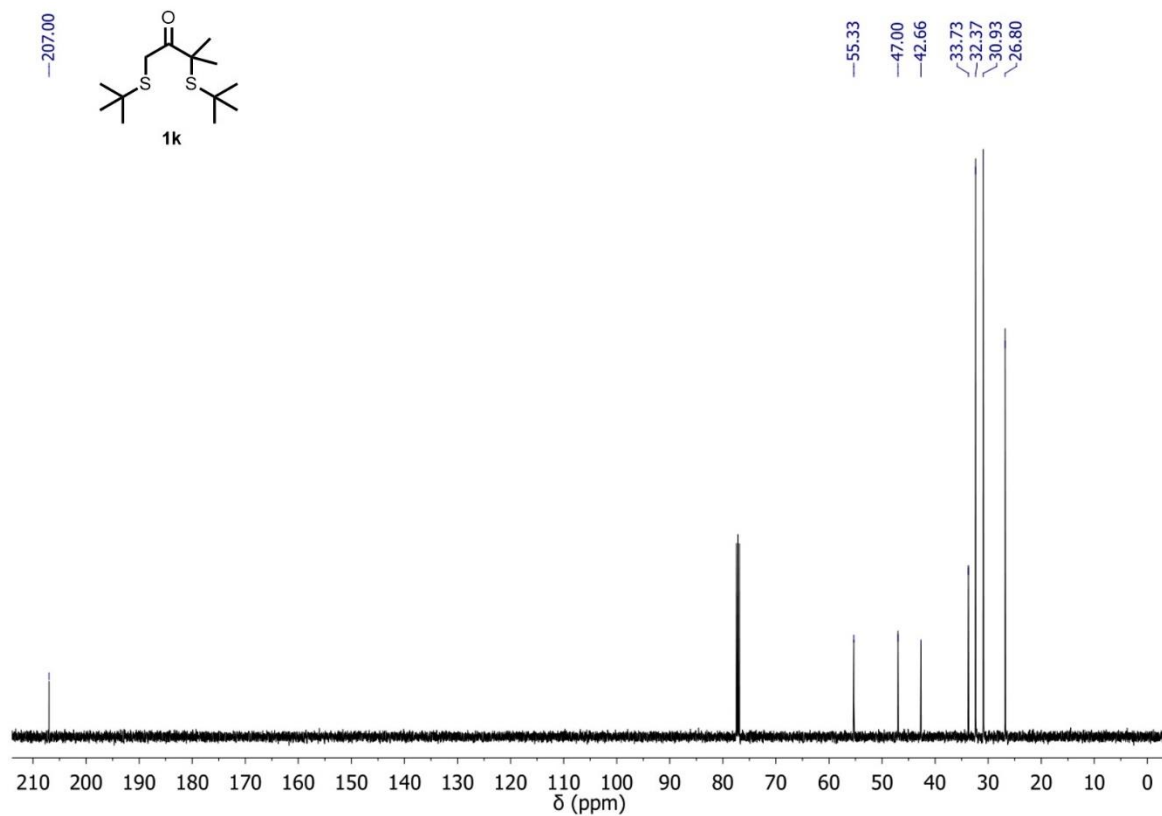


Figure S66. ¹³C NMR spectrum of **1k** in CDCl₃.

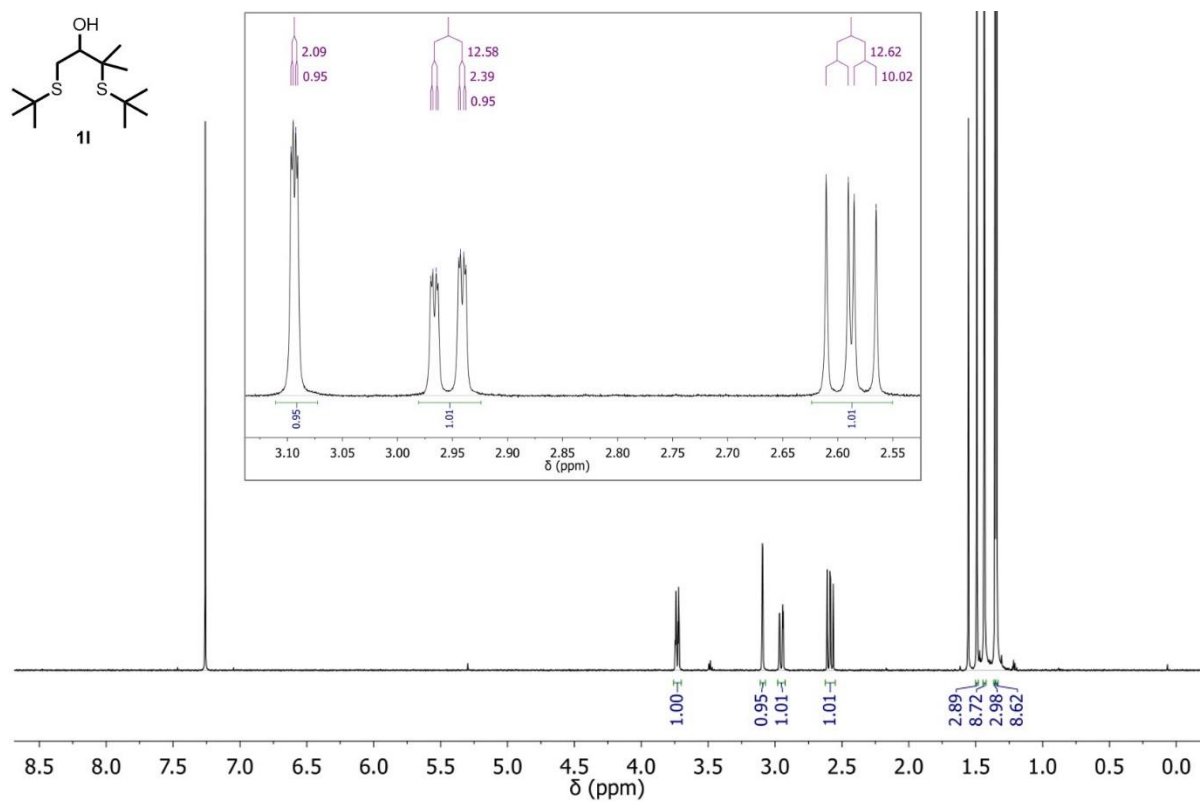


Figure S67. ¹H NMR spectrum of **11** in CDCl₃.

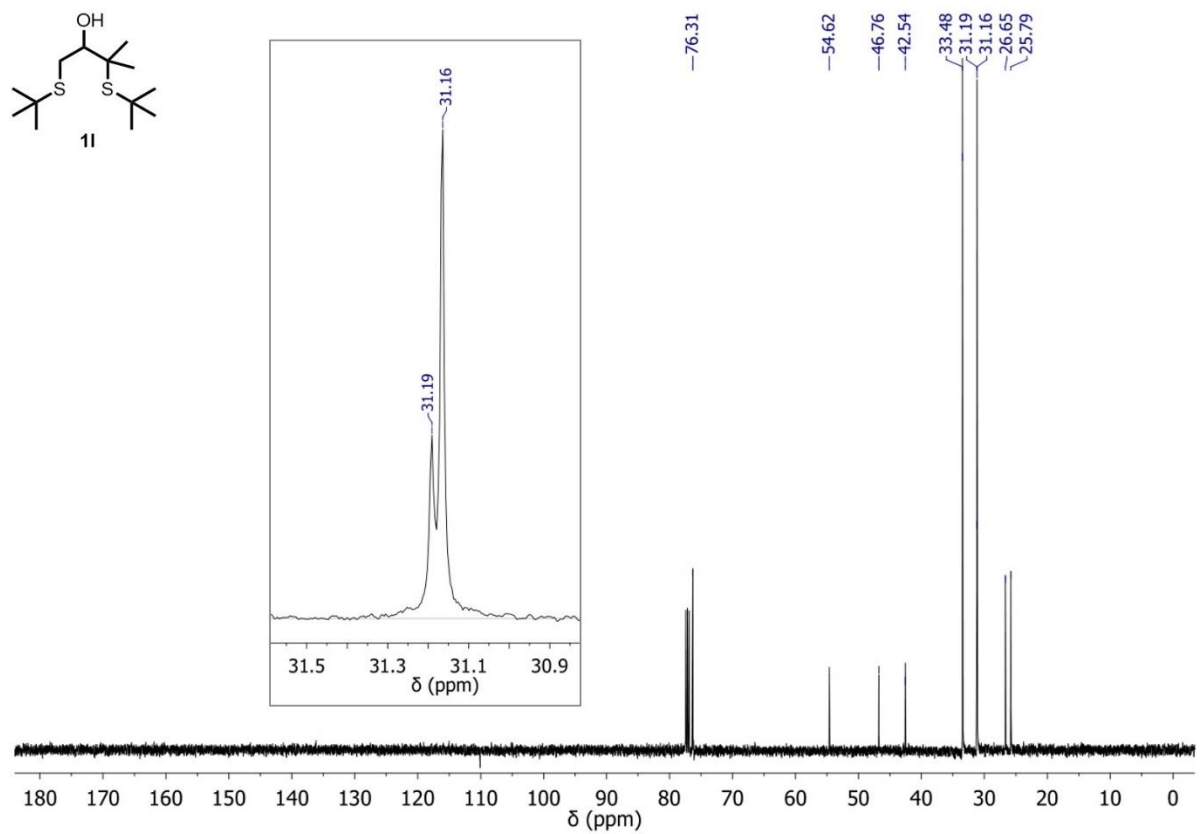


Figure S68. ¹³C NMR spectrum of **11** in CDCl₃.

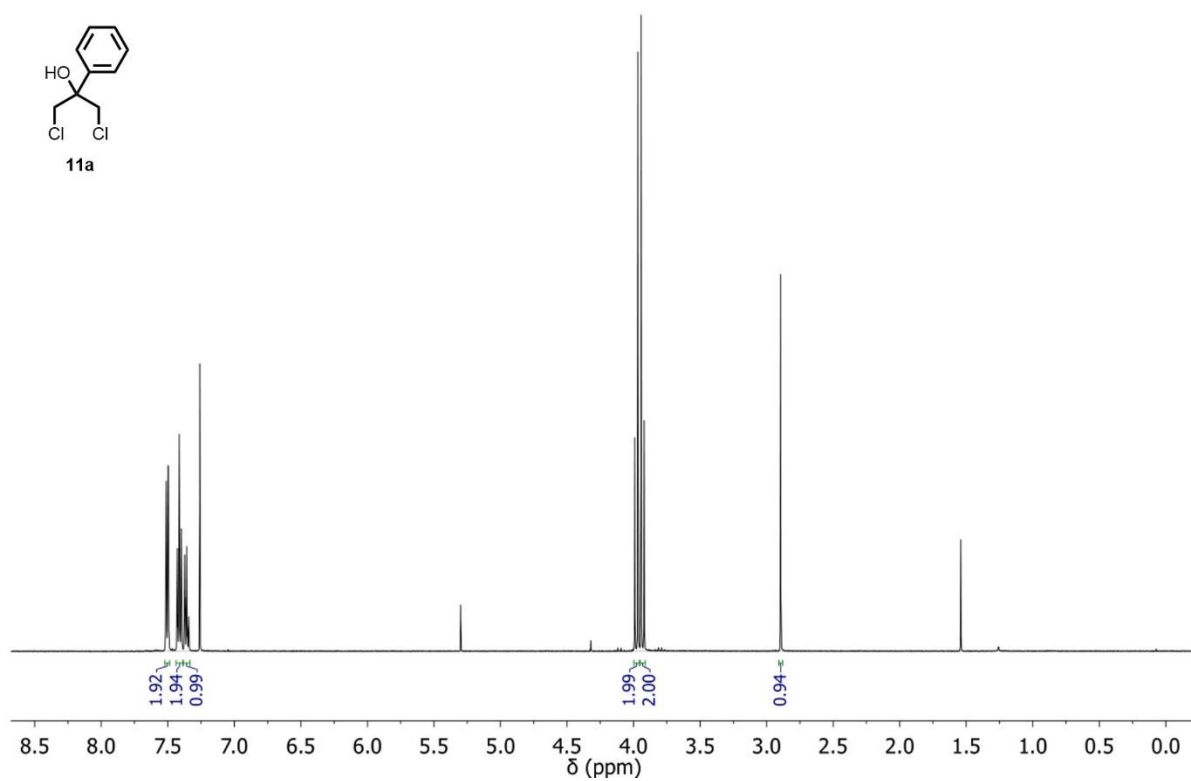


Figure S69. ^1H NMR spectrum of **11a** in CDCl_3 .

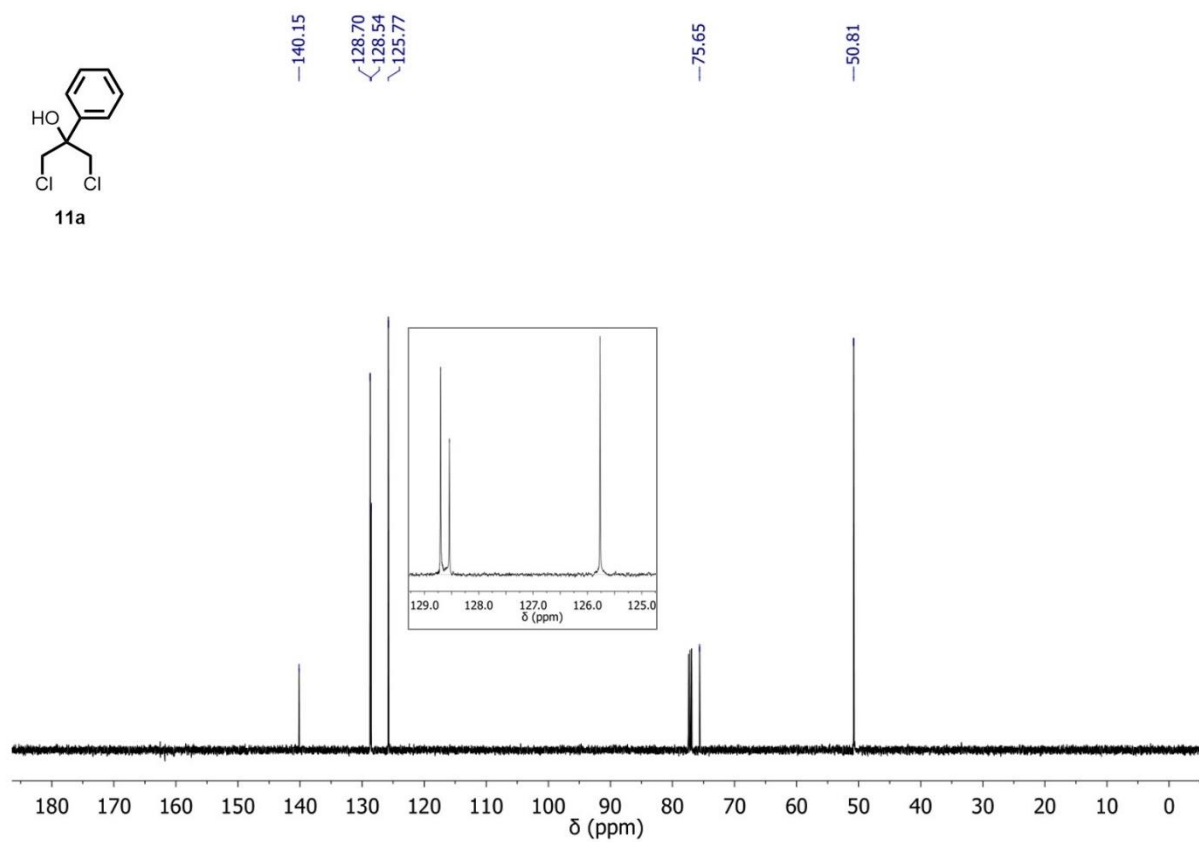


Figure S70. ^{13}C NMR spectrum of **11a** in CDCl_3 .

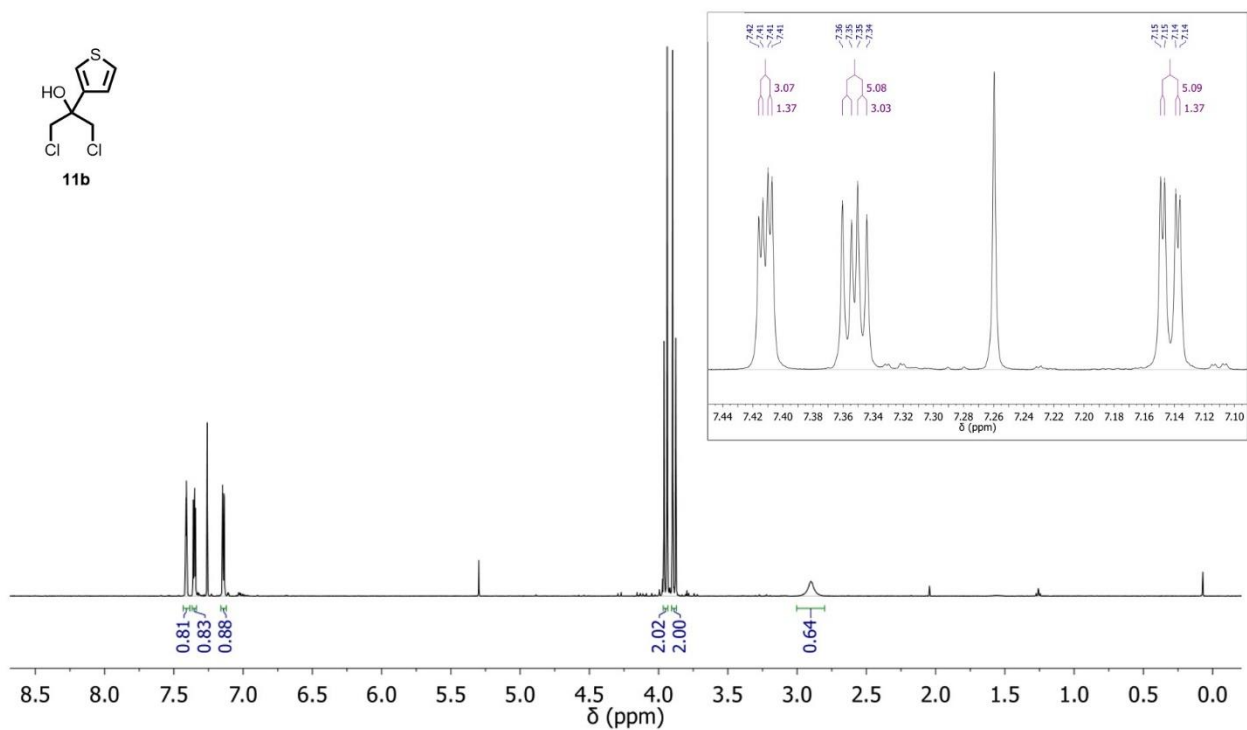


Figure S71. ^1H NMR spectrum of **11b** in CDCl_3 .

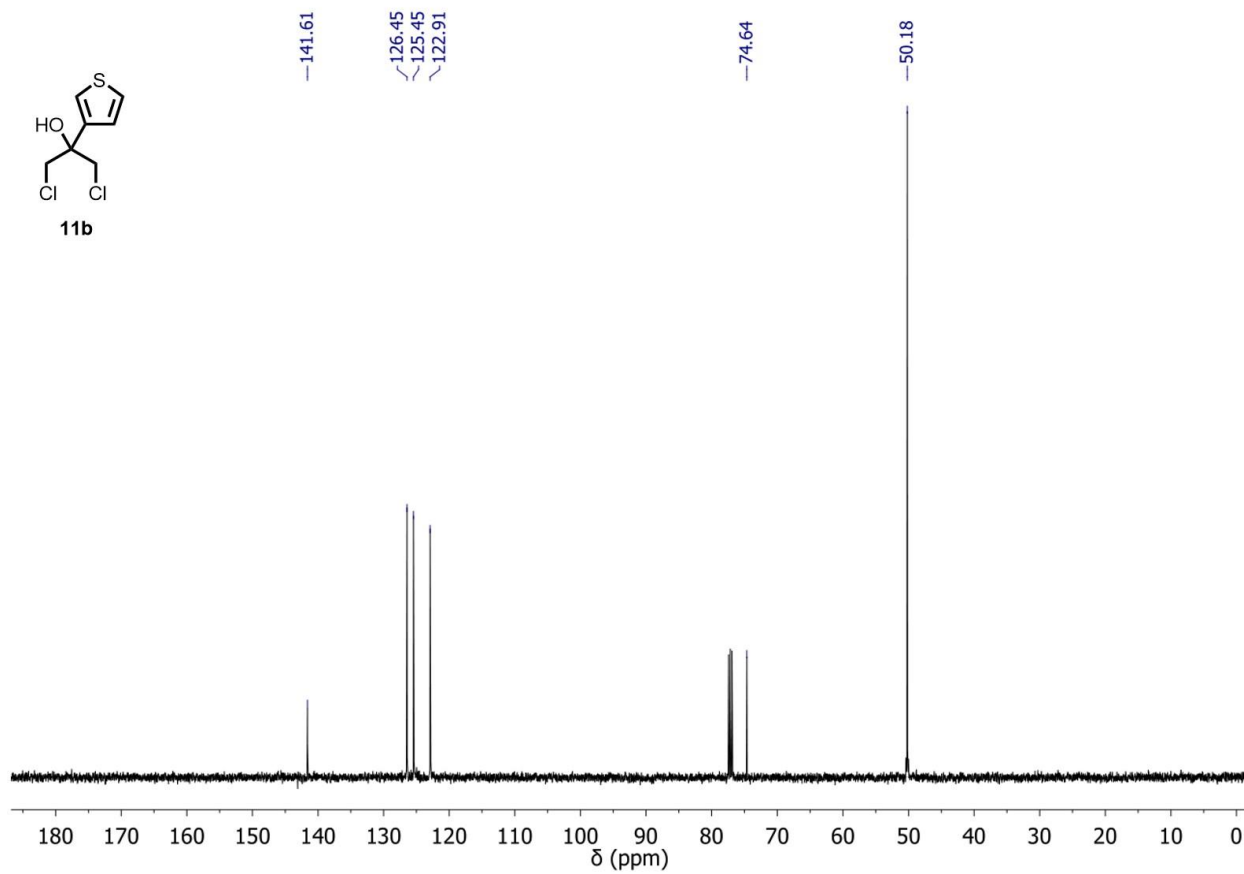


Figure S72. ^{13}C NMR spectrum of **11b** in CDCl_3 .

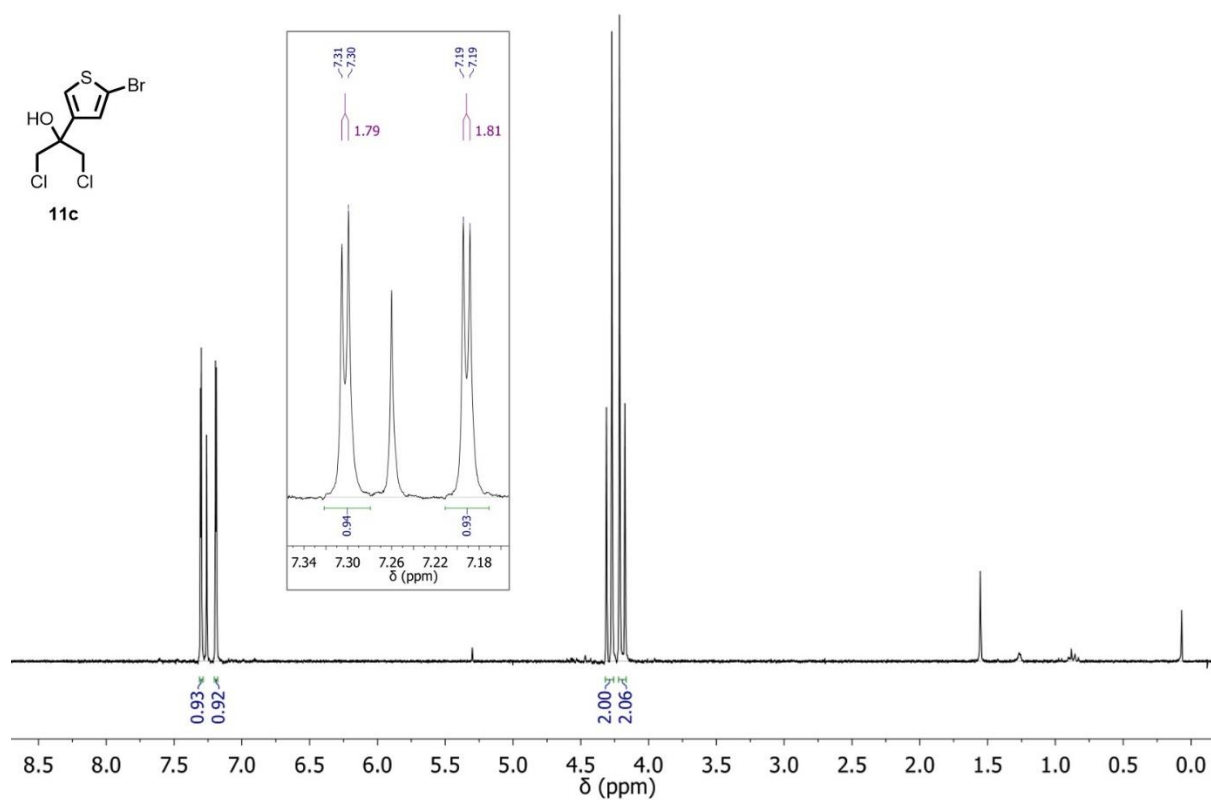


Figure S73. ^1H NMR spectrum of **1g** in CDCl_3 .

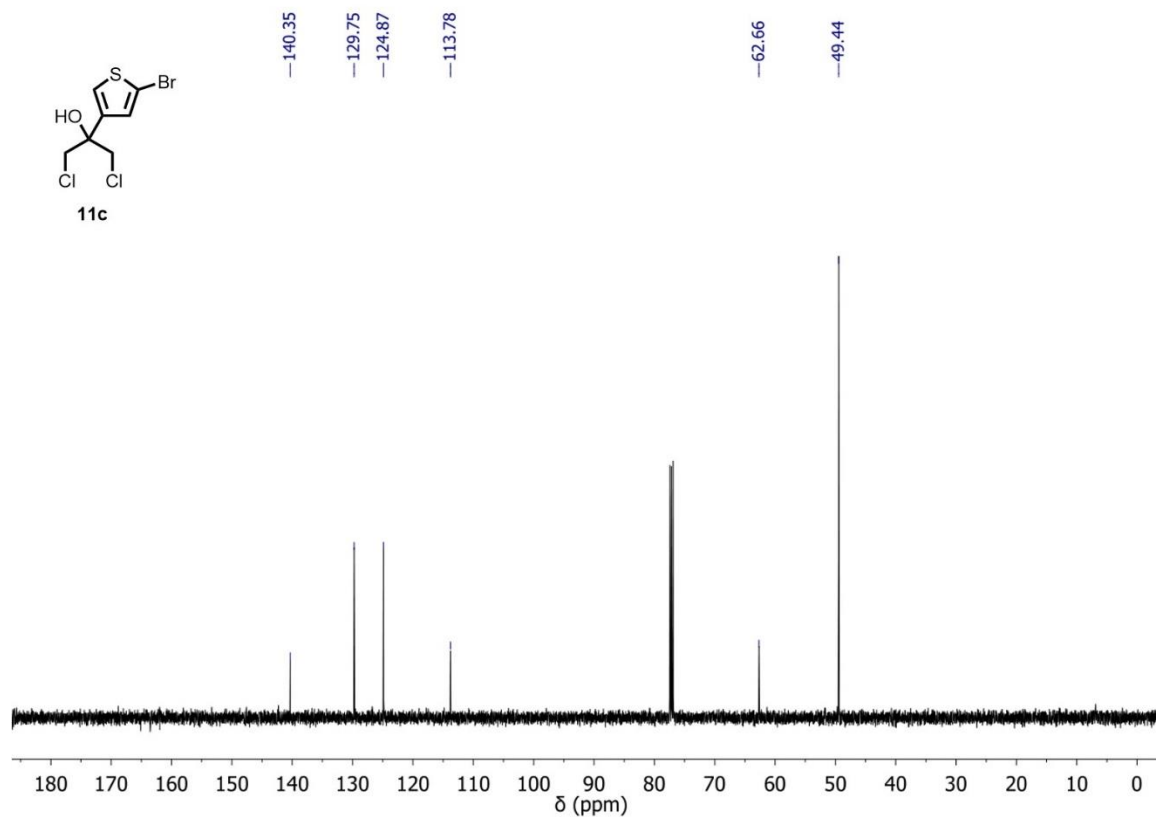


Figure S74. ^{13}C NMR spectrum of **1g** in CDCl_3 .

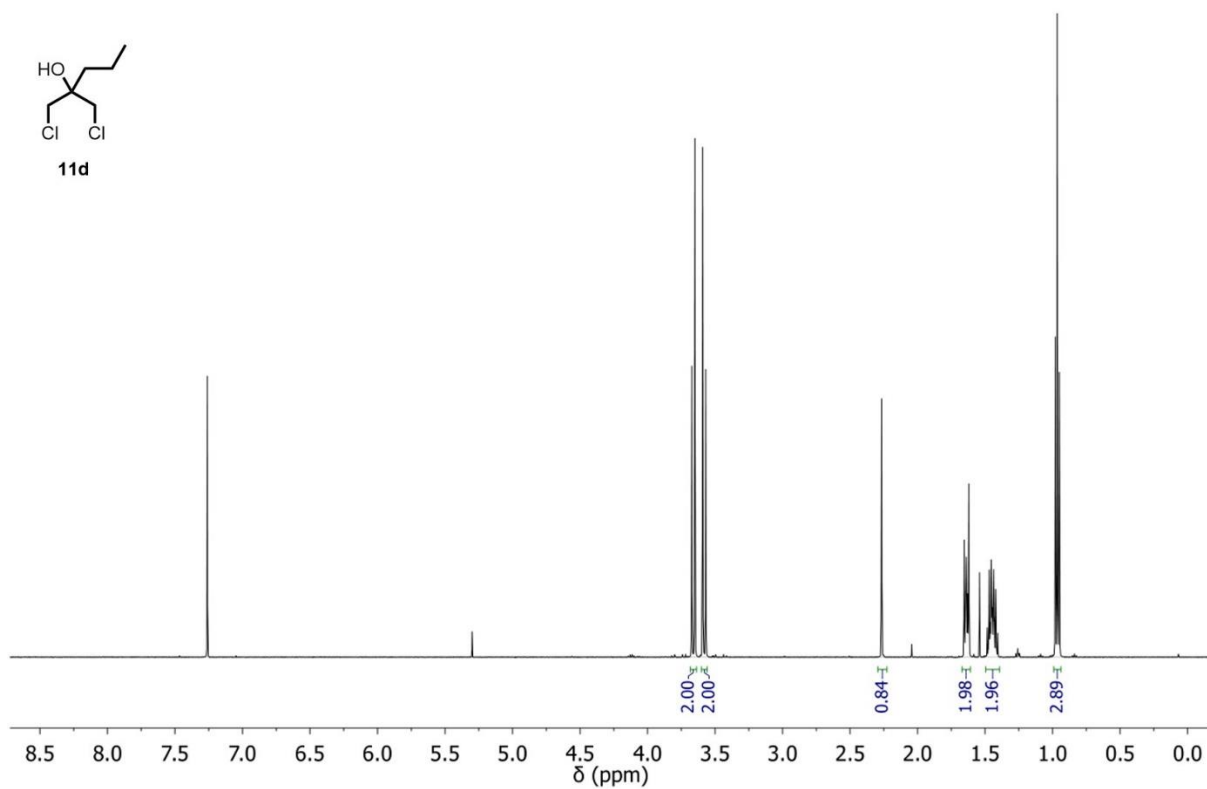


Figure S75. ^1H NMR spectrum of **11d** in CDCl_3 .

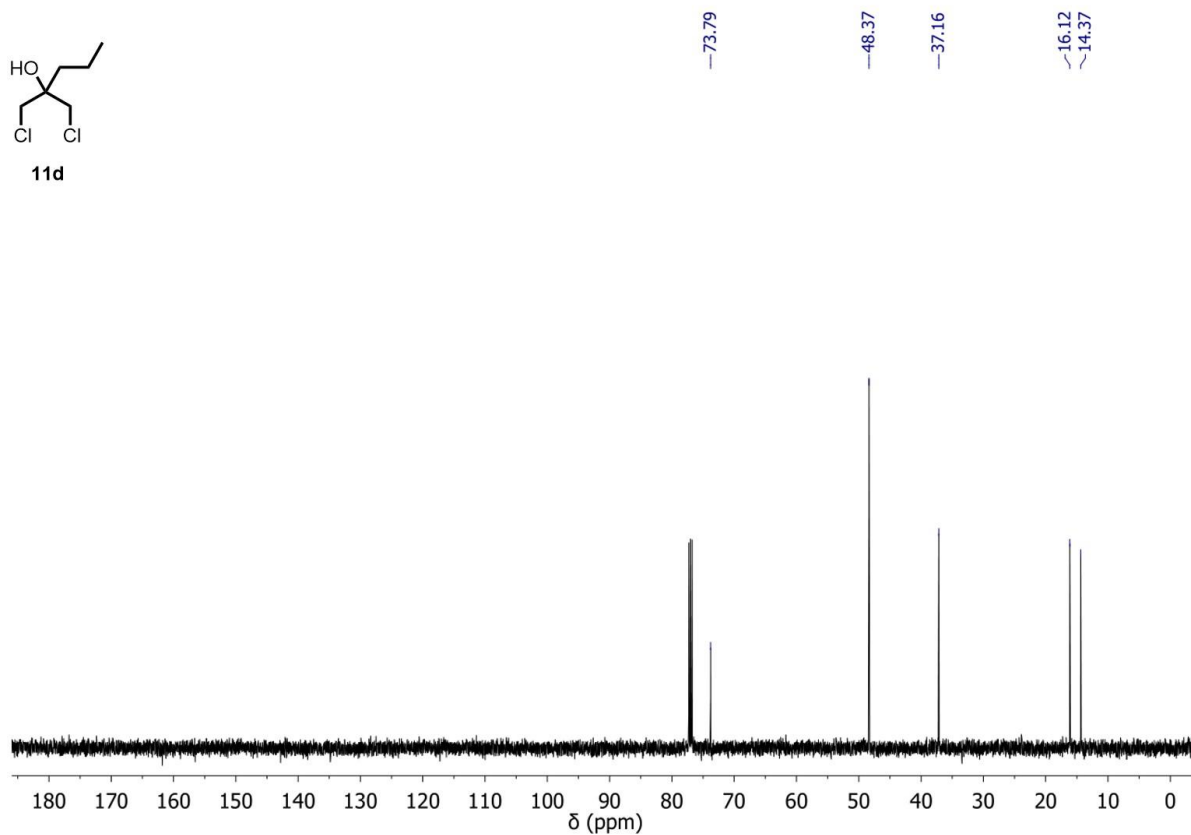
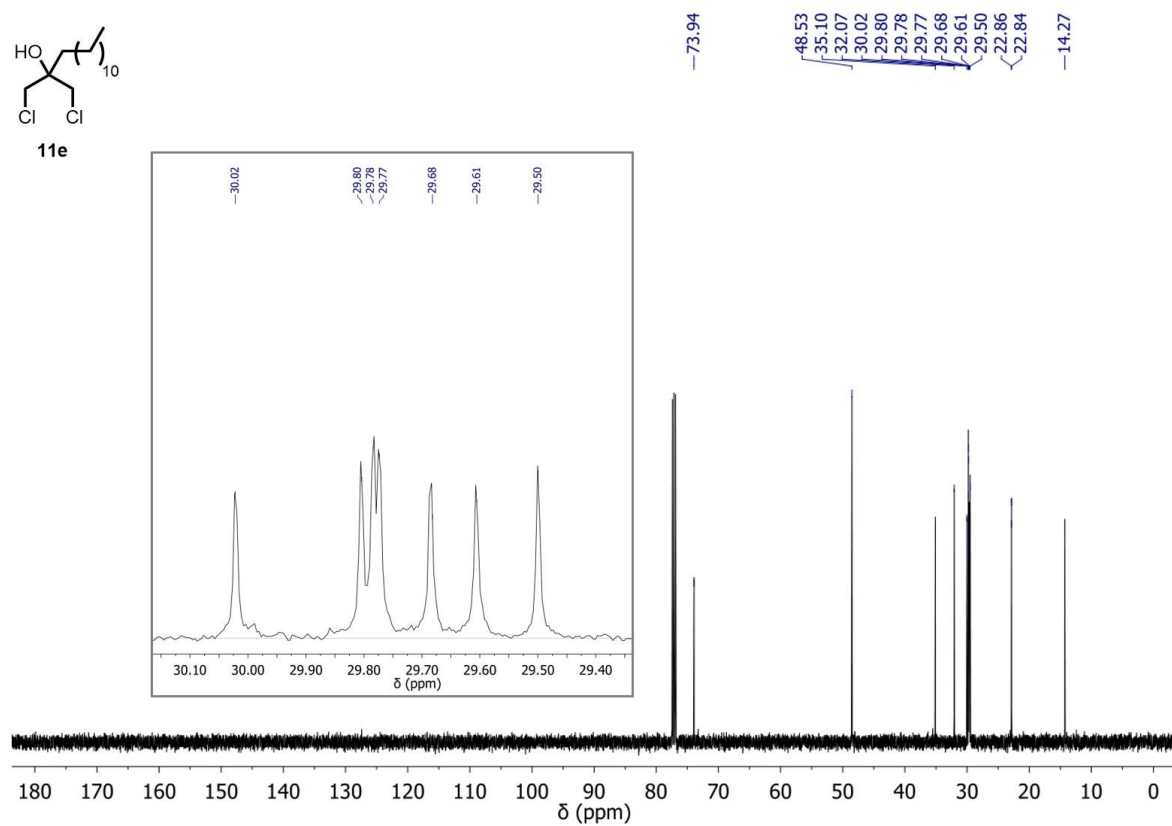
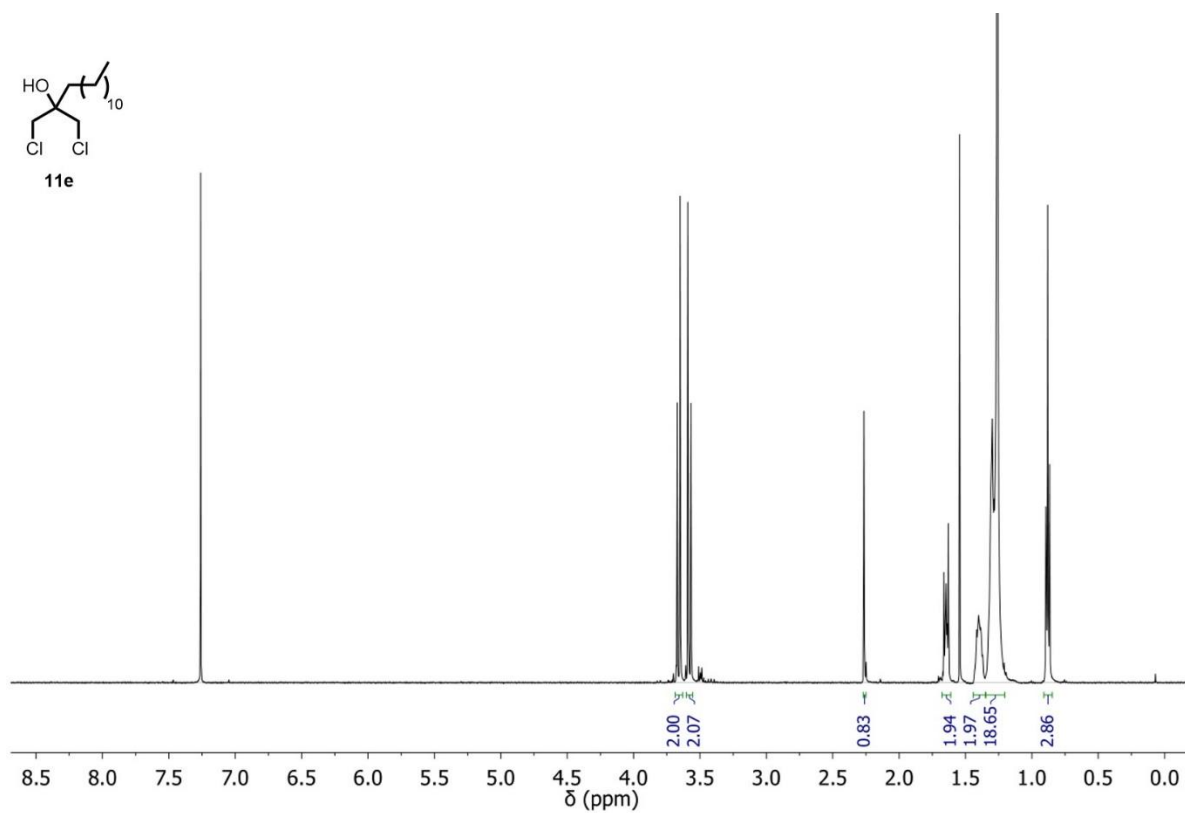


Figure S76. ^{13}C NMR spectrum of **11d** in CDCl_3 .



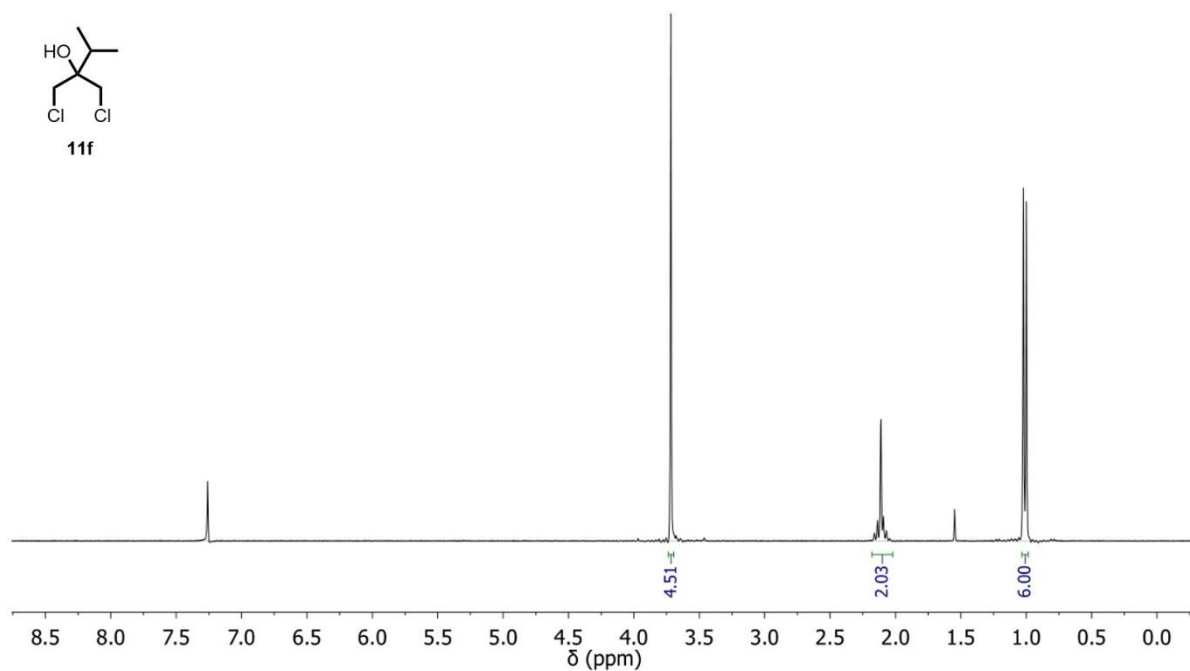


Figure S79. ^1H NMR spectrum of **11f** in CDCl_3 .

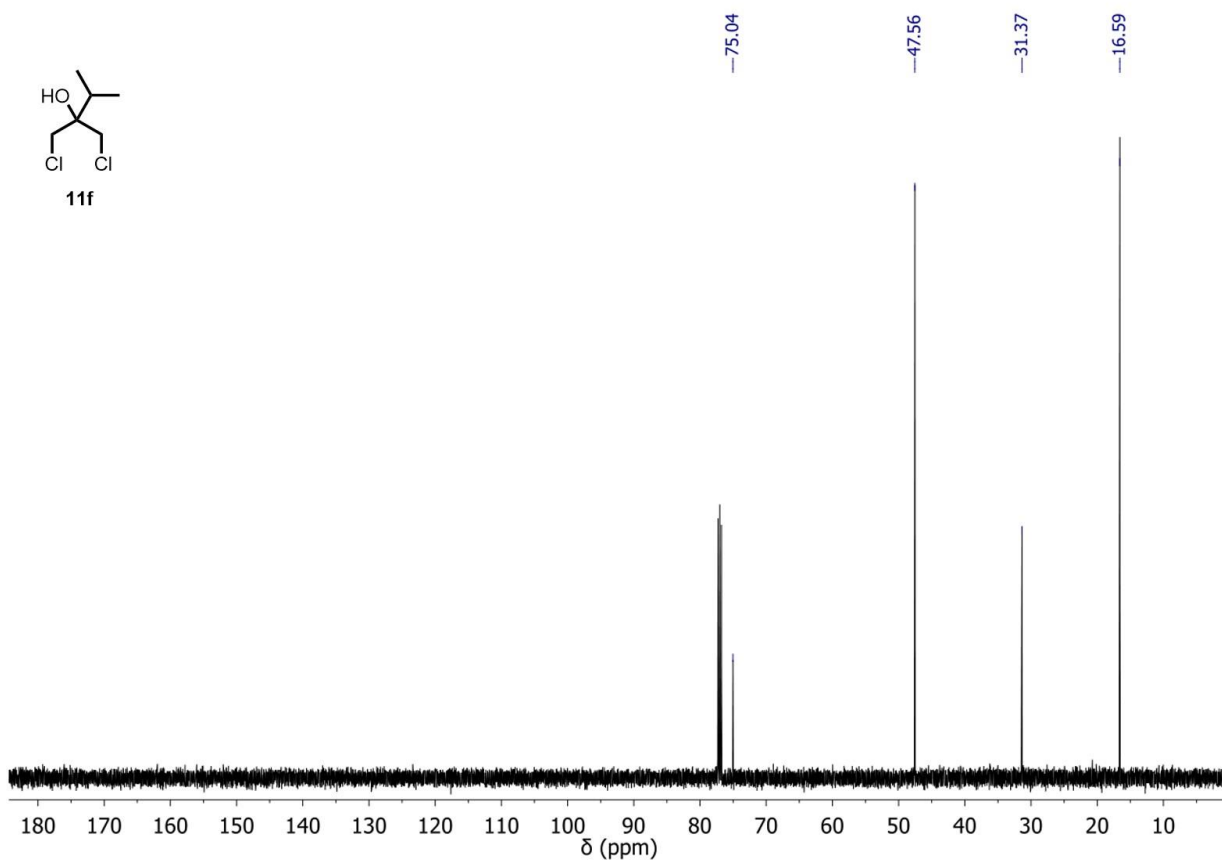


Figure S80. ^{13}C NMR spectrum of **11f** in CDCl_3 .

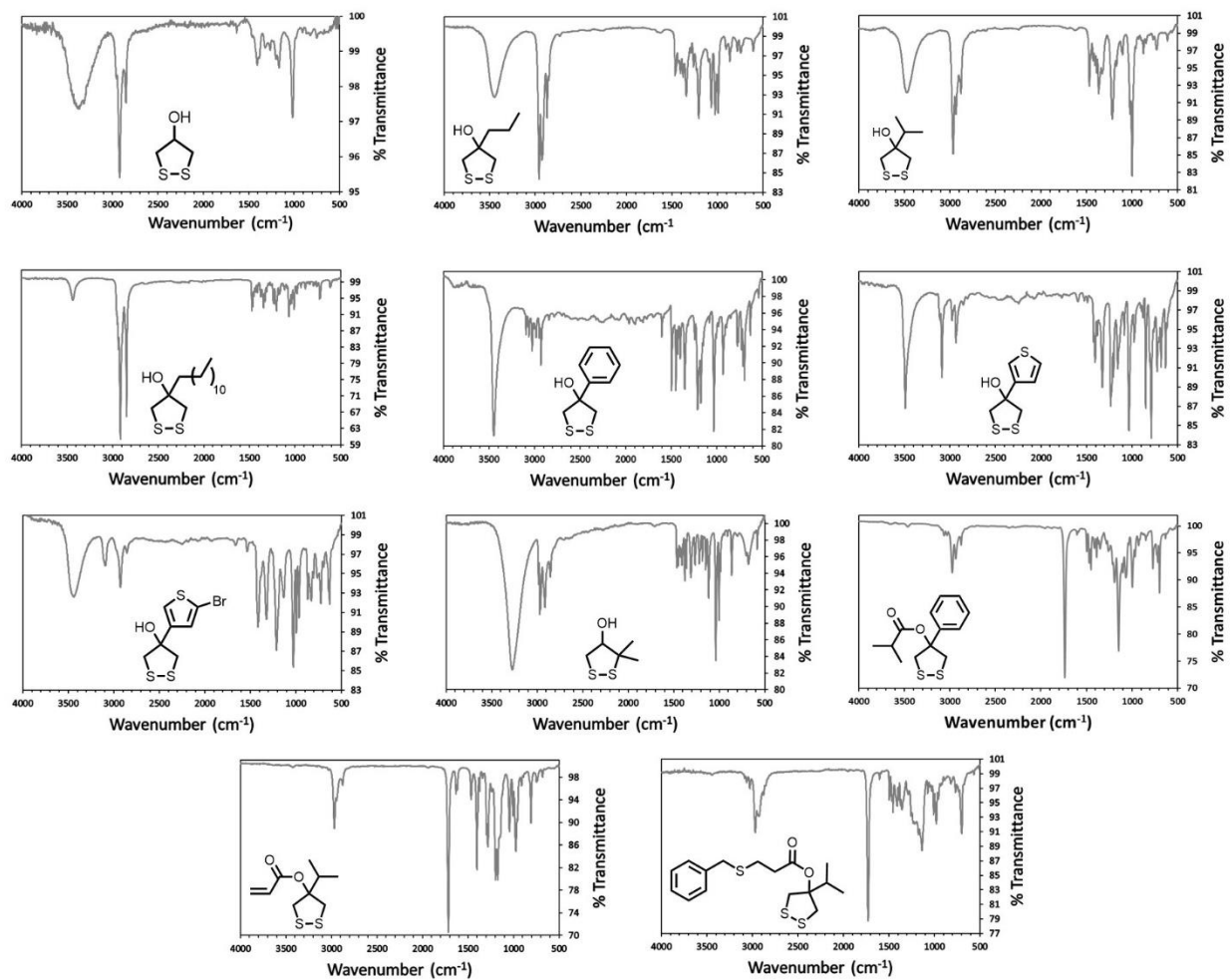


Figure S81. FTIR spectra of the 1,2-dithiolane products.

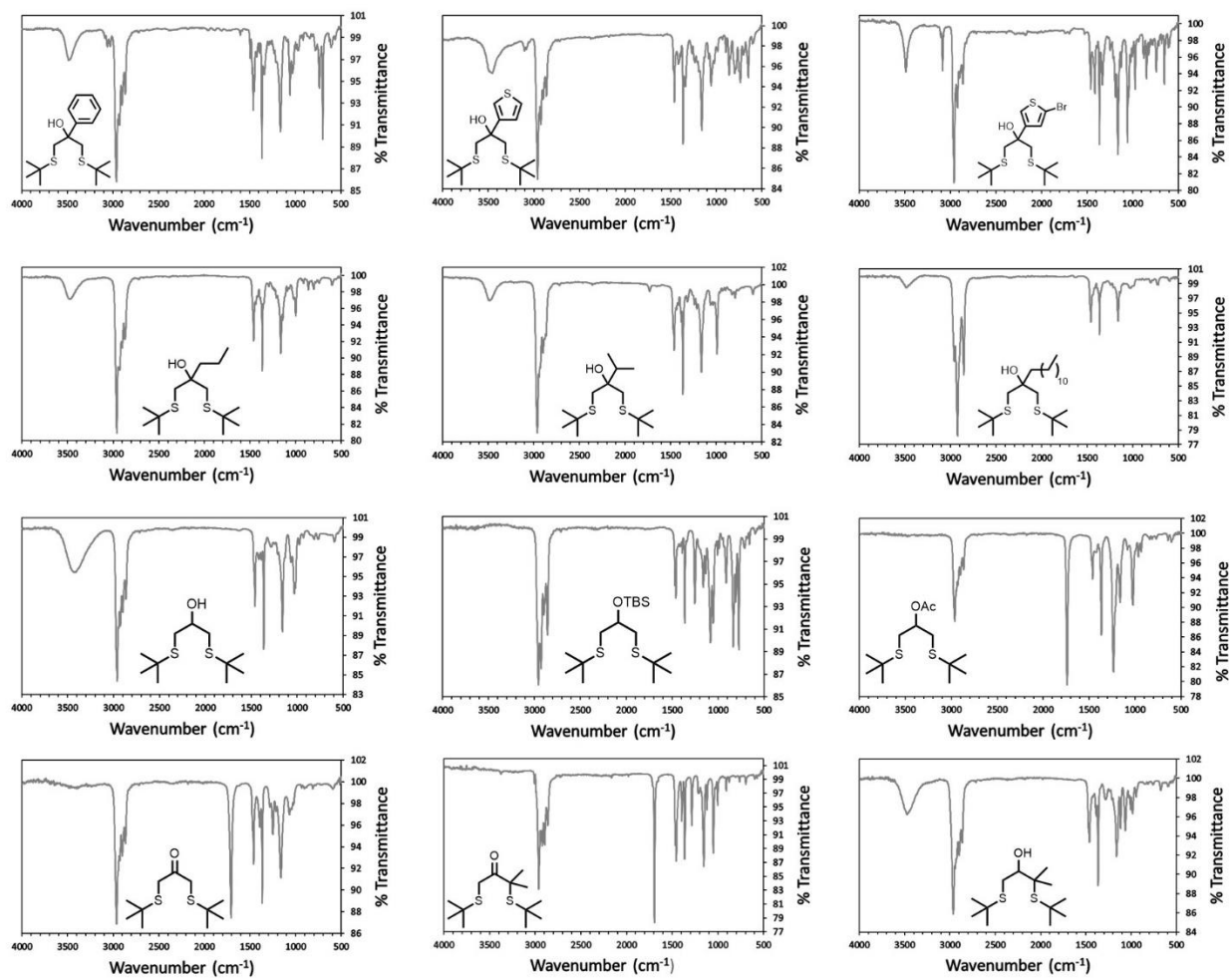


Figure S82. FTIR spectra of the 1,3-bis-*tert*-butyl thioether substrates.

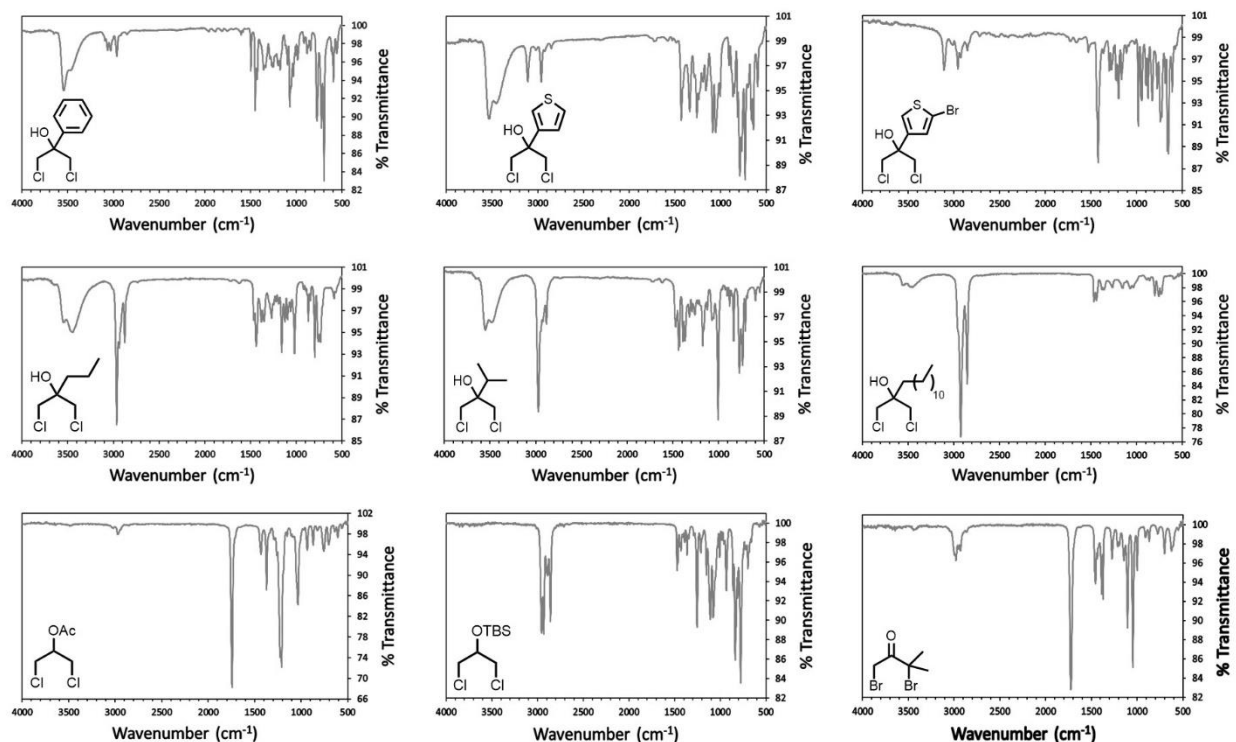


Figure S83. FTIR spectra of the 1,3-dihalide starting materials.

S8. X-Ray Crystallography

X-Ray Intensity data were collected at 100 K on a Bruker D8 Venture diffractometer using MoKa radiation ($\lambda = 0.71073 \text{ \AA}$) and a Photon III area detector.

Raw data frames were read by program SAINT¹ and integrated using 3D profiling algorithms. The resulting data were reduced to produce hkl reflections and their intensities and estimated standard deviations. The data were corrected for Lorentz and polarization effects and numerical absorption corrections were applied based on indexed and measured faces.

SHELXTL6 (2008). Bruker-AXS, Madison, Wisconsin, USA.

SHELXTL2014 (2014). Bruker-AXS, Madison, Wisconsin, USA.

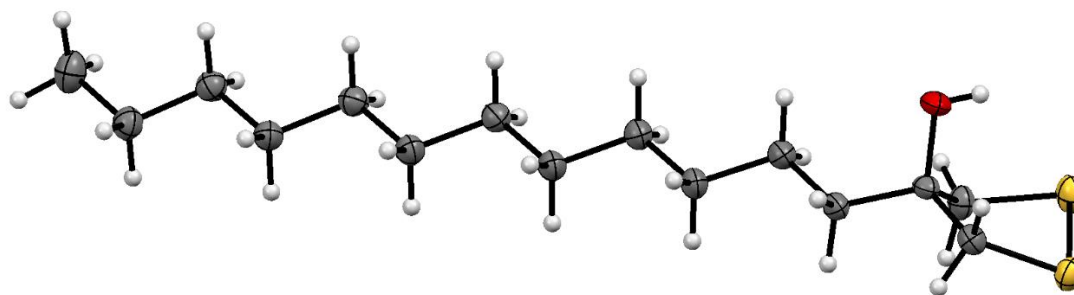


Figure S84. Molecular structure of **C12DL** with thermal displacement ellipsoids drawn at the 50% probability level.

The structure was solved and refined in SHELXTL2014, using full-matrix least-squares refinement. The non-H atoms were refined with anisotropic thermal parameters and all of the H atoms were calculated in idealized positions and refined riding on their parent atoms. In the final cycle of refinement, 4854 reflections (of which 4580 are observed with $I > 2s(I)$) were used to refine 168 parameters and the resulting R1, wR2 and S (goodness of fit) were 2.78%, 6.89% and 1.100, respectively. The refinement was carried out by minimizing the wR2 function using F2 rather than F values. R1 is calculated to provide a reference to the conventional R value but its function is not minimized.

The structure was solved and refined in SHELXTL6.1, using full-matrix least-squares refinement.

Crystal data and structure refinement for C12DL

Identification code	georg7	
Empirical formula	C ₁₅ H ₂₉ O S ₂	
Formula weight	289.50	
Temperature	173(2) K	
Wavelength	0.71073 Å	
Crystal system	Orthorhombic	
Space group	P 21 21 21	
Unit cell dimensions	a = 5.0392(2) Å	α = 90°.
	b = 8.4897(3) Å	β = 90°.
	c = 38.3953(13) Å	γ = 90°.
Volume	1642.60(10) Å ³	
Z	4	
Density (calculated)	1.171 Mg/m ³	
Absorption coefficient	0.313 mm ⁻¹	
F(000)	636	
Crystal size	0.198 x 0.185 x 0.052 mm ³	
Theta range for data collection	2.457 to 31.154°.	

Index ranges	-7≤h≤7, -12≤k≤12, -55≤l≤55
Reflections collected	22184
Independent reflections	4854 [R(int) = 0.0223]
Completeness to theta = 25.000°	99.7 %
Absorption correction	Semi-empirical from equivalents
Max. and min. transmission	0.9851 and 0.9490
Refinement method	Full-matrix least-squares on F ²
Data / restraints / parameters	4854 / 0 / 168
Goodness-of-fit on F ²	1.100
Final R indices [I>2sigma(I)]	R1 = 0.0278, wR2 = 0.0689 [4580]
R indices (all data)	R1 = 0.0313, wR2 = 0.0711
Absolute structure parameter	-0.006(17)
Extinction coefficient	n/a
Largest diff. peak and hole	0.346 and -0.201 e.Å ⁻³

$$R1 = \frac{\sum(|F_o| - |F_c|)}{\sum F_o}$$

$$wR2 = \frac{[\sum[w(F_o^2 - F_c^2)^2] / \sum[w(F_o^2)^2]]^{1/2}}$$

$$S = \frac{[\sum[w(F_o^2 - F_c^2)^2] / (n-p)]^{1/2}}$$

$$w = 1/[\sigma^2(F_o^2) + (m*p)^2 + n*p], p = [\max(F_o^2, 0) + 2 * F_c^2] / 3, m \& n \text{ are constants.}$$



Figure S85. Molecular structures of (*S*)-DiMeDL and (*R*)-DiMeDL with thermal displacement ellipsoids drawn at the 50% probability level.

The structure was solved and refined in *SHELXTL2014*, using full-matrix least-squares refinement. The non-H atoms were refined with anisotropic thermal parameters and all of the H atoms were calculated in idealized positions and refined riding on their parent atoms. The hydroxyl proton was obtained from a Difference Fourier map and refined freely. The hydrogen bonding among hydroxyl groups lead to the formation of double layered sheets connected by S...S interactions. In the final cycle of refinement, 1815

reflections (of which 1382 are observed with $I > 2\sigma(I)$) were used to refine 77 parameters and the resulting R_1 , wR_2 and S (goodness of fit) were 4.03 %, 9.34 % and 1.134, respectively. The refinement was carried out by minimizing the wR_2 function using F^2 rather than F values. R_1 is calculated to provide a reference to the conventional R value but its function is not minimized.

Crystal data and structure refinement for DiMeDL

Identification code	georg8	
Empirical formula	C5 H9 O S2	
Formula weight	149.24	
Temperature	173(2) K	
Wavelength	0.71073 Å	
Crystal system	Tetragonal	
Space group	I 41/a	
Unit cell dimensions	$a = 19.7501(18)$ Å	$\alpha = 90^\circ$.
	$b = 19.7501(18)$ Å	$\beta = 90^\circ$.
	$c = 7.4965(6)$ Å	$\gamma = 90^\circ$.
Volume	2924.1(6) Å ³	
Z	16	
Density (calculated)	1.356 Mg/m ³	
Absorption coefficient	0.635 mm ⁻¹	
F(000)	1264	
Crystal size	0.210 x 0.060 x 0.035 mm ³	
Theta range for data collection	2.906 to 28.300°.	
Index ranges	-26 ≤ h ≤ 26, -26 ≤ k ≤ 26, -9 ≤ l ≤ 9	
Reflections collected	19828	
Independent reflections	1815 [R(int) = 0.0824]	
Completeness to theta = 25.000°	99.9 %	
Absorption correction	Semi-empirical from equivalents	
Refinement method	Full-matrix least-squares on F^2	
Data / restraints / parameters	1815 / 0 / 77	
Goodness-of-fit on F^2	1.134	
Final R indices [$I > 2\sigma(I)$]	$R_1 = 0.0403$, $wR_2 = 0.0934$ [1382]	
R indices (all data)	$R_1 = 0.0609$, $wR_2 = 0.1126$	
Largest diff. peak and hole	0.600 and -0.334 e.Å ⁻³	

$$R_1 = \frac{\sum(|F_o| - |F_c|)}{\sum F_o}$$

$$wR_2 = \left[\frac{\sum[w(F_o^2 - F_c^2)^2]}{\sum[w(F_o^2)^2]} \right]^{1/2}$$

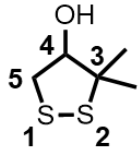
$$S = \left[\frac{\sum[w(F_o^2 - F_c^2)^2]}{(n-p)} \right]^{1/2}$$

$$w = 1/[\sigma^2(F_o^2) + (m^*p)^2 + n^*p], p = [\max(F_o^2, 0) + 2 * F_c^2]/3, m \& n \text{ are constants.}$$

S9. Computational Details

DFT calculations were performed with Gaussian 09 package.³¹ Geometry optimizations were calculated at B3LYP/6-311G** level of theory.^{32,33} All final geometries were verified as minima with frequency calculations. All the thermal energies were obtained from frequency calculation as well for the bond dissociation enthalpies at 298 K. The calculation provided a good match between calculated geometry and X-ray structure for DiMeDL (Table S4).

Table S4. Comparison of X-ray and calculated metrical parameters for DiMeDL.

	X-Ray Structure	B3LYP/6-311G**
Bond Length (Å)		
S-S	2.065	2.134
S-C3	1.840	1.863
C3-C4	1.539	1.547
C4-C5	1.522	1.539
C5-S	1.827	1.856
Bond Angle (°)		
C5SS	96.6	95.5
SSC3	94.0	93.5
SC3C4	104.7	104.7
C3C4C5	110.6	110.9
C4C5S	110.8	111.2
Dihedral Angle (°)		
C5SSC3	23.4	23.7
SSC3C4	43.2	44.0
SC3C4C5	51.3	52.5
C3C4C5S	32.2	32.8
C4C5SS	1.0	0.9

The enthalpy of formation ($\Delta_f H$) in the isodesmic reaction was determined from the calculated sum of electronic and thermal enthalpies for each compound and converted into kJ/mol via 1 Ha = 2625.5 kJ/mol.

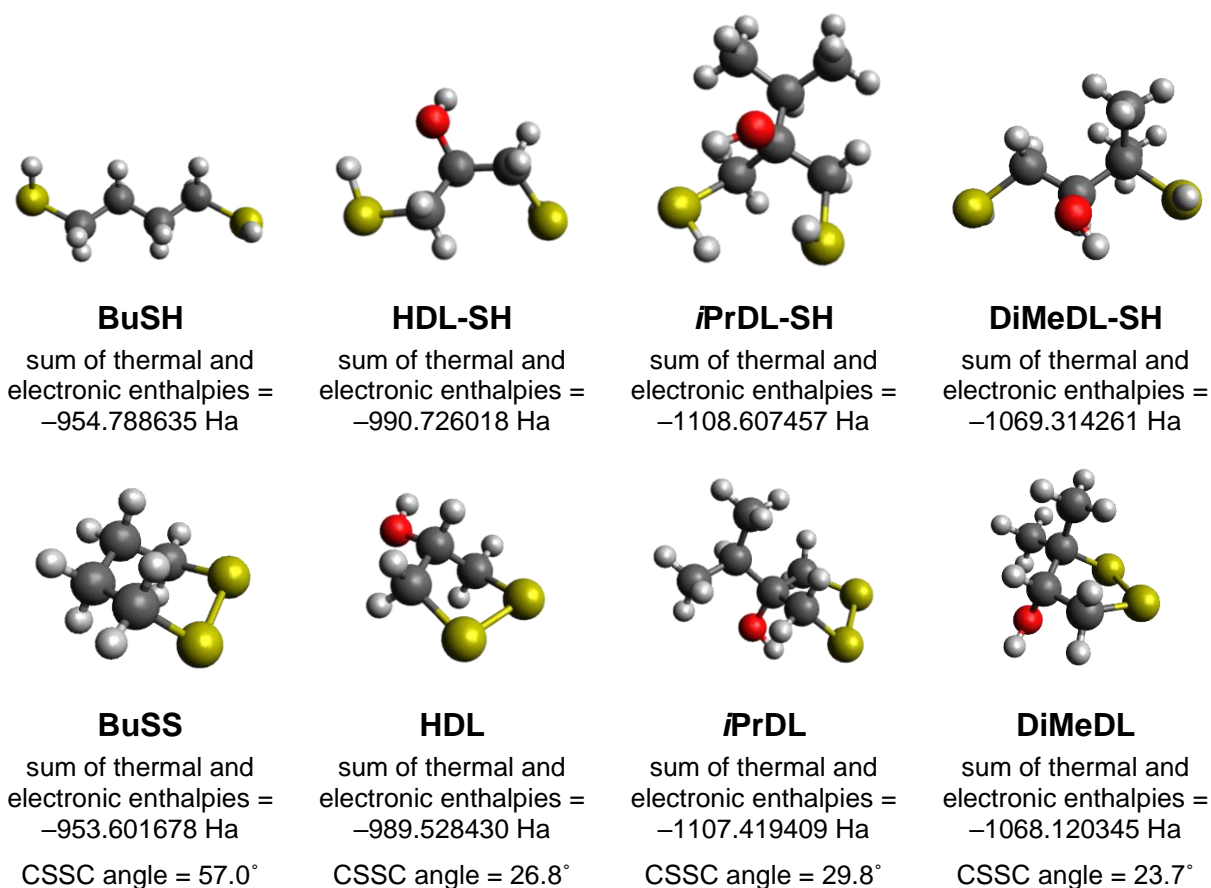


Figure S86. Optimized structures and energies of open and ring-closed 1,2-dithiane (BuSS) and selected 1,2-dithiolanes using a B3LYP/6-311G** basis set. Calculated CSSC dihedral angles are indicated for the ring-closed compounds. The CSSC dihedral angle for **HDL** and **iPrDL** in the optimized geometries are lower than the estimated values based λ_{\max} values from UV-vis spectroscopy. However, the values are very similar to each other and therefore the calculated energy difference should directly reflect the effect of the isopropyl substituent.

Cartesian coordinates of optimized structures

BuSH

C	-1.84089	-0.65362	0.01220
C	-0.68566	0.34688	0.00460
C	0.68566	-0.34688	0.00460
H	-0.76740	1.00128	0.88033

H	-0.77779	0.99289	-0.87437
C	1.84089	0.65362	0.01220
H	0.77779	-0.99290	-0.87436
H	0.76740	-1.00127	0.88034
S	3.51404	-0.11229	-0.07709
H	1.79795	1.30306	0.88880
H	1.79763	1.29753	-0.86952
H	3.45697	-0.75602	1.10740
S	-3.51404	0.11229	-0.07709
H	-1.79795	-1.30305	0.88881
H	-1.79763	-1.29754	-0.86951
H	-3.45697	0.75603	1.10739

BuSS

C	1.66829	-0.75655	0.14055
C	1.66829	0.75655	-0.14055
C	0.46952	-1.52131	-0.42822
H	1.71591	-0.92807	1.22125
H	2.58064	-1.18670	-0.28835
C	0.46952	1.52131	0.42822
H	1.71591	0.92808	-1.22125
H	2.58064	1.18670	0.28835
S	-1.12928	-1.00437	0.31894
H	0.55029	-2.58778	-0.20211
H	0.39475	-1.40430	-1.51157
S	-1.12928	1.00437	-0.31894
H	0.55029	2.58778	0.20211
H	0.39475	1.40430	1.51157

HDL-SH

C	-0.01838	0.60571	-0.22779
---	----------	---------	----------

C	-0.79721	-0.46197	0.52789
C	1.43506	0.73782	0.25506
S	-2.48042	-0.75626	-0.14329
H	-0.87053	-0.18212	1.58103
H	-0.28231	-1.41991	0.45968
H	-2.89441	0.52076	-0.02171
S	2.50889	-0.72387	-0.05555
H	1.45287	0.88630	1.33666
H	1.89593	1.61659	-0.20029
H	2.52514	-0.62567	-1.40121
O	-0.69636	1.84383	0.00525
H	-0.40013	2.48493	-0.64773
H	-0.02813	0.36118	-1.29792

HDL

C	1.22362	-0.07202	0.34254
C	0.45507	-1.18032	-0.39151
C	0.53268	1.28234	0.11260
S	-1.27730	-1.07029	0.16549
H	0.82484	-2.17288	-0.12321
H	0.52533	-1.04042	-1.47193
S	-1.28659	1.05802	-0.13651
H	0.93715	1.72655	-0.79690
H	0.70491	1.95342	0.95298
O	2.55953	0.06527	-0.12871
H	1.20945	-0.29936	1.41500
H	3.07621	-0.67322	0.20820

iPrDL-SH

C	0.37833	-0.10152	-0.05221
C	-0.19049	-1.49756	-0.38256

C	-0.39120	0.99388	-0.86794
C	1.89586	-0.03411	-0.44332
C	2.54733	1.26156	0.06740
H	2.03429	2.16569	-0.26861
H	3.57994	1.32519	-0.28519
H	2.55613	1.27060	1.15874
C	2.70976	-1.23372	0.07084
H	1.93833	-0.03669	-1.54124
H	3.77417	-1.06755	-0.11434
H	2.44105	-2.17174	-0.41853
H	2.57263	-1.35359	1.14872
O	0.27772	0.07690	1.35589
H	-0.30254	0.83716	1.51849
S	-1.62505	2.00181	0.05259
H	-0.89528	0.54322	-1.72159
H	0.30054	1.73783	-1.25826
H	-2.57546	1.04604	0.12289
S	-1.98361	-1.73419	-0.02611
H	0.34770	-2.25805	0.17700
H	-0.08031	-1.71729	-1.44726
H	-1.87180	-1.54914	1.30503

iPrDL

C	-0.15491	0.84429	0.21891
C	1.03009	1.26729	-0.68022
C	0.45265	0.03588	1.37667
S	2.14100	-0.16157	-1.01300
H	1.58937	2.05186	-0.17105
H	0.68167	1.63710	-1.64719
S	1.47671	-1.31679	0.70326
H	-0.31838	-0.41933	1.99781

H	1.05589	0.70311	1.99316
C	-1.22765	0.09117	-0.58721
C	-2.42109	-0.42468	0.22489
H	-0.75763	-0.73559	-1.12634
H	-1.59290	0.78657	-1.35693
C	-3.54914	-0.95173	-0.66706
H	-2.79770	0.37964	0.86463
H	-2.09191	-1.22773	0.89226
H	-3.94052	-0.16476	-1.31953
H	-4.38176	-1.33017	-0.06853
H	-3.20113	-1.76862	-1.30646
O	-0.71295	2.00888	0.83973
H	-1.20445	2.49728	0.17040

DiMeDL-SH

C	-0.30565	-0.27142	-0.16087
C	1.07061	0.42481	0.07343
C	-1.49866	0.53342	0.36319
S	2.41244	-0.73215	-0.54813
H	2.36056	-1.59910	0.48296
S	-3.12658	-0.10602	-0.22290
H	-1.43362	1.58863	0.10576
H	-1.53455	0.45196	1.44978
H	-3.20459	0.65689	-1.33256
O	-0.37148	-1.52871	0.50231
H	-0.41757	-0.40779	-1.24283
H	0.03794	-2.18585	-0.06833
C	1.31464	0.73921	1.55242
H	1.16020	-0.14949	2.16707
H	0.62418	1.51499	1.89887
H	2.33222	1.10133	1.70751

C	1.20860	1.68247	-0.79642
H	1.04515	1.46001	-1.85471
H	2.20598	2.11405	-0.69150
H	0.48505	2.44382	-0.49449

DiMeDL

C	0.36555	1.17673	0.36847
C	-1.12741	1.13637	0.73871
C	0.94042	-0.25299	0.23631
S	-1.96495	-0.34195	-0.00896
H	-1.62401	2.04044	0.38276
H	-1.25857	1.06622	1.81943
S	-0.21132	-1.11873	-0.94533
O	0.58814	1.86269	-0.85257
H	0.90898	1.67725	1.18538
H	0.27104	2.76521	-0.75496
C	0.95784	-0.95771	1.59789
H	-0.04460	-1.07623	2.01167
H	1.56507	-0.38964	2.31190
H	1.39490	-1.95234	1.49655
C	2.33618	-0.25302	-0.39763
H	2.33362	0.26507	-1.35446
H	2.69192	-1.27609	-0.54096
H	3.04134	0.25324	0.26929

S10. References

1. Bergson, G. Molecular orbital treatment of the 3p(pi) interaction in five-membered cyclic disulphides. *Ark. Kemi* **1958**, *12*, 233–237.
2. Boyd, D. B. Conformational dependence of the electronic energy levels in disulfides. *J. Am. Chem. Soc.* **1972**, *94*, 8799–8804.
3. Houk, J. W., Whitesides, G. M. Structure-Reactivity Relations for Thiol-Disulfide Interchange. *J. Am. Chem. Soc.* **1987**, *109*, 6825–6835.
4. NIST: 2-Bromo-2-methylpropane; NIST MS number 227729.
<https://webbook.nist.gov/cgi/cbook.cgi?ID=C507197&Mask=200#Mass-Spec> (accessed 05.10.2020).;

5. NIST: 1,2-Dibromo-2-methylpropane; NIST MS number 73436.
<https://webbook.nist.gov/cgi/formula?ID=C594343&Mask=200> (accessed 05.10.2020).
6. Gafner, G.; Admiraal, L. J. The crystal and molecular structure of the alkaloid gerrardine. *Acta Crystallogr. B* **1971**, *27*, 565–568.
7. Kato, A.; Ichimaru, M.; Hashimoto, Y.; Mitsudera, H. Guinesine-A, -B and -C: new sulfur containing insecticidal alkaloids from *cassipourea guianensis*. *Tetrahedron Lett.* **1989**, *30*, 3671–3674.
8. Siemeling, U.; Bruhn, C.; Bretthauer, F.; Borg, M.; Träger, F.; Vogel, F.; Azzam, W.; Badin, M.; Strunskus, T.; Wöll, C. Photoresponsive SAMs on gold fabricated from azobenzene-functionalised asparagusic acid derivatives. *Dalton Trans.* **2009**, 8593–8604.
9. Stroud, R. M.; Carlisle, C. H. A single-crystal structure determination of DL-6-thioctic acid. *Acta Crystallogr. B* **1972**, *28*, 304–307.
10. Morera, E.; Lucente, G.; Ortar, G.; Nalli, M.; Mazza, F.; Gavuzzo, E.; Spisani, S., Exploring the interest of 1,2-Dithiolane ring system in peptide chemistry. Synthesis of a chemotactic tripeptide and x-ray crystal structure of a 4-amino-1,2-dithiolane-4-carboxylic acid derivative. *Bioorg. Med. Chem.* **2002**, *10*, 147–157.
11. Sureshkumar, D.; Koutha, S. M.; Chandrasekaran, S. Chemistry of Tetrathiomolybdate: Aziridine Ring Opening Reactions and Facile Synthesis of Interesting Sulfur Heterocycles. *J. Am. Chem. Soc.* **2005**, *127*, 12760–12761.
12. Sureshkumar, D.; Koutha, S.; Ganesh, V.; Chandrasekaran, S. Tetrathiomolybdate Mediated Rearrangement of Aziridinemethanol Tosylates: A Thia-Aza-Payne Rearrangement. *J. Org. Chem.* **2010**, *75*, 5533–5541.
13. Kilgore, H. R.; Raines, R. T. Disulfide Chromophores Arise from Stereoelectronic Effects. *J. Phys. Chem. B* **2020**, *124*, 3931–3935.
14. Sugeta, H.; Go, A.; Miyazawa, T. Vibrational Spectra and Molecular Conformations of Dialkyl Disulfides. *Bull. Chem. Soc. Jpn.* **1973**, *46*, 3407–3411.
15. Van Wart, H. E.; Scheraga, H. A. Raman spectra of strained disulfides. Effect of rotation about sulfur-sulfur bonds on sulfur-sulfur stretching frequencies. *J. Phys. Chem.* **1976**, *80*, 1823–1832.
16. Eliel, E. L. Conformational Analysis in Mobile Cyclohexane Systems. *Angew. Chem., Int. Ed.* **1965**, *4*, 761–774.
17. McDaniel, D. H.; Brown, H. C. An Extended Table of Hammett Substituent Constants Based on the Ionization of Substituted Benzoic Acids. *The Journal of Organic Chemistry* **1958**, *23*, 420-427.
18. Van Wart, H. E.; Lewis, A.; Scheraga, H. A.; Saeva, F. D. Disulfide Bond Dihedral Angles from Raman Spectroscopy. *Proc. Natl. Acad. Sci. U.S.A.* **1973**, *70*, 2619–2623.
19. Martin, R. B. Invariance of disulfide stretching wave numbers to disulfide dihedral angles. *J. Phys. Chem.* **1974**, *78*, 855–856.
20. Van Wart, H. E.; Scheraga, H. A.; Martin, R. B. Agreement concerning the nature of the variation of disulfide stretching frequencies with disulfide dihedral angles. *J. Phys. Chem.* **1976**, *80*, 1832–1832.
21. Brunet, E.; Garcia-Ruano, J. L.; Rodriguez, H.; Alcudia, F. Stereochemistry of organic sulphur compounds. part 14. synthesis and conformation analysis of 1-thioderivatives of 3,3-dimethyl-2-butanol and its acetates. *Tetrahedron* **1984**, *40*, 4433–4445.
22. Zhang, L.; Duan, D.; Liu, Y.; Ge, C.; Cui, X.; Sun, J.; Fang, J. Highly selective off-on fluorescent probe for imaging thioredoxin reductase in living cells. *J. Am. Chem. Soc.* **2014**, *136*, 226–233.
23. Barth, S.; Biegger, F.; Puchberger, M. Synthesis and characterisation of thioether functionalised gallium and indium alkoxides. *Dalton Trans.* **2015**, *44*, 16439–16445.
24. Tan, X.; Li, C.; Yu, Z.; Wang, P.; Nian, S.; Deng, Y.; Wu, W.; Wang, G. Synthesis of Substituted 6-Amino-4-(2,4-dimethoxyphenyl)-[1,2]dithiolo[4,3-*b*]pyrrol-5-ones and Their Raising Leukocyte Count Activities. *Chem. Pharm. Bull.* **2013**, *61*, 351–357.
25. Hatano, M.; Ito, O.; Suzuki, S.; Ishihara, K. Zinc(ii)-catalyzed Grignard additions to ketones with RMgBr and RMgI. *Chem. Commun.* **2010**, *46*, 2674–2676.
26. Hatano, M.; Suzuki, S.; Ishihara, K. Highly Efficient Alkylation to Ketones and Aldimines with Grignard Reagents Catalyzed by Zinc(II) Chloride. *J. Am. Chem. Soc.* **2006**, *128*, 9998–9999.
27. Pugia, M. J.; Knudsen, B. E.; Cason, C. V.; Bartsch, R. A. Synthesis and alkali-metal complexing abilities of crown ether tertiary alcohols. *J. Org. Chem.* **1987**, *52*, 541–547.
28. Axenrod, T.; Watnick, C.; Yazdekhasti, H.; Dave, P. R. Synthesis of 1,3,3-Trinitroazetidone via the Oxidative Nitrolysis of N-p-Tosyl-3-azetidone Oxime. *J. Org. Chem.* **1995**, *60*, 1959–1964.

29. Iranpoor, N.; Zeynizadeh, B. Efficient and Regioselective Conversion of Epoxides into Vicinal Chloroesters with TiCl_4 and Imidazole in Ethyl Acetate. *J. Chem. Research (S)* **1998**, 582–583.
30. Tang, Q.; Chen, X.; Tiwari, B.; Chi, Y. R., Addition of Indoles to Oxyallyl Cations for Facile Access to α -Indole Carbonyl Compounds. *Org. Lett.* **2012**, *14*, 1922–1925.
31. Gaussian 09, Revision D.01, M. J. Frisch, G. W. Trucks, H. B. Schlegel, G. E. Scuseria, M. A. Robb, J. R. Cheeseman, G. Scalmani, V. Barone, B. Mennucci, G. A. Petersson, H. Nakatsuji, M. Caricato, X. Li, H. P. Hratchian, A. F. Izmaylov, J. Bloino, G. Zheng, J. L. Sonnenberg, M. Hada, M. Ehara, K. Toyota, R. Fukuda, J. Hasegawa, M. Ishida, T. Nakajima, Y. Honda, O. Kitao, H. Nakai, T. Vreven, J. A. Montgomery, Jr., J. E. Peralta, F. Ogliaro, M. Bearpark, J. J. Heyd, E. Brothers, K. N. Kudin, V. N. Staroverov, T. Keith, R. Kobayashi, J. Normand, K. Raghavachari, A. Rendell, J. C. Burant, S. S. Iyengar, J. Tomasi, M. Cossi, N. Rega, J. M. Millam, M. Klene, J. E. Knox, J. B. Cross, V. Bakken, C. Adamo, J. Jaramillo, R. Gomperts, R. E. Stratmann, O. Yazyev, A. J. Austin, R. Cammi, C. Pomelli, J. W. Ochterski, R. L. Martin, K. Morokuma, V. G. Zakrzewski, G. A. Voth, P. Salvador, J. J. Dannenberg, S. Dapprich, A. D. Daniels, O. Farkas, J. B. Foresman, J. V. Ortiz, J. Cioslowski, and D. J. Fox, Gaussian, Inc., Wallingford CT, **2013**.
32. Becke, A. D. Density-functional thermochemistry. III. The role of exact exchange. *J. Chem. Phys.* **1993**, *98*, 5648–5652.
33. McLean, A. D. Chandler, G. S. Contracted Gaussian-basis sets for molecular calculations. I. 2nd row atoms, $Z=11-18$. *J. Chem. Phys.* **1980**, *72*, 5639–5648.